The impact of pre-receptor metabolism on the adverse effects of exogenous glucocorticoids

Submitted in accordance with the requirements for the degree of
Doctor of Medicine

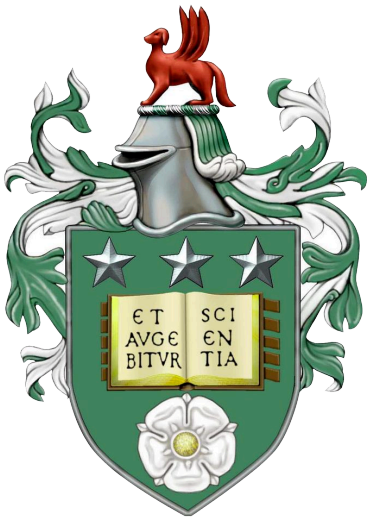

by

Nantia Othonos

The University of Leeds
Faculty of Medicine and Health
School of Medicine

Oxford Centre for Diabetes, Endocrinology and Metabolism (OCDEM)
Radcliffe Department of Medicine, University of Oxford

December 2020

Intellectual Property and Publication Statements

The candidate confirms that the work submitted is her own, except where work which has formed part of jointly authored publications has been included. The contribution of the candidate and the other authors to this work has been explicitly indicated below. The candidate confirms that appropriate credit has been given within the thesis where reference has been made to the work of others.

Work that forms part of a jointly authored publication is found in Chapter 3 and is from "Co-administration of 5α-reductase Inhibitors Worsens the Adverse Metabolic Effects of Prescribed Glucocorticoids" Othonos N, Marjot T, Woods C, Hazlehurst JM, Nikolaou N, Pofi R, White S, Bonaventura I, Webster C, Duffy J, Cornfield T, Moolla A, Isidori AM, Hodson L, Tomlinson JW. JCEM (Sep 2020). I conducted sample processing and analysis and prepared the manuscript. JWT and CW designed the study and was implemented by TM and SW. RP, IB, JMH, NN, CW, JD, TC, AM conducted sample analysis. RF, AMI, LH and JWT conducted data analysis.

Acknowledgements

I am deeply grateful to my primary supervisor Prof Jeremy Tomlinson for his unwavering encouragement, support and guidance throughout the length of my degree. I would also like to express my gratitude to my co-supervisor Prof Paul Stewart for his time and effort, considered opinion and supportive guidance.

A special thank you to all my colleagues in the Tomlinson group (Dr Nikolaos Nikolaou, Dr Jonathan Hazlehurst, Dr Ahmad Moolla, Dr Riccardo Pofi, Dr Niall Dempster, Dr Shelley Harris, Anastasia Arvaniti and Dr Ilaria Bonaventura), the CRU nurses (particularly Sarah White and Rachel Franklin), Tom Cornfield, Dr Catriona Charlton and Dr Leanne Hodson for their vital support on both a professional and personal level.

I am indebted to the ongoing support of my family and friends in the UK and in Cyprus, particularly my wonderful parents Stavros and Maria and brother Michael, my loving and supportive husband Michael and incredible son Victor.

This thesis is dedicated to the memory of my grandmother Ntina Omorphou who sadly passed away this year.

Abstract

Glucocorticoids (GC), commonly prescribed for their anti-inflammatory actions, have adverse metabolic and bone effects. 5α-reductase inhibitors (5αRI) inhibit the metabolism of cortisol to its active metabolites and 11β-hydroxysteroid dehydrogenase type 1 (11β-HSD1) inhibitors inhibit the re-activation of cortisol from the inactive cortisone. Two clinical studies were performed to investigate how co-administration of prednisolone with a 5αRI and prednisolone with an 11β-HSD1 inhibitor affects the GC-induced metabolic effects in healthy volunteers.

The FindIt2 clinical study is a prospective randomized study. 19 healthy male volunteers were recruited and underwent detailed metabolic assessment before and after administration of prednisolone (10mg daily) or prednisolone (10mg daily) and a 5αRI (finasteride 5 mg daily or dutasteride 0.5 mg daily) for 7 days. The results showed that 5αRIs can exacerbate the adverse effects of prednisolone such as hepatic, peripheral and adipose tissue insulin resistance. This study has significant translational implications, including the need to consider GC dose adjustments, but also the necessity for increased vigilance for the development of adverse effects.

The TICSI study is a randomized, double-blind, placebo-controlled study. 32 healthy male volunteers were recruited, of which 30 were eligible for analysis. They were randomized to receive prednisolone + placebo or prednisolone + AZD4017 for 7 days. They also, underwent detailed metabolic assessment before and after treatment. The results showed that co-administration of 11β-HSD1 inhibition limits the adverse metabolic and bone effects of prednisolone. 11β-HSD1 inhibition provides a potential strategy for selectively limiting the adverse side effects of prescribed GC.

The outcomes of these two clinical studies suggest that pre-receptor metabolism plays a fundamental role in the effect of GCs in metabolic tissues. Assessment of pre-receptor enzyme activity could be used to predict response, as well as risk of side-effects, in patients requiring treatment with GCs.

Table of Contents

Table of figures

Table of tables

Publications and Communications

Publication

Othonos N, Marjot T, Woods C, Hazlehurst JM, Nikolaou N, Pofi R, White S, Bonaventura I, Webster C, Duffy J, Cornfield T, Moolla A, Isidori AM, Hodson L, Tomlinson JW. Co-administration of 5α-reductase Inhibitors Worsens the Adverse Metabolic Effects of Prescribed Glucocorticoids. J Clin Endocrinol Metab. 2020 Sep 1;105(9):e3316-28.

Oral presentations

Othonos N, Pofi R, Arvaniti A, Whittaker A, Stewart P, Coleman R, Agbaje O, Milton J, Holman R, Tomlinson JW. 11β-Hydroxysteroid dehydrogenase type 1 inhibition protects against the development of adverse metabolic and bone effects of prednisolone: A randomized, double-blind, placebo-controlled trial. 22nd European Congress of Endocrinology, eECE, September 2020.

Othonos N, Marjot T, Woods C, Hazlehurst J, Moolla A, Hodson L, Tomlinson JW. Co-administration of 5α-reductase inhibitors worsens the adverse metabolic effects of prescribed glucocorticoids. Society for Endocrinology BES, Harrogate, UK November 2017. **(Awarded Society of Endocrinology Highly Commended Clinical Oral Communication Prize)**

Poster presentations

Othonos N, Marjot T, Woods C, Hazlehurst J, Moolla A, Hodson L, Tomlinson JW. The adverse effects of prescribed glucocorticoids are worsened by co-administration of 5α-reductase inhibitors. 19th European Congress of Endocrinology, Lisbon, Portugal, May 2017.

Glossary abbreviations

11β-HSD	11β-Hydroxysteroid Dehydrogenase
11β-HSD1	11β-Hydroxysteroid Dehydrogenase Type 1
11β-HSD2	11β-Hydroxysteroid Dehydrogenase Type 2
5aR	5a-Reductase
5aRI	5a-Reductase Inhibitor
5αR1	5a-Reductase Type 1
5αR2	5a-Reductase Type 2
ACACA	Acetyl-CoA Carboxylase 1
ACRD	Apparent Cortisone Reductase Deficiency
ACTH	Adrenocorticotropic Hormone
AKR1B10	Aldo-Keto Reductase Family 1 Member B10
ALAS2	5'-Aminolevulinate Synthase 2
allo-THF	5α-Tetrahydrocortisol
ALP	Alkaline Phosphatase
ALT	Alanine Aminotransferase
APOD	Apolipoprotein D
Approx	Approximately
ARHGAP20	Rho GTPase Activating Protein 20
ARNTL	Aryl Hydrocarbon Receptor Nuclear Translocator-like Protein 1
AST	Aspartate Aminotransferase
ATP	Adenosine Triphosphate
AUC	Area Under the Curve
BD	Twice Daily
BHT	Butylated Hydroxytoluene
BMI	Body Mass Index
BP	Blood Pressure
BPH	Benign Prostate Hyperplasia
BPM	Beats Per Minute
CA1	Carbonic Anhydrase 1
CBG	Cortisol Binding Globulin
cDNA	Complementary DNA
CI	Confidence Interval
CNS	Central Nervous System
CO2	Carbon Dioxide
CRD	Cortisone Reductase Deficiency
CRU	Clinical Research Unit

Ct	Cycle Threshold
CTX	Carboxy-Terminal Cross-linked Telopeptide of Type 1 Collagen
CYP1A1	Cytochrome P450 Family 1 Subfamily A Member 1
CYP1A2	Cytochrome P450 Family 1 Subfamily A Member 2
CYP2B1/2	Cytochrome P450 Family 2 Subfamily B Polypeptide 1
CYP2E1	Cytochrome P450 Family 2 Subfamily E Member 1
CYP3A	Cytochrome P450 Family 3 Subfamily A
DACT2	Dishevelled Binding Antagonist Of Beta Catenin 2
DBP	Diastolic Blood Pressure
DEXA	Dual Energy X-ray Absorptiometry
DHCR24	24-Dehydrocholesterol Reductase
DHEA	Dehydroepiandrosterone
DMARDs	Disease Modifying Anti-Rheumatic Drugs
DNA	Deoxyribonucleic Acid
dNTP	Deoxynucleoside Triphosphate
DPP-4	Dipeptidyl Peptidase-4
ECM	Extracellular Matrix
EDN1	Endothelin 1
eGFR	Estimated Glomerular Filtration Rate
EGP	Endogenous Glucose Production
ELISA	Enzyme-Linked Immunosorbent Assay
ER	Endoplasmic Reticulum
ETNK2	Ethanolamine Kinase 2
FABP7	Fatty Acid Binding Protein 7
FAM13A	Family With Sequence Similarity 13 Member A
FAM166B	Family With Sequence Similarity 166 Member B
FASN	Fatty Acid Synthase Gene
G6PD	Glucose-6-Phosphate Dehydrogenase
GADD45B	Growth Arrest and DNA-damage-inducible Beta
GC	Glucocorticoids
GC/C/IRMS	Gas Chromatography/ Combustion/ Isotope Ratio Mass Spectrometry
GC/MS	Gas Chromatography/ Mass Spectrometry
Gd	Glucose Disposal
GH	Growth Hormone
GILZ	Glucocorticoid-Induced Leucine Zipper
GLP-1	Glucagon-Like Peptide 1
GLUT4	Glucose Transporter Type 4
GR	Glucocorticoid Receptor

H6PDH	Hexose-6-Phosphate Dehydrogenase Reduced
HBA1	Haemoglobin Alpha 1
HBA2	Haemoglobin Subunit Alpha 2
HBB	Haemoglobin Subunit Beta
HBD	Haemoglobin Subunit Delta
HC	Hydrocortisone
HDL	High-Density Lipoprotein
HFD	High Fat Diet
HGP	Hepatic Glucose Production
HIV	Human Immunodeficiency Virus
HMOX1	Haem Oxygenase 1
HPA	Hypothalamus Pituitary Adrenal
HR	Hour
HRPC	Hormone-Refractory Prostate Cancer
IGF-1	Insulin-like Growth Factor 1
IIH	Idiopathic Intracranial Hypertension
IMP	Investigational Medicinal Product
IQR	Interquartile Ranges
KCNQ3	Potassium Voltage-Gated Channel Subfamily Q Member 3
KG	Kilograms
KLHL25	Kelch Like Family Member 25
KO	Knock Out
KRT1	Keratin 1
LDL	Low-Density Lipoprotein
LINC00844	Long Intergenic Non-Protein Coding RNA 844
lincRNA	Long Intergenic Non-Coding RNA
LIPE	Hormone-Sensitive Lipase Gene
LPL	Lipoprotein Lipase Gene
LPS	Lipopolysaccharides
M	Molar
MALL	Mal T Cell Differentiation Protein Like
Min	Minute
MMP3	Matrix Metalloproteinase-3
MR	Mineralocorticoid Receptor
NaCl	Sodium Chloride
NADP	Nicotinamide-Adenine Dinucleotide Phosphate
NADPH	Nicotinamide-Adenine Dinucleotide Phosphate Reduced
NEFA	Non-Esterified Fatty Acids

NF-kB	Nuclear Factor Kappa-light-chain-enhancer of Activated B cells
NFKBIA	NFKB Inhibitor Alpha
NTX	N-Telopeptide of Type 1 Collagen
OCDEM	Oxford Centre for Diabetes, Endocrinology and Metabolism
OD	Once Daily
OHB	3-Hydroxybutyrate
P1NP	Procollagen Type 1 N-terminal Pro-peptide
PADI4	Peptidyl Arginine Deiminase 4
PCOS	Polycystic Ovarian Syndrome
PCR	Polymerase Chain Reaction
PEPCK	Phosphoenolpyruvate Carboxykinase
PHA	Phytohaemagluttinin
PLA2G2A	Phospholipase A2 Group IIA
PNPLA2	Patatin-like Phospholipase Domain-containing Protein 2
PPAR	Peroxisome Proliferator-Activated Receptor
PPARa	Peroxisome Proliferator-Activated Receptor Alpha
QPCR	Quantitative Polymerase Chain Reaction
RASD1	Dexamethasone-induced Ras-related Protein 1
RNA	Ribonucleic Acid
RPL41P1	Ribosomal Protein L41 Pseudogene 1
RPM	Revolutions Per Minute
RR	Relative Rate
rRNA	Ribosomal Ribonucleic Acid
RT	Reverse transcription
RT-PCR	Reverse transcription polymerase chain reaction
S100A8	S100 Calcium-binding Protein A8
S100A9	S100 Calcium-binding Protein A9
SBP	Systolic Blood Pressure
SC	Subcutaneous
SD	Standard Deviation
SE	Standard Error
Sec	Seconds
SEGRM	Selective Glucocorticoid Receptor Modulators
SGK1	Serum/Glucocorticoid Regulated Kinase 1
SNCA	Synuclein Alpha
SNP	Single Nucleotide Polymorphisms
SOX7	SRY-related HMG-box 7
SPINK2	Serine Protease Inhibitor Kazal-type 2

T2DM	Type 2 Diabetes Mellitus
TAG	Triglycerides
THE	Tetrahydrocortisone
THF	5β-Tetrahydrocortisol
TMB	3,3',5,5'-Tetramethylbenzidine
TRIM58	Tripartite Motif Containing 58
TrisHCL	Tris(hydroxymethyl)aminomethane Hydrochloride
TSH	Thyroid Stimulating Hormone
TSPYL2	Testis-Specific Y-Encoded-Like Protein 2
TTR	Tracer-to-Tracee Ratio
VZV	Varicella-Zoster virus
γGT	Gamma-Glutamyl Transferase

1 General Introduction

1.1 General introduction

Steroids were first isolated and characterized in the 1930s by Kendall and Reichstein from the adrenal cortex (1-4). In 1949, compound E (cortisone), was synthesized and it was trialled in patients who suffered from rheumatoid arthritis and rheumatic fever (5). The extraordinary success in treating these conditions lead to a surge of trials using cortisone as a treatment for nearly every disease. Through these trials, it was discovered that cortisone was beneficial in adrenal deficiency disorders, inflammatory disorders and malignancies such as lymphoma but was harmful in infections. 2 years later, in 1951, compound F (cortisol) was synthesized and soon became evident that this was the active compound suggesting that glucocorticoids (GC) undergo metabolism in vivo (6). This prompted a new wave of studies investigating steroid metabolism in rodents and in humans. Amelung et al. (1953) reported that cortisone is converted to cortisol in a number of tissues in rats and was highest in the liver (7). During the next decade, 11beta-hydroxysteroid dehydrogenase (11β-HSD) activity was identified in a number of organs (8, 9) but it wasn't until the late-80s that it was first purified from rat liver cells (10) and 2002 when Maser et al. purified the human enzyme (11).

Steroids are synthesized and secreted from the adrenal cortex of the adrenal glands. Mineralocorticoids are synthesized in the zona glomerulosa, GCs in the zona fasciculata and sex steroids in the zona reticularis. GC are highly lipophilic therefore can easily cross the cell membrane and bind to and activate the mineralocorticoid (MR) and glucocorticoid (GR) intracellular receptors. The activated receptors then initiate a cascade of events which lead to the promotion or repression of a specific gene expression.

Cortisol is mainly bound (>90%) to cortisol binding protein with high affinity and the rest is "free" circulating and available to transfer into cells. Cortisol has a circulating half-life of between 70 and 120 minutes. Circulating GC levels vary significantly depending on external and internal factors; there are very low circulating levels during sleep and extremely high during severe stress or illness. The circulating levels of GCs are closely regulated through a balance between secretion and metabolism. The principal organ in GC metabolism is the liver, where a variety of metabolising enzymes can be found as follows (**Figure *1.1-1***):

- 11β-HSD type 1 (11β-HSD1) interconverts the active cortisol to the inactive cortisone.
- A-ring-reductases metabolise cortisol to 5α- or 5β-dihydrocortisol which is then subsequently metabolised to 5α-tetrahydrocortisol (allo-THF) and 5β-tetrahydrocortisol (THF) respectively, by 3α-hydroxysteroid dehydrogenase. Similarly, cortisone is converted to tetrahydrocortisone (THE). These metabolites are conjugated with glucuronic acid and excreted in the urine.
- 6β-hydroxylase converts cortisol to 6β-hydroxycortisol and cortisone to 6β-hydroxycortisone.
- 20β-oxoreductase reduces cortisol to 20β-dihydrocortisol and cortisone to 20β-dihydrocortisone.

In vivo, metabolism of GCs is particularly important as their bioactivity is dependent on the C11-hydroxyl group. Therefore, 11β-HSD, and in particular 11β-HSD1, is considered to be the most important enzyme in the metabolism and activation of GCs as they oxoreduce the C11-oxo group of the inactive cortisone and convert it to

cortisol. There are two types of 11β-HSD; 11β-HSD1 and 11β-HSD2 which are discussed extensively in the following sections.

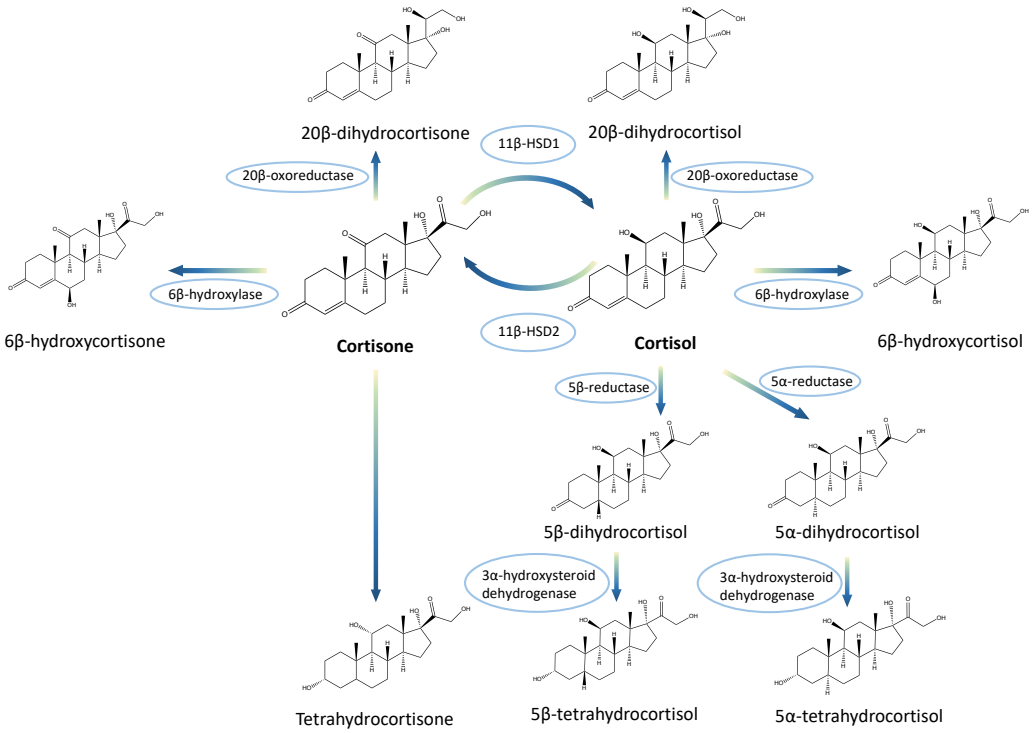

Figure 1.1-1 *Pre-receptor cortisol metabolism*

1.2 Glucocorticoid action

Over the last 70 years, GCs have been used extensively for their anti-inflammatory and immunosuppressive actions in conditions such as asthma, arthritis, inflammatory bowel disease and other systemic diseases, as well as in allotransplantation. The plasma half-life of synthetic GCs ranges from 80 min (cortisol) to 270 min (dexamethasone). As mentioned earlier, 90% of endogenous cortisol is bound to cortisol binding globulin (CBG), however, most synthetic steroids, with the exception of prednisolone, are bound to albumin. They are metabolized by the liver and 95%

are excreted by the kidney and the rest through the gut. Their biological action is mediated via the GR, in the same way as endogenous GCs (**Figure 1.2-1**).

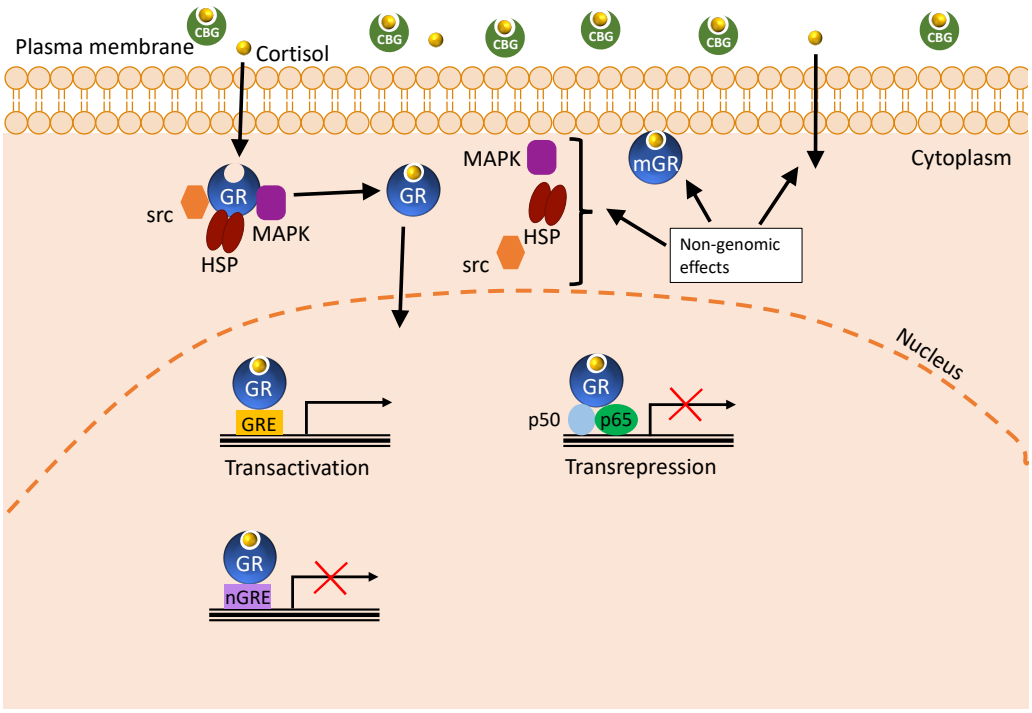

Figure 1.2-1 *Genomic and nongenomic GC signalling pathways. GCs pass through the plasma membrane to bind to the GR, displacing associated proteins (HSP, MAPK and co-chaperones like src) that mediated nongenomic effects. The GC-GR complex moves into the nucleus to affect transcription by binding of GR to positive and negative glucocorticoid responsive elements and by transrepression due to direct or indirect interaction of the GR with transcription factors such as nuclear factor-kB at its binding site). Nongenomic effects are also mediated through membrane bound GR and by interactions with cellular membranes. CBG= Cortisol binding globulin. GR= Glucocorticoid receptor. GRE= Glucocorticoid responsive element. HSP= heat shock protein. MAPK= mitogen activated protein kinase. mGR= membrane bound GR. nGRE= negative GRE.*

Prescribed GCs can induce a variety of side-effects which are discussed in the next sections. The side-effects are dependent on the duration, dosage and potency of the synthetic GCs.

1.2.1 Metabolic effects of glucocorticoids

GC-induced hyperglycaemia, in non-diabetic patients, is a common side-effect with an odds ratio that ranges from 1.36 to 2.31 (12). Risk factors of developing steroid

diabetes include: dosage and treatment duration (13, 14), age (15), weight (16, 17), race (18), impaired glucose tolerance (19) and family history of diabetes (20, 21). The pathophysiology of GC-induced hyperglycaemia is not completely understood but the main mechanisms include increase in insulin resistance, increase in glucose production and reduction in production and secretion of insulin.

Organ system	Glucocorticoid side-effects and the mechanism of action
Metabolic	• Increase in endogenous glucose production by: - Stimulating genes involved in hepatic metabolism of carbohydrates - Increasing the substrate availability for hepatic gluconeogenesis by their action on muscular and adipose tissues - Enhancing the effects of hormones such as glucagon and epinephrine • Increase in insulin resistance by: - Inhibit translocation of the GLUT4 glucose transporter to the cell surface in response to insulin and other stimuli
Bone	• Decrease bone formation markers • Slightly reduce bone resorption markers
Cutaneous	• Decrease cutaneous cell proliferation and protein synthesis • Decrease the proliferative activity of keratinocytes and dermal fibroblasts
Muscular	• Inhibit glucose uptake which may contribute to the breakdown of muscle proteins • Inhibit protein synthesis and stimulate protein degradation
Ophthalmic	• Induces cataract via: - increased glucose levels - inhibition of Na^+/K^+-ATPase - increased cation permeability - inhibition of G6PD - inhibition of RNA synthesis - loss of ATP - covalent binding of steroids to lens proteins • Induces ocular hypertension via morphological and functional changes in the trabecular meshwork
Neurological	• Steroid-induced psychosis could be caused by impairment of the hippocampal function following direct exposure • Depression may be caused by inhibition of the 5-HT1A receptor
Cardiovascular	• Cause hypertension by oversaturating mineralocorticoid receptors at the renal tubule, thus preventing 11β-HSD2 to deactivate GCs
Gastrointestinal	• Increase gastric acid secretion • Reduce gastric mucus • Induce gastrin and parietal cell hyperplasia • Delay the healing of ulcers

Table 1-1 *Glucocorticoid side-effects and the mechanism of action in each organ system*

Endogenous glucose production (EGP) is augmented by the direct stimulation of genes involved in hepatic metabolism of carbohydrates by GCs (22-24) (***Table 1*-1**). This is also enhanced by increasing the substrate availability for hepatic gluconeogenesis by their action on muscular and adipose tissues (25, 26), and by enabling transfer of metabolites across the mitochondrial membranes (25, 27). Moreover, GCs could be enhancing the effects of hormones such as glucagon and epinephrine which increase the gluconeogenesis (26, 28). Peroxisome proliferator-activated receptor (PPAR) α is an important receptor for this GC-induced mechanism as demonstrated by PPARα-knockout (KO) mice (29).

GCs induce peripheral insulin resistance by affecting parts of the insulin signalling cascade (24, 30), which causes mainly muscle insulin resistance (24). GLUT4 glucose transporter is the first determinant of peripheral glucose uptake (***Table 1*-1**). It is mainly expressed in skeletal muscle and its expression is promoted by insulin, however, GCs inhibit its translocation to the cell surface in response to insulin and other stimuli (30-34). This subsequently leads to decrease in glucose uptake and glycogen synthesis (35-37). GC actions in protein (38) and lipid metabolism (39-41) may also contributed to GC-induced skeletal muscle insulin resistance. This is due to the catabolic effect of GCs which leads to increase in amino acids and free fatty acids. Amino acids are thought to exert skeletal muscle insulin resistance by direct inhibition of muscle glucose transport and/or phosphorylation with subsequent reduction in rates of glycogen synthesis. Free fatty acids, on the other hand, contend with glucose for mitochondrial oxidation and thus subsequently give rise to intracellular glucose-6-phosphate dehydrogenase (G6PD) which reduces muscular glucose uptake.

GCs cause a dosage and duration dependant, inhibition of the production and secretion of insulin (42-44). Acute GC administration (45-47) can produce an acute inhibition of insulin secretion in healthy people without changes to fasting insulin despite a rise in plasma glucose levels, suggesting an acute inhibitory effect on β-cells. However, longer exposure (2-5 days) to high-dose GCs can induce fasting hyperinsulinemia as well as increased insulin secretion during hyperglycaemic clamp studies or intravenous glucose tolerance tests (20, 45, 48-51). Unfortunately, there are no well-defined data on the long-term effects of GCs on β-cell function as patients requiring chronic use of GCs often have a systemic inflammatory processes which can also affect β-cell function (52). Furthermore, chronic GC use may induce β-cell failure indirectly by lipotoxicity, by accumulation of pancreatic fatty acids, secondary to elevated plasma triglyceride and free fatty acids levels (53). The pathophysiology of this process is unclear but potential mechanisms include increase in α2-adrenergic receptor expression (54), and upregulation of kinases which regulate the activity of ion channels essential for insulin secretion from pancreatic β-cells (55).

1.2.2 Bone effects of glucocorticoids

GCs are known to induce osteoporosis as well as increase fracture risk (56, 57), which presents within of 3-6 months of treatment initiation and is dose-related. This is likely due to the higher GC doses administered and disease activity at the beginning of treatment. Fracture risk remains raised throughout the duration of treatment, but decreases after it discontinues (58-61).

Van Staa et al. (2002), showed that the risk of vertebral fracture in people taking oral GCs was increased almost three-fold (relative rate (RR) 2.86, 95% CI 2.56-3.16) whilst the risk of hip fracture was doubled (RR 2.01, 95% CI 1.74-2.29) (61). Amiche

et al. (2016), reported that the average incidence of fracture for those who were initiated on GC therapy in the last 6 months was 5.1% (95% CI 2.8-8.2%) for vertebral fracture and 2.5% (95% CI 1.2-4.2%) for non-vertebral fracture, while the risks in chronic users (>6 months use) were 3.2% (95% CI 1.8-5.0%) and 3.0% (95% CI 0.8-5.9%), respectively (62). Balasubramanian et al. (2016) found that the average fracture incidence rates were 9.0 (95% CI 5.7-13.7) per 1,000 person-years at a current daily (prednisolone equivalent) dose <5mg per day and increased to 16.0 (95% CI 11.0-22.6) at ≥5mg per day (63). For cumulative doses, average fracture incidence rates were 4.6 (95% CI 3.8-5.4) per 1,000 person-years at cumulative doses <0.675g and rose up to 13.4 (95% CI 10.7-16.7) at cumulative doses ≥5.4g (63).

The effect of GC therapy on biochemical bone makers have been reported in both healthy people and patients. Lems et al. (1998) showed that in healthy male volunteers, prednisolone treatment decreased bone formation markers (serum osteocalcin levels, procollagen type 1 N-terminal pro-peptide (P1NP) and alkaline phosphatase (ALP)) (***Table 1*-1**). Additionally, bone resorption markers (urinary excretion of pyridinolines, hydroxyproline and serum carboxy-terminal cross-linked telopeptide of type 1 collagen (CTX)) remained unchanged or were slightly reduced (64). Kauh et al. (2012) also reported that serum and urinary osteocalcin levels, and P1NP were significantly decreased by glucocorticoid administration in healthy adults (***Table 1*-1**) . They also reported significant increase in another marker of bone resorption, serum N-telopeptide of type I collagen (NTX), but only at higher prednisone doses (65). Two studies found that in patients with collagen, haematological and neuroimmune diseases, glucocorticoid therapy caused decrease in serum osteocalcin levels and increase in urinary NTX levels (66, 67).

1.2.3 Other effects of glucocorticoids

Both topical and systemic administration of GCs can cause significant cutaneous side-effects. Potency and duration of treatment are particularly critical in determining the incidence and severity of these effects. GCs can cause epidermis and dermis atrophy which can result in striae rubrae distensae and poor wound healing. This is caused by suppression of cutaneous cell proliferation and protein synthesis and reduction in the proliferative activity of keratinocytes and dermal fibroblasts (68) (***Table 1*-1**). GCs can also cause hypetrichosis which can be particularly problematic in women.

GCs can induce steroid myopathy, particularly in the proximal muscles, through catabolic effects. GCs inhibit glucose uptake which may contribute to the breakdown of muscle proteins (***Table 1*-1**) . They also inhibit protein synthesis and stimulate protein degradation (69).

The eyes are also affected by GC treatment, as they can cause the development of cataract and glaucoma. In more rare instances, they can also cause retinal emboli and maculopathy. Cataract occurs via a number of pathways including: increased glucose levels, inhibition of Na^+/K^+-ATPase, increased cation permeability, inhibition of G6PD, inhibition of RNA synthesis, loss of ATP, and covalent binding of steroids to lens proteins (70) (***Table 1*-1**). GC-induced ocular hypertension occurs mainly via morphological and functional changes in the trabecular meshwork (***Table 1*-1**). These occur due to increased accumulation of polymerized glycosaminoglycans (71). Additionally, there is an increased production of fibronectin and collagen type IV that contribute to the extracellular matrix (ECM) excess (72).

GCs are known to cause "steroid psychoses" in people without any pre-existing mental health illnesses but can also aggravate pre-existing psychiatric conditions (***Table 1*-1**).. Hall et al. (1979), Carpenter & Gruen (1982) and Sapolsky et al. (1990) showed that GCs can impair the hippocampal function by direct exposure (73-75). Animal studies have shown that direct GC exposure can lead to decreased dendritic branching (76), change in synaptic terminal structure (77), decreased neurons (78), and inhibition of neuronal regeneration (79). GCs can also cause a range of CNS effects that ranges from interference in cellular metabolism (80) to an increase in the susceptibility of hippocampal neurons (81) and an augmented accumulation of extracellular glutamate (82) (***Table 1*-1**). Additionally, GCs can cause inhibition of the 5-HT1A receptor expression (83) which may be involved in the pathophysiology of depression. This is brought about by GC inhibition of the NF-kB elements in the promoter of the 5-HT1A receptor gene (84).

Exogenous GCs induced hypertension by a variety of mechanisms which include increased systemic vascular resistance, increased extracellular volume, and increased cardiac contractility. Excess GCs act on the MR at the renal tubule as 11β-HSD2 enzyme, which normally deactivates active GCs, is oversaturated (85) (***Table 1*-1**).. It occurs more commonly in patients on high GC doses and in elderly patients with a family history of essential hypertension (86, 87).

Adverse effects of GCs on the gastrointestinal system include peptic ulcers, upper gastrointestinal bleeding, pancreatitis (88), and oral candidiasis (89) (***Table 1*-1**). The pathophysiology of these effects is not completely understood but animal studies have

shown that GCs can increase gastric acid secretion, reduce gastric mucus, cause gastrin and parietal cell hyperplasia, and delay the healing of ulcers (90).

1.3 Cushing's syndrome

Cushing's syndrome is characterized by a collection of signs and symptoms which are caused by chronic exposure to excess in circulating levels of GCs. The aetiology of Cushing's is divided into two categories: ACTH-dependent and ACTH-independent. ACTH-dependent forms are defined by excessive ACTH production which in turn stimulates the adrenal cortex to produce excess GCs. ACTH-independent forms comprise of adrenal or exogenous GCs excess. The clinical features of Cushing's syndrome include a wide range of signs and symptoms as described below.

Cushing's syndrome consists of a variety of metabolic conditions such as weight excess, seen in 57-100% of patients, hypertension in 25-93% of patients, impaired glucose tolerance is described in 7-64% of patients, type 2 diabetes mellitus (T2DM) in 11-47% of patients and dyslipidaemia in 12-72% (91). There is also an increased risk for myocardial infarction (hazard ratio 2.1, 95% CI 0.5-8.6) and heart failure (6.0, 95% CI 2.1-17.1). Cushing's syndrome also affects bone structure. Osteopaenia develops in 40-78% of patients, osteoporosis in 22-57% and skeletal fractures in 11-76% (91). There is also a significant increase (more than ten-fold) risk of venous thromboembolism (91). Reproductive and sexual dysfunction is also common in Cushing's syndrome. There is decreased libido in 24-90% of patients, hypogonadism in 50-75% of men and menstrual irregularities in 43-80% of women (91). Cushing's syndrome is also associated with psychiatric diseases such as major depression (50-

81%), anxiety (66%), and bipolar disorders (30%) (91). It also causes impairment of immune function which subsequently increase the risk of severe infections and sepsis.

All the clinical features and disorders caused by Cushing's syndrome, as described above, can be induced by both endogenous and exogenous excess of GCs. Exogenous GC excess is the most frequent cause of hypercortisolism and is termed Iatrogenic Cushing's. Despite significant advances in medicine, GCs remain one of the most common medications used in inflammatory conditions, due to their potent anti-inflammatory and immunosuppressive action, with GC therapy prevalence ranging from 0.5 to 21.1% (for both short and long-term courses) (92-95). However, the biggest caveat of this treatment is its adverse metabolic effects which limits its use.

Nevertheless, high circulating levels of glucocorticoids does not always equal to clinical characteristics of Cushing's syndrome. Two cases have been described in the literature where partial defect of 11β-HSD1 activity prevented the development of Cushing's phenotype. The first was a patient who was found to have a corticotroph pituitary adenoma (96) and the second in a patient with an adrenocortical adenoma (97). This indicates that 11β-HSD1 activity plays a role in the development of the adverse metabolic effects of GCs.

The importance of 11β-HSD1 action on the effects of GCs has also been reported in animal models. Fenton et al. (2020) studied the effect of corticosterone on mouse models of polyarthritis with global, myeloid and mesenchymal deletion of 11β-HSD1 (98). They reported that global deletion of 11β-HSD1 caused profound resistance to the anti-inflammatory action of corticosterone. Myeloid 11β-HSD1 deletion resulted

in partial resistance, but mesenchymal 11β-HSD1 deletion did not prevent corticosterone therapy to suppress the inflammatory processes. These findings suggest that 11β-HSD1 is required for peripheral reactivation and amplification of GCs at sites of inflammation to deliver their anti-inflammatory therapeutic effects (98).

1.4 11-beta hydroxysteroid dehydrogenase type 1 (11β-HSD1)

11β-HSD1 is a bidirectional enzyme which acts as an oxoreductase converting cortisone to cortisol or as a dehydrogenase converting cortisol to cortisone. However, in vivo it acts mainly as an oxoreductase (99). Within the cell it is located in the endoplasmic reticulum (ER) membrane and its catalytic domain is placed in the ER lumen (100). Its oxoreductase activity is achieved via the activity of a tightly associated enzyme, hexose-6-phosphate dehydrogenase (H6PDH) which is also located in the ER lumen and facilitates the maintenance of the high intra-lumen NADPH/$NADP^+$ ratio which confers the directionality of 11β-HSD1 (101). In the absence of H6PDH, 11β-HSD1 acts as dehydrogenase and oxidizes cortisol to cortisone. In humans, 11β-HSD1 is coded by the gene HSD11B1 found on chromosome 1q32.2, is made up of 292 amino acids and it is 30 kb in length (102).

11β-HSD1 is mainly expressed in the liver, adipose, gonads, skeletal muscle and brain but can also be found in the cardiovascular system, immune system, bone, eyes, gastrointestinal tract, kidneys, pancreas, skin and placenta (99). There are many factors that regulate its expression. GCs, pro-inflammatory cytokines, PPARγ agonists and CCAAT/Enhancer binding protein increase expression and activity. Conversely, growth hormone and liver X receptor agonists decrease its expression

(99). Oestradiol reduces 11β-HSD1 expression in rat liver and kidney but testosterone has no effect (103).

1.4.1 Genetic defects

Cortisone reductase deficiencies

There are two clinical phenotypes of cortisone reductase deficiency (CRD). The first one is caused by loss of function mutations in the HSD11B1 gene and is termed as "true" CRD and the second caused by mutations in the H6PD gene, is termed "apparent" CRD (ACRD). ACRD is the more severe form of the condition as the loss of H6PDH activity instigates a decrease of the intra-lumen NADPH/$NADP^+$ ratio thus favouring the dehydrogenase activity of 11β-HSD1 where cortisol is inactivated to cortisone (104). The cortisol inactivation seen in ACRD induces a compensatory HPA axis activation and ACTH-mediated adrenal GC and androgen secretion. Clinically this condition presents as polycystic ovary syndrome (PCOS) in adult females or as premature adrenarche in children. The urinary steroid profiles show extremely high cortisone metabolites and low cortisol metabolites demonstrating impairment in the activity of 11β-HSD1. True CRD is a milder form of the condition; two cases have been reported where two male children presented with premature adrenarche. The urinary steroid profile was not as abnormal as seen in cases of ACRD, with THF+allo-THF/THE ratios of 0.26 and 0.16 (105). However, similarly to the ACRD there was secondary HPA axis activation and increased androgen secretion causing this phenotype. Lavery et al. (2013) reported that gas chromatography/ mass spectrometry (GC/MS) urinary steroid profile can be used to distinguish between cases of CRD and ACRD (106).

HSD11B1 polymorphisms

Several studies have been conducted to investigate possible links between single nucleotide polymorphisms T2DM and cardiovascular disease have been investigated but there is currently conflicting data on the association between HSD11B1 SNPs and these diseases (107).

H6PD polymorphisms

H6PD genetic variations have been examined as they are expected to have more significant clinical effects due to the importance of H6PDH in modulating 11β-HSD1 activity. Multiple sclerosis, carotid intima-medial thickness and atherosclerosis are conditions that have been linked to genetic variations of H6PD (108-110). Additionally, PCOS has been associated with the rs668832 H6PD SNP as reported by two small case-control studies (111, 112).

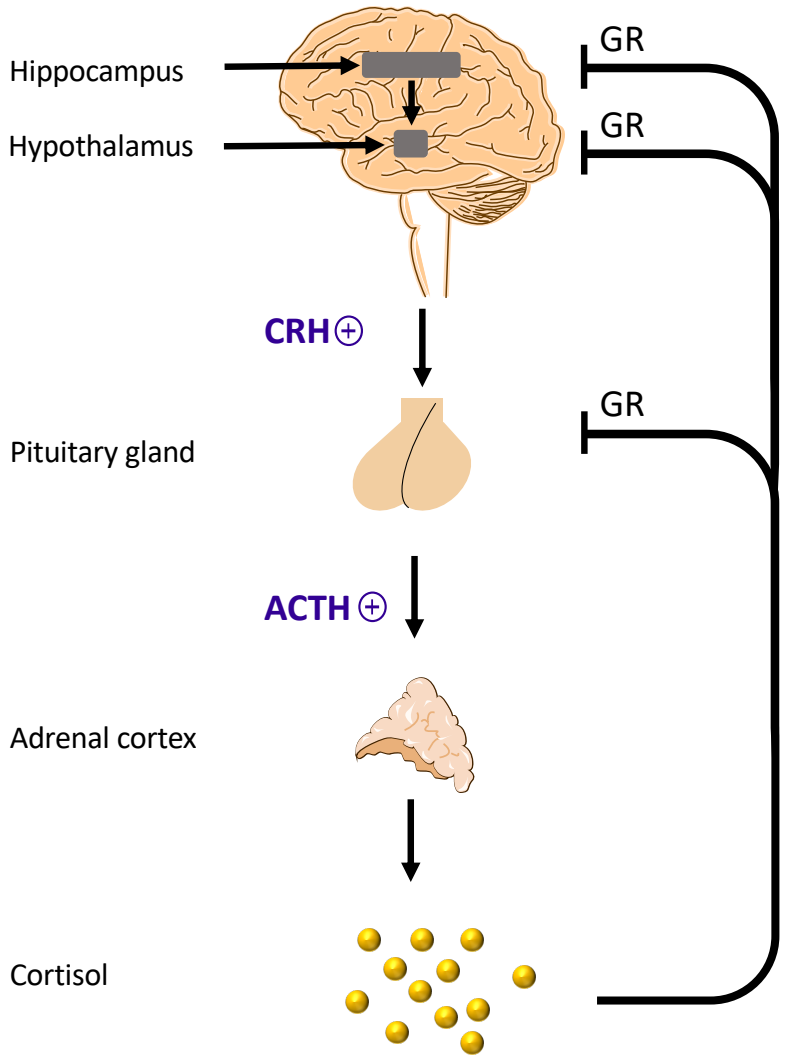

Figure 1.4-1 *Hypothalamic-Pituitary-Adrenal axis. CRH stimulates the anterior pituitary gland to release ACTH, which in turn stimulates cortisol production by the adrenal glands. Cortisol exerts negative feedback on the pituitary gland, hypothalamus and hippocampus via the GR to control the synthesis of this hormone. CRH=Corticotropin-releasing hormone. ACTH=Adrenocorticotropic hormone. GR=Glucocorticoid receptor.*

1.4.2 Adipose tissue

As mentioned earlier, 11β-HSD1 is highly expressed in both white and brown adipose tissue and acts predominantly as an oxoreductase. H6PDH and GRα receptors are found in higher amounts in omental adipose tissue compared to subcutaneous (SC) and therefore the oxoreductase action is more pronounced in this tissue, even though

expression of 11β-HSD1 is similar in both omental and SC adipose tissue in humans (113). In mice, on the other hand, 11β-HSD1 is expressed in higher levels in SC tissue (114). GCs play an important role in promoting adipocyte differentiation and 11β-HSD1 is involved in both induction of adipogenesis and maturation of adipocytes (115).

It is proposed that 11β-HSD1 activity is dysregulated in obesity (116), with stable circulating GC levels (117). In fact, there is a two to three-fold increase of 11β-HSD1 activity in SC adipose tissue in simple obesity and a decrease in hepatic 11β-HSD1 activity. However, in obese individuals with T2DM, the hepatic 11β-HSD1 activity does not decrease (116). There are fewer consensuses on the effect of obesity on visceral 11β-HSD1 activity partly due to the low number of studies performed and the fact that the tissue obtained is usually from patients who have undergone a surgical procedure. Woods et al. (2015) reported a positive correlation between visceral adipose tissue 11β-HSD1 gene expression and body mass index (BMI) but not in SC adipose tissue. They did however report that there was a reduction in 11β-HSD1 gene expression in SC adipose tissue following weight loss. On the other hand, 11β-HSD1 gene expression in hepatocytes was negatively correlated with BMI which is consistent with previous evidence (118). These findings are in accordance to the reports by Mlinar et al. (2011) (119) and Michailidou et al. (2007) (120) who reported that visceral adipose tissue 11β-HSD1 gene expression correlates with adiposity and adipocyte size. However, in contrast, Goedecke et al. (2006) reported that 11β-HSD1 gene expression in omental adipose tissue did not correlate with obesity (121).

11β-HSD1 activity in adipose tissue has been investigated in rodent models where it has been both deleted and overexpressed. Masuzaki et al. (2001) (122) overexpressed 11β-HSD1 in adipose tissue in mice using the aP2 promoter. They found that the mice developed visceral obesity but no changes in circulating GC levels. They did however report an increase in corticosterone in the portal vein. These mice developed similar features to the metabolic syndrome including insulin resistance, dyslipidaemia and hypertension. Therefore, it is possible that 11β-HSD1 plays a role in the development of metabolic syndrome in obese individuals. Additionally, Morton et al. (2004) studied the 11β-HSD1 KO mouse model and reported that these mice have lower visceral adipocyte accumulation on high fat diet (HFD) and resisted developing insulin resistance and diabetes, rendering them metabolically "healthier" (123).

Several factors appear to play a role in the regulation of 11β-HSD1 in adipose tissue in rodents. These include GCs, pro-inflammatory cytokines and stearate feeding in upregulation and PPAR and HFD in downregulation (116). It is still not clear how 11β-HSD1 is regulated in human adipose tissue.

1.4.3 Liver

11β-HSD1 is highly expressed in the liver and in humans it is mainly located centripetally and found in high levels around the central vein (124), and it acts entirely as an oxoreductase (125, 126). In simple obesity, the 11β-HSD1 activity in the liver is lower, however in patients who also have T2DM, activity is unchanged (127). This is in accordance to the findings reported by Torrecilla et al. (2012) who reported that there was higher expression of GR, 11β-HSD1, H6PDH and PEPCK in hepatocytes of obese patients with metabolic disease compared to obese patients (128). However,

more recently, Shukla et al. (2019) showed that 11β-HSD1 activity was increased in patients with T2DM, particularly in lean individuals (129). These findings are comparable to the db/db diabetes murine model, where 11β-HSD1 and GR expression are both increased (130). Dube et al. (2015) reported the results of a clinical trial where they showed that GCs increase the intrahepatic conversion of cortisone to cortisol via the 11β-HSD1 pathway (131). This could be the mechanism by which GCs induce or exacerbate hepatic insulin resistance (131).

Hepatic 11β-HSD1 activity has been explored by developing mouse models with both overexpressing and deleting 11β-HSD1. Overexpression of 11β-HSD1 in liver was achieved by using the apolipoprotein E promoter. These mice developed hypertension, dyslipidaemia and hypertriglyceridaemia which lead to hepatic steatosis but did not progress to steatohepatitis (132). They also became insulin resistant but were not obese. In mice with hepatic 11β-HSD1 deletion, they develop a mild metabolic phenotype but there is no significant change in insulin sensitivity, hepatic or serum lipids. There was however, an increase in adrenal size, despite circulating corticosterone levels being stable, signifying an increase in HPA axis activation (133). In 11β-HSD1 KO mice, 11β-HSD1 deficiency has little effect on liver function in the fed state but in the fasted state there is no rise in PPARα which is consistent with reduced GC action. On refeeding these mice, there is an exaggerated generation of lipogenic enzymes and reduction of fat catabolism enzymes. Therefore, 11β-HSD1 deficiency causes a more favourable lipid profile and improved liver insulin sensitivity (134). Morgan et al. (2014) studied the metabolic effects of corticosterone in 11β-HSD1 KO mice. The circulating levels of corticosterone were similar in both 11β-HSD1 KO mice and wild-type but there was a significant

reduction in serum free fatty acids, fatty acid translocase and hepatic triglycerides (TAG) in the KO mice. Additionally, features of hepatic steatosis were also noted in the wild-type mice, whereas the KO mice appear to be protected (135).

1.4.4 Muscle

11β-HSD1 is present in skeletal muscle but at lower levels compared to the liver (136). In human muscle, it has been demonstrated that it acts as an oxoreductase and its role in metabolic disease has been controversial. Whorwood et al. (2001) (136) reported that 11β-HSD1 levels did not correlate with adiposity in human muscle ex vivo but Abdallah et al. (2005) (137) reported that there was an increased expression in myotubes from obese patients with T2DM. Similar findings were also shown in obese rodents with diabetes where there were increased levels of 11β-HSD1 mRNA and protein (138). 11β-HSD1 inhibition in the hyperglycaemic KK/Ta jcl mouse induced an increase in skeletal muscle insulin receptor substrate 1 and a decrease in expression of genes involved in lipid metabolism (107).

It has also been suggested that 11β-HSD1 may be involved in age-related sarcopaenia as it was discovered that 11β-HSD1 is upregulated with age in women and also associated with reduced grip strength, insulin resistance and an adverse composition profile (139).

1.4.5 Pancreas

11β-HSD1 mRNA has been identified in rodent and human pancreatic islets but there has been controversy regarding its exact location with reports proposing it is found in α-cells (140) and β-cells (141).

The relationship between pancreatic 11β-HSD1 activity and metabolic disease has been investigated using several rodent models and has been suggested that increased 11β-HSD1 levels are associated with β-cell failure (141). However, the relationship between 11β-HSD1 expression and metabolic disease is not very clear. In a diabetes-prone rodent model, where 11β-HSD1 is overexpressed in the pancreas, there is enhanced glucose-stimulated insulin secretion (142). On the other hand, increase in 11β-HSD1 expression in the pancreatic islets of obese ob/ob mice (143) and Zucker diabetic fatty fa/fa rats (144), correlates to increasing hyperglycaemia. This increase is reversed by troglitazone which inhibits hyperglycaemia and hyperlipidaemia. It is possible that there is an inverted U-shaped relationship between 11β-HSD1 expression and glucose stimulated insulin secretion, similar to what is observed with GC dose and β-cell function. In mouse strains that are susceptible to β-cell failure, HFD causes a decrease in 11β-HSD1 expression whereas in mice that are not prone to metabolic disease there is some increase in 11β-HSD1 expression. In normal mice, HFD causes a compensatory insulin secretion via upregulation of 11β-HSD1, whereas in severe obesity, very high islet 11β-HSD1 levels and therefore GC regeneration, contributes to β-cell failure (116).

In the global 11β-HSD1 KO mouse, there is impairment in the β-cell function. However, when these mice are fed HFD, there was improved glucose tolerance (142).

1.4.6 Cardiovascular

11β-HSD1 is mainly found in the vascular smooth muscle and is involved in angiogenesis and vascular remodelling (145). As, GCs inhibit angiogenesis, mice deficient in 11β-HSD1 exhibit increased angiogenesis particularly in cases of

myocardial injury (146). 11β-HSD1 KO mice show increased vascularization following myocardial infarction which indicates the potential use of 11β-HSD1 selective inhibitors. However, pathological neovascularisation such as diabetic retinopathy has not been thoroughly investigated yet (146).

1.4.7 Nervous system

11β-HSD1 can be found in the adult brain with highest expression in the hippocampus, cortex, cerebellum and anterior pituitary. 11β-HSD1 mainly acts as an oxoreductase but H6PDH is not frequently found with 11β-HSD1 in the brain (147). 11β-HSD1 is thought to be involved in cognition as the use of 11β-HSD inhibitors in elderly mice (148) and humans (149) improves cognitive function. It is also involved in the regulation of aqueous humour production in the ocular ciliary epithelium (150).

1.4.8 Inflammation and immunity

11β-HSD1 is detected in neutrophils where there is increased expression during inflammation and lacking during apoptosis (151). It is also present in mouse CD4 and CD8 positive lymphocytes, B cells and dendritic cells (152). 11β-HSD1 KO mice show defects in anti-inflammatory response and in particular in models of joint inflammation, peritonitis and lung inflammation there was a greater inflammatory reaction with a slower recovery suggesting a possible drawback in the use of selective 11β-HSD1 inhibitors in these conditions (153). In humans, 11β-HSD1 activity has been found to be augmented in rheumatoid arthritis (154) and increased expression in inflammatory bowel disease (155). Specifically, there is higher expression during acute exacerbation compared to remission suggesting that 11β-HSD1 has an active role in acute inflammation (155).

1.4.9 Bone and joint

11β-HSD1 is mainly expressed in osteoblasts and its activity is induced by pro-inflammatory cytokines and GCs. 11β-HSD1 KO mice do not exhibit any changes in bone mass, formation or resorption. Cooper et al. (2003) reported that urinary cortisol to cortisone metabolites, following a 7-day course of prednisolone in healthy male volunteers, correlate to bone formation markers. Therefore, this has the potential to be utilized in clinical practice, where 11β-HSD1 could predict an individual's susceptibility to GC-induced osteoporosis (156).

1.4.10 Skin and salivary glands

11β-HSD1 is expressed in human and mouse skin (157-159), specifically in the epidermis and dermis (160) with higher numbers in keratinocytes and it acts as a reductase (159).

1.4.11 11β-HSD1 inhibitors

The 11β-HSD1 enzyme is a promising therapeutic target as its inhibition can potentially improve the pathological features of metabolic disease and age-associated cognitive impairment.

There are several natural products that inhibit the 11β-HSD1 enzyme, however, their clinical use is limited due to their poor bioavailability, rapid metabolism and 11β-HSD2 inhibition. Glycyrrhizin acid is a non-selective 11β-HSD inhibitor which was discovered from the Glycyrrhiza glabra (liquorice) root (161). Carbenoxolone is another non-selective 11β-HSD1 inhibitor which was derived from 18α-glycyrrhetinic acid, a metabolite of glycyrrhizin acid (162). It inhibits 11β-HSD1 in the liver but not in the adipose tissue or skeletal muscle, which improved plasma lipid

metabolism with no change on body weight, food intake, glucose tolerance, and insulin sensitivity in obese insulin-resistant Zucker rats (163). Curcumin is a selective 11β-HSD1 inhibitor which is effective in protecting against morbid obesity, maintaining serum glucose, and lipid profiles in the HFD-induced obese rats (164). However, due to poor bioavailability and rapid metabolism it was modified to a new curcumin analogue, compound, LG13. This compound was more efficacious as an 11β-HSD1 inhibitor and as a result was found to decrease fasting blood glucose, lipid deposition, and hepatic glucose metabolism in the type 2 diabetic mice (165). Epigallocatechine-3-gallate is an aqueous extract of green tea and can inhibit 11β-HSD1, as well as affect drug metabolism by downregulating enzymes such as CYP1A1, CYP1A2, CYP2B1/2, CYP2E1, CYP3A (166). Resveratrol is an endogenous steroid hormone, 17β-oestradiol, which inhibits the 11β-HSD1 murine adipose activity (167). Citrinal B, another natural 11β-HSD1 inhibitor, is a tricyclic compound which is extracted from Colletotrichum capsica (168). In vitro studies showed that it inhibits cortisone-cortisol cycles in hepatocytes and forms fat droplets in pre-adipocytes.

Various synthetic 11β-HSD1 inhibitors have been developed for potential clinical use in conditions such as T2DM and hypercholesterolaemia. However, clinical studies showed that they have low therapeutic potency and there were also some safety concerns.

In particular, Biovitrum compound BVT2733 has shown reduction in fasting blood glucose, insulin and cholesterol levels in hyperglycaemic rodent models (169-171). However, BVT2733 weakly inhibited human 11β-HSD1 and thus clinical trials were

not performed. Compound A, showed tissue specific effects in that there was reduction in mesenteric fat mass and hepatic steatosis (172, 173). KR-67183 improved insulin sensitivity and glucose tolerance in the HFD-induced mice and also enhanced osteoblastogenesis in osteoblasts and inhibited osteoclastogenesis in osteoclasts (174). It also showed no effect on HPA axis activation. In vivo data following treatment with KR-67105 showed improvement in insulin sensitivity and glucose tolerance in diabetic mice, and also suppression of diabetes-related genes, such as G6Pase and phosphoenolpyruvate carboxykinase in the liver and tumour necrosis factor-α and PPARγ in SC adipose tissue. Additionally, KR-67105 inhibited cortisone-induced inflammation (175). SKI-2852 was tested on mice and results showed that it can inhibit hepatic gluconeogenesis and partially improve lipid profiles, as well as improve many aspects of metabolic parameters in metabolic disorders. This drug has not been trialled in humans yet (176, 177). PF-877423 also indicates clinical potential as a preclinical study showed it could prevent human lipogenesis in vitro (115).

UI-1499 improved insulin sensitivity and glucose tolerance in ex vivo studies. The anti-obesity effect and improvement of lipid profiles were also reported in both diabetic mice and monkeys (178). BI-135585 is another 11β-HSD1 inhibitor which has been assessed ex vivo, in human pre-adipocytes, adipocytes and liver tissue of cynomolgus monkey (179). The outcome suggested adequate 11β-HSD1 inhibition and entered Phase I clinical studies. However, the clinical data indicated that there was inadequate 11β-HSD1 inhibition in the adipose tissues following 2 weeks of treatment (180). HSD-621 was tested in diet-induced obesity mice, which demonstrated a modest effect in symptoms of the metabolic syndrome (181).

Compound 531, indicated improvement in insulin sensitivity and reduced hepatic glucose production when tested in dogs (182).

In humans, INCB013739 was investigated in patients with T2DM and after two weeks of administration there was decrease in fasting blood glucose, particularly in patients with higher hyperglycaemia and there was also reduction in low-density cholesterol but no change in high-density cholesterol (183, 184). Clinical data suggested that a 12-week treatment with MK-0736 and MK-0916 did not lower blood glucose significantly in healthy subjects but had modest dose-dependent decreases in blood pressure, low-density lipoprotein (LDL) level and body weight in overweight and obese non-diabetic patients with hypertension (185). MK0916 was also trialled in patients with T2DM and the results showed a reduction in the weight and waist-hip ratio and an HbA_{1c} reduction of 0.3% in the 6mg group. However, there was no alteration in fasting plasma glucose, post-prandial glucose or insulin levels. There was also increase in LDL and non-high-density lipoprotein cholesterol (185). With both agents, there was an activation of the HPA axis and in the case of INCB013739 there was significant increase in total testosterone in women but this side-effect was not evident in MK0916.

AZD4017, the 11β-HSD1 inhibitor used in our clinical trial which is presented in **Chapter 4**, was originally developed as a potential treatment for T2DM, obesity, and metabolic syndrome (186). AZD4017 was tested in rats and cynomolgus monkey. It is an effective inhibitor in humans and non-human primates but not in other animal models (186). In terms of safety, reversible liver hypertrophy was observed in rats, which was adaptive rather than degenerative. There were no safety issues in the

cynomolgus monkey. AZD4017 underwent five phase I and II human clinical trials assessing the drug in healthy males, obesity, T2DM, and raised intraocular pressure (186). The efficacy in these trials were modest and with regards to adverse effects elevated transaminases were noted, without concomitant rise in bilirubin, in a few subjects treated in the multiple-ascending dose study (186). The findings were reversible on drug discontinuation, and no subjects were clinically symptomatic.

1.5 5-alpha reductase

5α-reductases are key enzymes in the metabolism of testosterone, cortisol and progesterone, as they all contain a 3-oxo-Δ4,5, structure in the steroid A-ring (187). They were initially described in the 1950s in rat liver cells. There are three isoforms of 5α-reductase enzymes: 5α-reductase type 1 (5αR1), 5α-reductase type 2 (5αR2) and 5α-reductase type 3 (5αR3). The first two types are described in more detail in the following sections (187, 188). 5αR3 was identified in hormone-refractory prostate cancer (HRPC) cells (189). It converts testosterone to 5α-dihydrotestosterone in HRPC cells (188). It is mainly found in prostatic cancer cells with little or no expression in normal tissue.

Tomkins et al. (1962) discovered that the 5α-reductase enzyme utilized reduced pyridine nucleotide as a cofactor and could metabolise a number of steroid substrates (190). The 5α-reductase (5αR) isoenzymes are hydrophobic proteins which explains their intrinsic membrane localization (190, 191). They 5α-reduce testosterone to 5α-dihydrotestosterone, cortisol to 5α-dihydrocortisol and progesterone to 5α-dihydroprogesterone. This metabolism makes the 5α-reduced steroid susceptible to further reduction by 3α-and 3β-hydroxysteroid dehydrogenase and to sulfation and

glucuronylation (187). In the case of 5α-dihydrocortisol, it is metabolised further to tetrahydrocortisol. Therefore, 5α-reductases increase androgen but reduce GC availability making it an important regulator enzyme in the activity of steroid hormones. The aforementioned steroid substrates have a much lower affinity to 5αR1 than to the 5αR2 isoform but the conversion yields are much higher in the 5αR1 (187).

1.5.1 5α-reductase Type 1

5α-reductase type 1 (5αR1) is expressed by gene SRD5A1 which is located on 5p15.31, in the human genome. The enzyme consists of 259 amino acids and has a molecular weight of 29 kDa. In humans, it is highly expressed in the liver, non-genital skin, muscle, adipose tissue and brain but poorly expressed in androgen target tissues (191). In rats, it is widely expressed in different tissues but at highest levels in the liver (191). Testosterone is the most recognized substrate for this isoform, even though progesterone has the highest affinity, and it is thought to be accountable for about a third of circulating dihydrotestosterone (192-194). There are no known mutations of SRD5A1.

1.5.2 5α-reductase Type 2

5α-reductase type 2 (5αR2) is expressed by gene SRD5A2 which is located on 2p23.1, in the human genome. The enzyme consists of 254 amino acids and has a molecular weight of 28 kDa (187). It is mainly expressed in the male reproductive tissues such as prostate, epididymis and seminal vesicles in both humans and rats (187).

A number of mutations and polymorphisms of SRD5A2 have been identified, some of which cause the clinical phenotype of 46XY Disorder of Sex Development (195).

This condition is also called 5α-reductase deficiency and affected males lack virilisation and have poor development of external genitalia due to reduction in the production of the potent androgen dihydrotestosterone. Conversely, increased dihydrotestosterone production via 5αR2 has been associated with disorders such as PCOS, breast and prostate cancer (196, 197).

1.5.3 5α-reductase tissue distribution and function

Both 5αR1 and 5αR2 are expressed in human liver whereas in rodents only 5αR1 is expressed. Therefore, 5αR1 function in the liver has been investigated using rodent models. 5αR1 KO male mice caused higher incidence of hepatosteatosis and consequently higher risk of liver fibrosis and scarring (198, 199). 5αR activity has been shown to be correlated with worsening metabolic phenotype as well as with PCOS (200-205).

5αR1 is expressed in adipose tissue in both humans and rodents. There is evidence to suggest it has a role in metabolism but its exact function is currently unknown (206, 207). 5αR1 is also expressed in skeletal muscle and dutasteride use causes decrease in glucose disposal in the muscle but its exact function is not described (208). It can also be found in vascular endothelium and smooth muscle and inhibition of 5αR causes endothelial damage and dysfunction but it is not currently known if it is involved in cortisol clearance (209). In the kidney, similarly to the aforementioned tissues 5αR1 is expressed however, 5αR2 is absent (210). There is currently no data reporting on the activity of 5αR1 with regards to steroid metabolism.

1.5.4 5α-reductase inhibitors

5α-reductase inhibitors (5αRI) are traditionally used for their anti-androgen effects and they are commonly prescribed in conditions such as benign prostate hyperplasia, prostate cancer, androgenic alopecia and acne. Several clinical and pre-clinical studies have been conducted to deduce the effect of 5α-reductase inhibition or deficiency in GC action.

Mak et al. (2019) administered a liver-selective GR antagonist in 5αR1 KO mice and their control, during consumption of HFD (211). They found that hepatic GR antagonism improved diet-induced insulin resistance, but liver steatosis was unaffected, in both 5αR1 KO mice and the controls. They also administered a 12-week course of dutasteride or vehicle in mice and reported that dutasteride reduced the excess weight gain and normalized the associated hyperinsulinaemia after glucose challenge (211). In vitro experiments have been conducted which showed that SRD5A2 overexpression in human hepatocytes reduced the effects of cortisol treatment to suppress lipogenesis. Conversely, treatment with 5αRIs, finasteride and dutasteride, augmented the cortisol action (212). Similarly to the pre-clinical experiments, clinical studies have been undertaken in order to investigate their potential implication in steroid metabolism and indeed metabolic phenotype.

As mentioned previously, cross-sectional and longitudinal studies have shown that 5α-reductase activity is higher in the presence of high BMI and insulin resistance (201-203). Hazlehurst et al. (2016) performed a randomised clinical trial on 12 healthy male volunteers where they were randomised to either take a three-week course of dutasteride (5αR1 and 5αR2 inhibitor) or finasteride (5αR2 selective

inhibitor). They reported that dual 5α-reductase inhibition using dutasteride was associated with increased hepatic lipid accumulation (213). Similar results have also been published by Upreti et al. (2014) where they randomised 46 men who took finasteride or dutasteride or placebo for 3 months and concluded that only dual 5α-reductase inhibition increases insulin resistance implying that dutasteride has an adverse impact on the metabolic phenotype (208). More recently, Wei et al. (2019) looked at the incidence of T2DM in a large cohort of men taking 5α-reductase inhibitors in Taiwan (214). They found that the risk of developing T2DM was higher in men with BPH taking a 5αRI (either finasteride or dutasteride) compared to those taking tamsulosin. There was no difference in T2DM incidence between the two 5αRIs (214).

1.6 Aims and Objectives

In summary, GCs are commonly prescribed medications for their anti-inflammatory action. The adverse metabolic effects they induce can cause significant clinical complications to patients such as development of hypertension, insulin resistance and muscular atrophy. Pre-receptor metabolism is considered to be critical in the regulations of active endogenous GCs. The work undertaken in this doctoral thesis aims to test the hypothesis that altering pre-receptor metabolism will have an impact upon GC metabolism that in turn has the potential to limit or enhance the adverse effects of prescribed GCs.

Specifically, my objectives are:

To demonstrate the adverse metabolic effects associated with prednisolone administration (**Chapters 3 & 4**).

To determine if 5αR inhibition worsens the adverse effects associated with prednisolone administration putatively through increased prednisolone availability (**Chapter 3**).

To explore the potentially beneficial impact of selective 11β-HSD1 inhibition to limit prednisolone regeneration and improve metabolic phenotype in healthy male volunteers (**Chapter 4**).

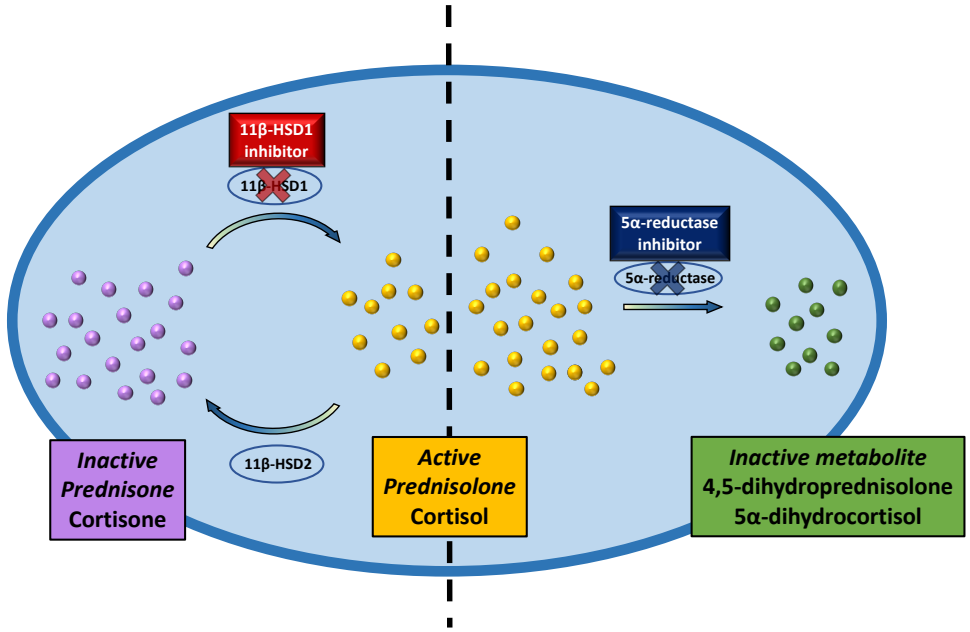

Figure 1.6-1 *Schematic representation of the action of 11β-HSD1 inhibitors and 5αR inhibitors.*

2 General Methods

The following methods were used in both clinical studies described in **Chapters 3 and 4** unless otherwise stated.

2.1 Two-step hyperinsulinaemic euglycaemic clamp

2.1.1 Principle

The hyperinsulinaemic euglycaemic clamp technique is commonly used to quantify insulin sensitivity. This method was utilised in the two clinical studies that are described in **Chapters 3 and 4**. The duration of the clamp was 6 hours and consisted of three phases lasting two hours each, which are described next.

In the first two hours of the clamp, no insulin was infused. This is considered the basal phase and allows for assessment and calculation of basal hepatic glucose production (HGP) in the fasting condition. In this case, we assume that hepatic glucose production is equal to endogenous glucose production (EGP) which is discussed later. During the next two hours, 20mU/m^2/min of insulin was infused (low-dose insulin). HGP is suppressed by low-dose insulin without affecting peripheral glucose uptake and this enables hepatic insulin sensitivity to be calculated. In the last two hours of the clamp, 100mU/m^2/min of insulin was infused (high-dose insulin). During this second step, this high-dose insulin infusion completely blunts HGP and stimulates peripheral glucose uptake. Therefore, this allows for calculation of peripheral insulin resistance.

2.1.2 Method

The participants arrived at the Clinical Research Unit (CRU), University of Oxford at around 8 o'clock in the morning, following an overnight fast. They were cannulated twice in the right arm to allow infusions of stable isotopes and a dextrose/insulin

infusion and once in the left arm to allow for blood sampling. The vein was kept patent using a warmed blanket and a slow infusion of 0.9% saline. Baseline bloods were taken and then the stable isotopes infusion began ([U-^{13}C]-glucose and [2,2-$^{2}H_2$]-palmitate). Blood glucose measurements were done every 15 min in the first two hours. At two hours, once the dextrose/insulin infusion had started, blood glucose was measured every 5 min. Euglycaemia was achieved throughout the clamp by using an algorithm to calculate the infusion rate of the dextrose needed to maintain the blood glucose (215). 3 sets of blood samples were taken in the last 30 min of each step, at the steady phase. At the end of the clamp, the infusions were stopped and the participants were fed a high carbohydrate meal and their blood glucose levels were monitored for 1-2 hours to ensure they were stable prior to them leaving the department.

2.2 [U-13C]-glucose isotope

2.2.1 Principle

Stable isotopes are alternative forms of elements with different molecular weights which occur naturally and do not decay. Carbon is an element which has a stable isotope and was infused in the form of [U-^{13}C]-glucose (Cambridge Isotope Laboratories, Andover, USA) during the hyperinsulinaemic euglycaemic clamp. Following analysis of the serum samples taken using GC/MS, the tracer:tracee ratio was calculated and thus the glucose metabolism during the clamp was estimated.

2.2.2 Method

20mL of sterile saline solution was added to 5g of [U-^{13}C]-glucose to give 0.25ng/mL solution. Using a sterile needle and 0.2μM filter, 5mL (2.5g) was inserted into a

500mL bag of 0.9% saline. This gave a concentration of 2.5mg/mL. The desired infusion rate was 0.02mg/Kg/min which was calculated as shown below:

Infusion rate (mL/h) = (0.02/2.5) * weight (kg) x 60 (min)

3.2mL (0.8g) of the [U-^{13}C]-glucose/saline solution was inserted into 500mL bags of 20% dextrose. A further 2mL (0.5g) was inserted into a 5mL syringe and then topped up to 5mL using sterile saline solution to give a 100mg/mL solution. The latter was given as a bolus. The bolus dose (2mg/Kg to be administered over 1 min) was then calculated as shown below:

Bolus volume = 2 * weight (Kg) / 100mg/mL

= *x* mL

The bolus volume was then drawn up and transferred to a 10mL syringe and sterile solution was used to make up to 10mL.

2.3 [2,2-2H2]-palmitate isotope

2.3.1 Principle

Hydrogen is another element which has a stable isotope and was infused in the form of [2,2-$^{2}H_2$]-palmitate (Cambridge Isotope Laboratories, Andover, USA). Similarly to the glucose isotope, the serum samples were analysed using GC/MS and the tracer:tracee ratio of palmitate was calculated and thus lipid metabolism throughout the clamp was determined.

2.3.2 Method

The required infusion rate for [2,2-$^2H_2$]-palmitate was 0.03μmol/Kg/min and this was calculated as illustrated below:

Total amount of [2,2-$^2H_2$]-palmitate infused = (0.03 * 296.54)/1,000 * weight (Kg) * (6 * 60)

296.54 is the molecular weight of [2,2-$^2H_2$]-palmitate

6 is the duration of the clamp in hours

60 is the minutes in an hour

Pre-determined infusion rate = 68mL/hr

Total volume of albumin infused = 68 * 6 = 408mL

Total amount of [2,2-$^2H_2$]-palmitate to be added to 500mL bag = (Total amount of [2,2-$^2H_2$]-palmitate infused * 500) / 408

The desired amount of [2,2-$^2H_2$]-palmitate was weighed and then dissolved in pre-heated (using a water bath at 70ºC) sterile water. Using a sterile needle and syringe, the solution was aspirated and injected into 500mL of preheated (using a water bath at 70ºC) human serum albumin.

2.4 RNA extraction

2.4.1 Principle

RNA extraction is the purification of RNA from biological samples. This procedure is complicated by the ubiquitous presence of ribonuclease enzymes in cells and tissues, which can rapidly degrade RNA. Several methods are used in molecular

biology to isolate RNA from samples, the most common of these is guanidinium thiocyanate-phenol-chloroform extraction (TriReagent® system).

2.4.2 Method

Snap frozen abdominal adipocyte and skeletal muscle tissue was placed in a 2ml Eppendorf® containing 1ml TriReagent® (SigmaAldrich, UK) and a stainless steel bead (Qiagen, UK) and homogenized mechanically for 30 seconds at 25 bpm. The samples were then centrifuged at 13000rpm for 15 min at 4ºC. The TriReagent® was then transferred to a 1.5ml Eppendorf® and 200µl of chloroform was added. The samples were agitated for 1 min and then allowed to stand at room temperature for 5 min. The samples were centrifuged again (13000rpm; 15 min; 4ºC) and the aqueous phase was removed and placed in a new 1.5ml Eppendorf®. A further 500µl of TriReagent® and 100µl of chloroform was added to the original tube, agitated for 1 min, allowed to stand for 5 min and finally centrifuged (13000rpm; 15 min; 4ºC). The aqueous phase was added to the new Eppendorf® from the previous step and then 600µl of isopronalol was added and the samples were placed at -4ºC overnight. Samples were centrifuged (13000rpm; 30 min; 4ºC) and the supernatant was discarded. The pellets were washed with 75% ethanol and then centrifuged (13000rpm; 15 min; 4ºC). The washing step was repeated once more. The pellets were allowed to dry at room temperature and then dissolved in nuclease-free water. The RNA quantity and quality was then measured using a Nanodrop (ND-1000, ThermoScientific, Wilmington, DE, USA). The RNA was diluted to reach a concentration of 50ng/µl which was used for complementary DNA (cDNA) synthesis and RNA sequencing.

2.5 cDNA synthesis

2.5.1 Principle

This method was used for the clinical study FindIt2 which is described in **Chapter 3**. Complementary DNA (cDNA) is synthesized by reverse transcription polymerase chain reaction (RT-PCR) using single stranded RNA. The extracted RNA is heated to denature secondary structures and subsequently cooled to allow annealing of random hexamers to the RNA template. Once annealed, the enzyme reverse transcriptase is used to extend the RNA-bound primer, in the presence of an RNase inhibitor. The final cDNA product is then used as a template for exponential amplification using PCR.

2.5.2 Method

The RT reactions were performed using the Applied Biosystems Reverse Transcription Kit (AppliedBiosystems, Warrington, UK). 10µl of RNA sample was used and 10µl of 2x RT master mix was added. The 2x RT master mix was made up of 2µl of 10x RT buffer, 0.8µl of 25x dNTPs mix (100mM), 2µl of 10x RT Random primers, 1µl of MultiScribe reverse transcriptase, 1µl of RNase Inhibitor, and 3.2µl of nuclease free water. Samples were then incubated at 25ºC for 10 min followed by 37ºC for 120 min, and then 85ºC for 5 min to denature the reverse transcriptase, using a thermal cycler (Applied Biosystems, Warrington, UK).

The cDNA quality was then checked using a Rotor Gene 6000 rotary cycler (Qiagen, Manchester, UK). 1µl of every sample was pooled together and diluted with 10mM TrisHCL to make a range of dilutions (1:10, 1:20, 1:40, 1:80, 1:60, 1:320) and tested against the housekeeping gene 18s rRNA. The reaction included 3.6µl of cDNA, 4µl

of 2x Taqman Universal PCR Master Mix (KapaBiosystems, Massachussets, USA) and 0.4µl of housekeeping gene.

2.6 Quantitative Polymerase Chain Reaction

2.6.1 Principle

This method was used for the clinical study FindIt2 which is described in **Chapter 3**. PCR is the method used to amplify DNA sequences exponentially. Quantitative polymerase chain reaction (qPCR) or real-time polymerase chain reaction is a laboratory method which is based on the PCR which monitors the amplification of a targeted DNA molecule during the PCR and not at its end, as in conventional PCR.

2.6.2 Method

All qPCR reactions were performed using the ABI 7900HT sequence detection system (Perkin-Elmer Applied Biosystems, Warrington, UK). The reactions were carried out in 6µl volume which included 3µl of 2x Taqman Universal PCR Master Mix (KapaBiosystems, Massachussets, USA), probe-primer mix for gene of interest (0.3µl) and 2.7µl of cDNA. Life Technologies supplied all the primers. The reaction conditions were as follows: 95ºC for 3 min followed by 40 cycles of 95ºC for 3 sec, and then 60ºC for 20 sec. The housekeeping gene used for adipocyte tissue was 18s rRNA. Data were expressed as Ct values which is the number of cycles at which logarithmic PCR plots crossed a calculated threshold line. ΔCt values were determined as follows: ΔCt = (Ct of target gene) - (Ct of housekeeping gene). Arbitrary units were then calculated using the formula (1000x2-ΔCt).

2.7 Biochemical serum sample analysis

2.7.1 Principle

Serum samples were run on 600/650 iLAB clinical chemistry analyser (Instrumentation Laboratory, Milano, Italy) in order to establish concentrations of TAG, NEFA, 3-hydroxybutyrate (OHB) and glycerol in the serum samples. The analyser uses a photometric method where it detects colour changes following a reaction for each given method.

2.7.2 Method

iLAB 600/650 analyzer was calibrated and had a quality check performed for each method prior to running the samples.

2.8 Solid phase extraction of NEFA from plasma samples

2.8.1 Principle

Solid-phase extraction is a technique by which compounds are separated from other compounds in the mixture according to their physical and chemical properties. The method used has been previously described (216, 217).

2.8.2 Method

500µl of sample (or saline solution; used as control) with 20µl of internal standard and 5ml of 2:1 (v:v) chloroform:methanol solution was added to each tube. The samples were mixed on the rotary mixer for 10 min and then 1ml of 1M NaCL was added. The samples were mixed once more on the rotary mixer for 15 min and then centrifuged (2000rpm; 10 min; 4ºC) (Beckman J6 floor-standing centrifuge, Palo Alto, CA, USA). The aqueous phase was aspirated and discarded, and the solvent

phase was placed in an LP4 tube and dried down using Zymark at 50ºC under nitrogen for 15 min.

The lipid extract was dissolved in 1ml of chloroform. The samples were then transferred into pre-washed columns (2 x 1ml acetone and then 2 x 1ml chloroform) and allowed to drip through. The NEFA fraction was eluted by adding 2 x 1ml of chloroform and 2 x 1ml of diethyl ether with 2% acetic acid and then dried using the Zymark.

Following the extraction, the samples then underwent methylation. 400µl of toluene-BHT solution was used (10mg butyl hydroxytoluene/100ml toluene) to dissolve the dried NEFA fraction. 800µl of methanol with 1.5% H_2SO_4 was added and the tubes were then placed in a water bath at 80ºC for at least an hour. 2ml of neutralising solution were then added ((25g $KHCO_3$ (0.125M) + 34.6g K_2CO_3 (0.125M) made up to 500ml with distilled water); diluted stock 1 in 5 for use) followed by 2 ml of cyclohexane. The samples were mixed using the rotary mixer for 15 min and afterwards were centrifuged (2000rpm; 10 min; 4ºC). The upper solvent phase was transferred into new tubes and dried down in Zymark. 100µl of chloroform was added to the dried samples and then transferred into gas chromatography vials containing inserts, where 20µl of external standard had been added.

The samples were then run on the GC (model 5890; Agilent Technologies, Cheshire, UK) and the relative amounts of individual fatty acids within the NEFA fraction were established. The samples were also run on the GC/MS (model 5973; Agilent

Technologies, Cheshire, UK) to be able to quantify the amount of labelled isotope ([2,2-$^2H_2$]-palmitate) relative to the unlabelled palmitate (tracer to tracee ratio (TTR)).

2.9 Ra palmitate calculations

2.9.1 Principle

Deuterium is the stable isotope of hydrogen (^2H) which is much less common in nature than ^1H. As mentioned previously, this isotope was used to measure the lipolysis rate throughout the clamp. ^2H was used as the tracer and ^1H as the tracee. The amount of each isotope was measured using the GC/MS (model 5973; Agilent Technologies, Cheshire, UK) and the TTR was calculated as described below.

2.9.2 Method

The Ra palmitate was calculated for individual time points (=10) throughout the clamp and the average of the three time points, at each stage of the clamp (basal, low-dose insulin, high-dose insulin), was used for analysis.

Ra palmitate = (Infusion rate of [2,2-$^2H_2$]-palmitate) / (TTR - background TTR)

Infusion rate of [2,2-$^2H_2$]-palmitate = 0.03μmol/Kg/min

TTR = Number of ions with mass-to-charge ratios of 270 (M+0) and 272 (M+2)

= 272/270

TTR background = Number of ions with mass-to-charge ratios of 270 (M+0) and 272 (M+2) (At time 0)

= 272/270 (At time 0)

2.10 Glucose extraction from plasma samples

2.10.1 Principle

Glucose was derivatised using N,O-Bis(trimethylsilyl)trifluoroacetamide + 1%Trimethylchlorosilane. This procedure introduces silyl group(s) which gives derivatives enhanced volatility, making them suitable for analysis by GC/MS.

2.10.2 Method

The analysis of ^{13}C glucose by GC/MS depends on accurate standards which are made up to the required dilution in deionised water. Unlabelled glucose (Do) was made to a working stock concentration of 100µg/ml. Isotopically labelled glucose (^{13}C) was made to two working dilutions (Dilution 1 = 10µg/ml; Dilution 2 = 1µg/ml). The subsequent dilutions to make up the 8 standards are detailed below.

Standard	^{13}C dilution	^{13}C Volume	Do Volume	Approx TTR
1		0	200	0
2	2	10	200	0.00065
3	2	80	200	0.00516
4	1	15	200	0.00968
5	1	40	200	0.02582
6	1	120	200	0.07745
7	1	140	200	0.09036
8	1	175	200	0.11295

Table 2-1 *The dilutions required to make standards for GC/MS analysis of D2 glucose*

The standards were then dried down in a centrifugal evaporator for 45 minutes. The plasma samples were thawed, vortexed and centrifuged (2500rpm; 10 min; 4ºC) (Beckman J6 floor-standing centrifuge, Palo Alto, CA, USA). 50µl of plasma was

pipetted into a LP4 tube followed by 500µl of ethanol. The samples were vortexed and then centrifuged (2500rpm; 5 min; 4ºC). The supernatant was transferred into 4.5ml tubes and dried down in a centrifugal evaporator for 45 minutes. 100µl of 2% methylhydroxamine hydrochloride in pyridine (2% w/v so 0.02g/1ml) was prepared and added to the samples. They were then capped, vortexed and placed in a heating block at 90ºC for 2 hours. Samples were allowed to cool and 50µl of BSTFA + 1%TMCS (N,O-Bis(trimethylsilyl)trifluoroacetamide + 1%Trimethylchlorosilane) was added. Samples were capped, vortexed and placed back in the heating block at 120ºC for 15 min. Samples were again cooled then dried in the centrifugal evaporator. 500µl of decane was added and samples vortexed. 50µl of sample was pipetted into GC vial containing 500µl decane. GC vials were capped, vortexed then run on the GC/MS to identify the enrichment of glucose with isotopically labelled glucose (^{13}C-glucose).

2.11 Glucose production and disposal calculations

2.11.1 Principle

As mentioned previously, ^{13}C was used as the stable isotope to label glucose. The stable isotope enrichment was then measured and used to calculate the glucose production and disposal rates throughout the clamp. The samples were taken in the last 30 min at each stage of the clamp when steady state was reached.

2.11.2 Method

The following calculations, based on the Steele equation (218), were used to basal Ra glucose, endogenous glucose production (EGP) and glucose disposal (Gd).

Basal Ra glucose = Infusion rate of ^{13}C-glucose in saline / (Plasma TTR - background TTR)

Infusion rate of ^{13}C-glucose in normal saline = 0.02mg/Kg/min

Plasma TTR = Number of ions with mass-to-charge ratios of 323 and 319

= 323/319

TTR background = Number of ions with mass-to-charge ratios of 323 and 319 (At time 0)

= 323/319 (At time 0)

EGP = Total glucose production (Ra) - 20% dextrose infusion rate

Total glucose production = [(20% dextrose infusion TTR - background TTR)*20% dextrose infusion rate + Infusion rate of ^{13}C-glucose in normal saline] / (Plasma TTR-background TTR)

Total glucose infused during the clamp = 20% dextrose infusion rate

20% dextrose infusion TTR = Number of ions with mass-to-charge ratios of 323 and 319 - background TTR

= 323/319 - background TTR

20% dextrose infusion rate = the rate of infusion at the time each sample was taken (mg/Kg/min)

Gd = Total amount of 20% dextrose infused (Due to high insulin rate it is assumed that EGP is 0)

= [(20% dextrose infusion TTR - background TTR)*20% dextrose infusion rate] / (Plasma TTR- background TTR)

2.12 Isotopic enrichment of CO2 in breath

2.12.1 Principle

Glucose oxidation was calculated by measuring the ^{13}C enrichment of CO_2 in breath from the infused ^{13}C-glucose. Expired breath was collected in tubes throughout the study and was stored at room temperature.

2.12.2 Method

CO_2 was separated from the other gases using a capillary column (CP-PoraPLOTQ; Variant Ltd, Oxford, United Kingdom) and by using the GC-combustion-isotope ratio mass spectrometer (GC/C/IRMS). This was performed using a splitless injection mode, with an injection volume of 10µl and an injector temperature of 110ºC. The oven temperature was maintained at 35ºC and the run time per sample was 10 min. The column flow was held constant at 1.2mL/min. The results ($\delta^{13}C$ $^{0}/_{00}$) were only accepted if the background enrichment was in accordance with the anticipate range of natural enrichment. The TTR (^{13}C:^{12}C) ratio was calculated according to the previously published calculation (219):

TTR (^{13}C:^{12}C) = [($\delta^{13}C^{0}/_{00}$/1000)+1] * 0.0112372 * 17/16

Background TTR = TTR (^{13}C:^{12}C) - TTR (^{13}C:^{12}C) (At time 0)

CO_2 production (mmol/hr/Kg) = [(TTR (^{13}C:^{12}C) - background TTR)*$\dot{V}CO_2$ (mmol/min)]/ participant weight (Kg)

The $\dot{V}CO_2$ (mmol/hr) was calculated based on the subjects' basal metabolic rate which itself was estimated by body composition measurement (TANITA®, Amsterdam-Zuidoost, Netherlands) as detailed below:

$\dot{V}CO_2$ = [(((KJ/(15.913/0.85)+5.207)/24)/60)*(1000/22.4)]*60

KJ is the basal metabolic rate + 20% to allow for bed rest, in kilojoules

15.913 is the energy expenditure per litre of O_2 consumed (220)

0.85 is the respiratory quotient

5.207 is energy expenditure per litre of CO_2 produced (220)

24 is the hours in a day

60 is the minutes in an hour

1000/22.4 is the conversion from litres/min to mmol/min (molar volume of gas = 22.4L/moles)

2.12.3 Analysis

CO_2 production (mmol/hr/Kg), at each time point, was calculated as shown above. Area under the curve analysis (AUC) was measured using the trapezoidal method for

each phase of the clamp (basal, low-dose insulin and high-dose insulin) and statistical analysis was performed as described in **Chapters 3 and 4**.

2.13 Microdialysis

2.13.1 Principle

Adipose interstitial fluid was collected for measurement of glycerol, pyruvate, glucose and lactate. These measurements were then analysed to study changes in metabolism during the clamp directly from the subcutaneous adipose tissue.

2.13.2 Method

A single microdialysis catheter (CMA Microdialysis, Solna, Sweden) was inserted under local anaesthetic (1-2 ml of 1% lidocaine) into the subcutaneous adipose tissue 5-10 cm to one side of the umbilicus. Using the microdialysis pump, a microdialysate solution (physiological sterile saline solution) was introduced into the catheter (perfusion rate = 0.3µl/minute). Microdialysis took place over the duration of the hyperinsulinaemic euglycaemic clamp. Samples were taken every 30 minutes throughout the study period and at the end of the sampling period the catheter was removed. Microdialysate fractions were stored at -80°C and subsequently analysed by automated analyser (CMA ISCUS Flex, Solna, Sweden) for glycerol, pyruvate, glucose and lactate according to manufacturer's instructions. Paired samples (i.e. pre and post treatment) from an individual were always processed sequentially. The analyser was first calibrated using pre-prepared reagents (Reagent Set A, Linton Instrumentation, UK). Samples were then run sequentially. Results that were not consistent with the time points pre and post the potentially anomalous sample were re-run.

2.13.3 Analysis

The concentrations of glycerol, pyruvate, glucose and lactate were measured for each time point, as described above. Similarly to the previous section of this chapter, AUC analysis was measured using the trapezoidal method for each phase of the clamp (basal, low-dose insulin and high-dose insulin) and statistical analysis was performed as described in **Chapters 3 and 4**.

2.14 Insulin ELISA

2.14.1 Principle

The Insulin ELISA (Mercodia, Uppsala, Sweden) used is a solid phase two-site enzyme immunoassay. It is based on the direct sandwich technique where two monoclonal antibodies are directed against separate antigenic determinants on the insulin molecule. During incubation, insulin reacts with peroxidase-conjugated anti-insulin antibodies and anti-insulin antibodies bound to the microplate. The washing step removes any unbound enzyme labelled antibody. The bound conjugate is detected by reaction with 3,3',5,5'-tetramethylbenzidine (TMB). The reaction is stopped by adding acid to give a colorimetric endpoint that is read using the SpectraMax Plus Microplate Reader (Molecular Devices, CA, USA) at 450 nm.

2.14.2 Method

25µl of calibrators, control and samples were pipetted in duplicates into the wells of the microplate. 100µl of 1X conjugate was added to each well and the microplate was placed on a plate shaker for an hour at 700-900rpm. The wells were then washed 6 times using the 1X wash buffer solution and allowed to dry. 200µl of TMB was then pipetted into each well and allowed to incubate at room temperature for 15 min. 50µl

of the Stop solution was added and the microplate was read at 450nm using the SpectraMax Plus Microplate Reader following a brief shake on the plate shaker.

2.14.3 Analysis

The insulin concentration of the samples was calculated from a standard curve with a logarithmic x-axis of the concentrations of the standards and a linear y-axis of the absorbance. The inter-assay co-efficient of variation of the ELISA was <15%.

2.15 Prednisolone/Prednisone serum levels

2.15.1 Method

The following procedure was performed by Joanne Duffy and Craig Webster (Department of Pathology, University Hospitals Birmingham, NHS Foundation Trust, Birmingham, B15 2GW, UK). Prednisolone, prednisone, cortisol and cortisone were extracted from participants' serum, calibration standards and quality control by liquid:liquid extraction using diethyl ether. The upper solvent layer containing the steroids was separated from the bottom aqueous layer using an ice-bath (Thermofisher) filled with ethanol (VWR). A rotary evaporator was used to dry down extracts and they were then reconstituted in 50:50 methanol water before analysis on the mass spectrometer.

2.15.2 Analysis

Analysis was performed by LC-MS/MS, specifically a Shimadzu HPLC system coupled to an API 5000 tandem mass spectrometer (Sciex, Warrington, UK). The ion source used was atmospheric pressure ionisation and the software was Analyst version 1.7.

3 The effect of Finasteride/Dutasteride & Prednisolone on metabolic (Insulin) action in healthy volunteers (FindIt2)

3.1 Introduction

2-3% of the population of the United Kingdom and United States are currently prescribed GC therapy (93). GC use, both acute and chronic, is known to be associated with a number of significant adverse effects. Recurrent short-course administration is also associated with increased morbidity and mortality (92). Adverse metabolic features include obesity, skeletal muscle myopathy, hypertension, insulin resistance and diabetes mellitus and are collectively termed '*Iatrogenic Cushing's syndrome'*.

5α-reductases (5αR) have a crucial role in the metabolism of testosterone and GCs (187). They metabolise testosterone to the more potent androgen, 5α-dihydrotestosterone, and inactivate cortisol to 5α-dihydrocortisol, which is then in turn metabolised to tetrahydrocortisol by 3α-hydroxysteroid dehydrogenase. The two main isoforms of 5αR are 5αR type 1 (5αR1) which is found in the liver, non-genital skin, muscle, adipose tissue and brain whilst 5αR type 2 (5αR2) is mainly expressed in the male reproductive tissues such as prostate, epididymis and seminal vesicles but also in the liver (187). 5αR, therefore, simultaneously enhances androgen, and limits active GC availability and represent a potent pre-receptor regulatory step in steroid hormone action.

The 5αRs have an established role in the regulation of metabolic phenotype. 5αR1 KO male mice are glucose intolerant, and have a higher incidence of hepatosteatosis and liver fibrosis (198, 199). Cross-sectional studies in humans have shown that 5αR activity correlates positivity with BMI (201-203) and tracks longitudinally over time with both weight and insulin resistance (201). Conversely, weight loss is associated

with reduced 5αR activity (201-203). 5αRIs such as dutasteride and finasteride are prescribed widely for their anti-androgenic effects in conditions such as benign prostate hyperplasia (BPH), prostate cancer, alopecia, as well as in some patients with PCOS. Dutasteride is a non-selective 5αRI inhibiting both 5αR1 and 2, whilst finasteride is a selective 5αR2 inhibitor. The ability of these drugs to regulate metabolic phenotype has only been examined in a very small number of studies. Dutasteride (and not finasteride) treatment worsened skeletal muscle and hepatic insulin sensitivity and increased hepatic triglyceride accumulation (208, 213). Most recently, analysis of data from primary care prescriptions as suggested a significant association between 5αRI prescriptions and the incidence of T2DM (214).

Patients who are prescribed GCs often have other comorbidities necessitating treatment with other medications and there are numerous examples of drug interactions altering GC exposure, leading to clinical signs and symptoms of GC excess. Such medications include protease inhibitors, anti-fungals, antibiotics immunosuppressive medications and combined oral contraceptives (171, 221, 222). Despite the well-recognised role of 5αR in GC metabolism (including synthetic GCs (187)), their ability to negatively impact upon the adverse effect profile associated with prescribed GC has not been explored.

We have therefore undertaken a detailed, proof-of-concept experimental medicine study in healthy volunteers, to test the hypothesis that 5αRIs can worsen the metabolic impact of prescribed prednisolone, putatively, through decreased metabolism and generation of inactive metabolites, and / or increased prednisolone clearance (223, 224).

3.2 Methods

3.2.1 Research strategy

In this chapter, we will examine the metabolic effects of co-administration of 5αRIs and prednisolone in healthy male volunteers. In particular, we will examine the effects of co-administration of these two types of medications on insulin action, on glucose oxidation, on tissue glucocorticoid metabolism and examine changes in the adipose tissue mRNA expression of genes involved in GC metabolism.

3.2.2 Statement of contributions

This study was designed by Dr Conor Woods and Prof Jeremy Tomlinson and implemented by Dr Thomas Marjot. Prof Craig Webster and Joanne Duffy processed serum samples to obtain prednisolone, prednisone, cortisol and cortisone levels, at the University Hospitals Birmingham NHS Foundation Trust, UK, as described in **Chapter 2**. I processed the samples with laboratory support and advice by Dr Catriona Charlton, Thomas Cornfield and Dr Jonathan Hazlehurst, with the exception of NEFA extractions which were processed by Dr Riccardo Pofi and glucose extractions, processed by Dr Ilaria Bonaventura. RNA sequencing was performed by the Wellcome Centre for Human Genetics, Oxford, UK. I undertook all of the analyses, with the exception of the statistical analysis done as groups of three (see below), which were performed by Dr Riccardo Pofi.

3.2.3 Clinical protocol

The clinical protocol received full ethical approval from the Wales 7 Research Ethics Committee (reference 15/WA/0071) (https://www.hra.nhs.uk/planning-and-improving-research/application-summaries/research-summaries/find-it-2/). Nineteen

healthy male volunteers were recruited from local advertisement, the Oxford Biobank, (reference 08/H0606/107+5), NHS hospitals and GP surgeries.

Inclusion criteria

- Male volunteers without diabetes (HbA_{1c} <48mmol/mol at screening)
- BMI 20-35kg/m^2
- Age 18-65 years
- BP <160/100mmHg or on stable antihypertensive therapy for >3months
- No contraindications to 5αRIs or prednisolone treatment

Exclusion criteria

- Age <18 or >65 years
- BMI <20 or >35kg/m^2
- Diagnosis of diabetes mellitus (type 1 or type 2)
- Any medication known to impact upon GC metabolism
- Unwilling, or unable, to give informed consent

The clinical study comprised of 3 study visits, are presented in **Figure 3.2-1** as a schematic summary of the investigations performed.

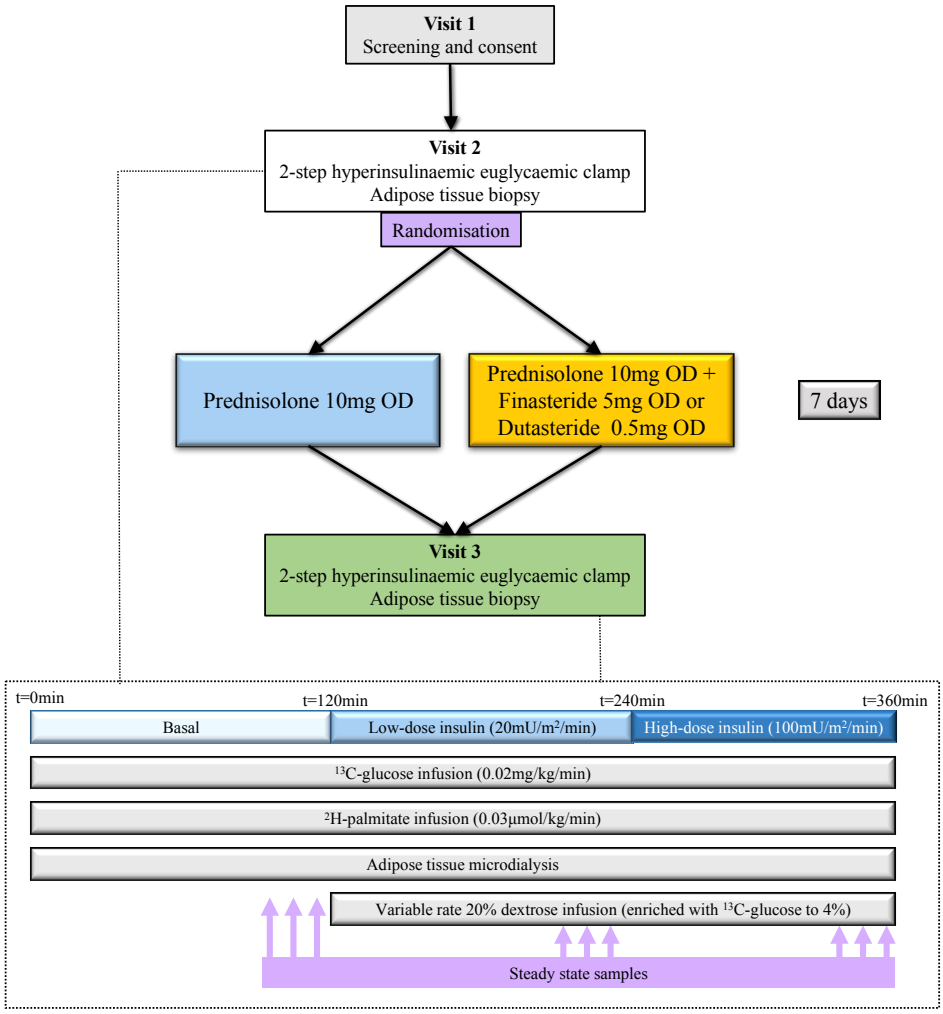

Figure 3.2-1 *FindIt2 Study design. Participants were screened and consented at Visit 1. At Visit 2, they underwent 2-step hyperinsulinaemic euglycaemic clamp, adipose tissue biopsy and they were randomized to receive prednisolone (10mg OD) for 7 days or prednisolone (10mg OD) and finasteride (5mg OD) for 7 days or prednisolone (10mg OD) and dutasteride (0.5mg OD) for 7 days. At Visit 3 the 2-step hyperinsulinaemic euglycaemic clamp and adipose tissue biopsy was repeated.*

Study visits

Visit 1 (Screening and consent):

Participants were screened for eligibility and baseline assessments were done which included:

- Height and weight measurements
- Blood tests: glycated haemoglobin
- Blood pressure

Visit 2:

The participants attended the Clinical Research Unit (CRU), at Oxford Centre for Diabetes, Endocrinology and Metabolism (OCDEM), Churchill Hospital (Oxford, UK) at 8:00 AM following a 12 hour fast.

Fasting blood tests were taken which included:

- Urea, creatinine, electrolytes and eGFR, AST, ALT, γGT, bilirubin, ALP and albumin
- Lipid profiles (total cholesterol, triglyceride, HDL cholesterol)

Subcutaneous adipose tissue biopsy was taken using a Pro-MagTM Ultra Biopsy 14g needle, a 20ml syringe and 100ml of 0.9% saline inserted into the abdominal subcutaneous tissue and adipocytes were aspirated using a negative pressure achieved with the needle and syringe. The skin had been cleaned and a local anaesthetic (3.5ml of 1% lidocaine) had been injected. Approximately 1g of tissue was taken and placed into liquid nitrogen.

An adipose tissue microdialysis catheter (CMA Microdialysis, Solna, Sweden) was then inserted under local anaesthetic into the abdominal subcutaneous adipose tissue, as described in **Chapter 2**. Immediately prior to the clamp procedure, indirect calorimetry was taken using a transparent hood for 15 minutes to measure resting energy expenditure and respiratory quotient. The two-step hyperinsulinaemic euglycaemic clamp was then performed, as described in **Chapter 2**. Throughout the clamp regular breath samples (every 60 minutes) were taken and blood samples over

the course of the following 6 hours to assess the incorporation of the stable-isotope into particles and molecules secreted by the liver and into the expired breath samples (Exetainer tubes, Labco Ltd, Bucks, UK).

At the end of this visit, the participants were randomized to receive prednisolone (10mg OD) for 7 days or prednisolone (10mg OD) and finasteride (5mg OD) for 7 days or prednisolone (10mg OD) and dutasteride (0.5mg OD) for 7 days.

Visit 3 was scheduled 7 days after visit 2.

Visit 3:

Participants underwent identical assessments to those described for visit 2. Volunteers took the prednisolone only or prednisolone and a 5αRI on the morning of the investigations.

3.2.4 Biochemical and stable isotope analysis

The data obtained from blood, adipose interstitial fluid, breath and adipose tissue biopsy samples were processed and analysed as described in **Chapter 2**.

3.2.5 RNA sequencing

Total RNA, extracted from adipose tissue biopsies, was enriched for polyA-tailed mRNA using oligo (dT) beads. The Illumina TruSeq Stranded mRNA HT Sample Prep Kit was used to prepare cDNA libraries for sequencing. In-house 8bp indexes (225) were used to multiplex samples (10-plex), which were then sequenced over 1 lane of an Illumina HiSeq4000 machine using HiSeq 3000/4000 PE Cluster Kit and

SBS Kit. Paired-end sequencing (75bp) was performed at a depth of ~25 million read pairs per sample.

Reads were mapped with STAR 2.5.1b (226) on default settings with GENCODE version 19 (227) as transcriptome and GRCh37 as genome reference. Gene level reads counts for all protein-coding and long intergenic non-coding RNA (lincRNA) transcripts present in GENCODE version 19 were quantified in a strand-specific manner with featureCounts (228) from the Subread package v1.5.0-p2. For plotting purposes, we also normalized the gene counts to transcripts per million (TPM).

3.2.6 Statistical analysis

Data are presented as mean (SD) or median (IQR) unless otherwise stated. In the first instance, data was analysed as three groups; prednisolone only, prednisolone + finasteride and prednisolone + dutasteride. Delta changes for the variables were calculated as the difference: follow-up (7 days post treatment) minus baseline. Shapiro-Wilk test was run to check for normality of distribution of the data. For normally distributed variables, one-way ANOVA was conducted to determine if there were differences between the three groups both for baseline measures and delta changes. For non-normally distributed variables, Kruskal-Wallis test was done instead. There were no outliers, as assessed by boxplot, and there was homogeneity of variances, as assessed by Levene's test of homogeneity of variances.

In cases where the differences between the three groups was not significant, further stratification was done by merging the two groups that received both prednisolone and a 5αRI, thus dividing the participants into two groups: prednisolone only and prednisolone + 5αRI. Paired t-tests were then used to compare individual variables before and after intervention within each participants' group where the data was

normally distributed and in cases the data was not normally distributed the Wilcoxon test was used instead. Absolute change between the two groups, as well as post-treatment comparisons, were calculated using unpaired t-test where the data was normally distributed or using the Mann-Whitney test where the data was not normally distributed.

Statistical analyses were performed using SPSS, version (IBM, Chicago, IL) and GraphPad Prism 8 software package (GraphPad Software, La Jolla, CA) for MacOS. Area under the curve (AUC) analysis was performed using the trapezoidal method. This was an exploratory study and therefore formal power calculations were not performed. However, sample size estimates suggested that 8 participants taking both prednisolone and 5αRIs would be needed to detect a 15% change in EGP (additional volunteers were recruited to account for potential drop-outs or failed sample analysis).

For RNA-sequencing data, differential expression analysis was performed using edgeR (229) in R 3.2.2 on normalised gene counts for all autosomal protein-coding and lincRNA genes that were expressed at >2 count per million (CPM) in all samples. A paired model was fitted to the data, and significance was determined by empirical Bayes moderated t-statistics implemented in edgeR. Differentially regulated genes were defined by a false discovery rate (Benjamini-Hochberg method) adjusted p-value <5%.

3.3 Results

3.3.1 Demographics and clinical characteristics of the participants

The participants were all male. There were 6 in the prednisolone only group, 7 in the prednisolone + finasteride group and 6 in the prednisolone + dutasteride group. The data was initially analysed as three groups (data not shown) but as there were no significant differences between the two 5αRI arms, the two intervention arms were grouped together. The results are shown as two arms; prednisolone only and prednisolone + 5αRI. The total cohort had a mean age of 45.2 (8.8) and a mean BMI of 27.1 (3.1) kg/m^2. The groups were well matched and there were no differences in demographic, anthropometric or metabolic values at baseline (**Table 3-1**).

Clinical/metabolic variable	**Prednisolone Only**	**Prednisolone + 5αRI**	***P* value**
Age, years	46.7 (9.5)	44.5 (8.8)	0.64
Weight, kg	89.4 (7)	86.2 (14)	0.51
Height, m	1.8 (0)	1.8 (0.1)	0.86
BMI, kg/m^2	27.8 (2.9)	26.7 (3.2)	0.50
Systolic BP, mmHg	140.8 (7.5)	141.8 (10.8)	0.38
Diastolic BP, mmHg	86.7 (6.1)	82 (9.5)	0.22
HbA1c, mmol/mol	34.3 (2.9)	32.1 (3.4)	0.17
Fasting glucose, mmol/L	4.8 (0.5)	4.5 (0.4)	0.29
Fasting insulin, pmol/L	20.4 (12.5)	33.4 (23.8)†	0.21
HDL cholesterol, mmol/L	1.4 (0.3)	1.2 (0.3)	0.38
Total cholesterol, mmol/L	5.1 (1.1)	4.8 (0.9)	0.60
AST, IU/L (15-42)	21.7 (4.6)	19 (4.2)	0.28
Bilirubin, mmol/L (<21)	19.2 (9.9)	12.9 (5.8)	0.12
ALT, IU/L (10-45)	22.7 (8.2)	22.1 (11.4)	0.59

ALP, IU/L (30-130)	58.7 (15.5)	62 (22)	0.72
Albumin, g/L (32-50)	37.5 (2.6)	37.6 (2.1)	0.91

Table 3-1 *The demographic and biochemical profiles of the participants. Data marked† is not normally distributed. Data are mean (SD).*

Circulating prednisolone levels were significantly high in participants taking 5αRIs compared to those taking prednisolone alone (482 (96) vs. 761 (57) nmol/L, p=0.029). There was no difference in circulating prednisone levels (95 (16) vs. 105 (8) nmol/L, p=0.54) (**Figure 3.3-1**).

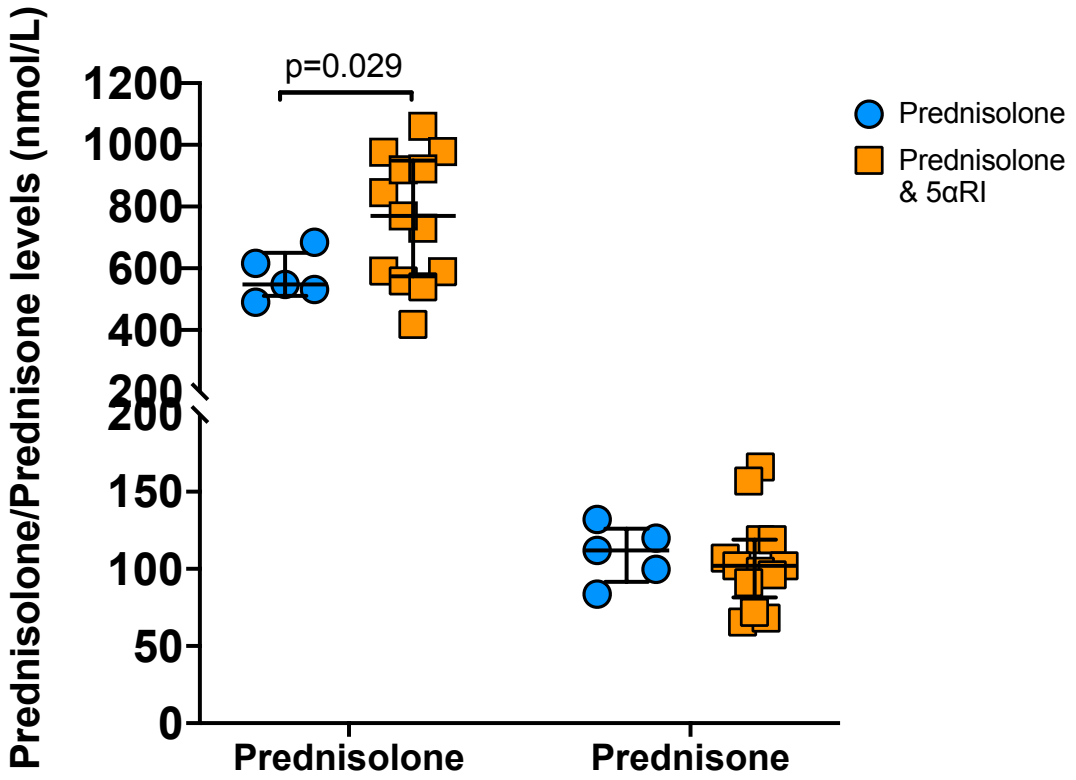

Figure 3.3-1 *The effect of prednisolone and co-administration with a 5αRI on circulating prednisolone and prednisone levels. Data are medians and error bars are IQR. Datapoints represent individual patients.*

There was no impact of either prednisolone alone or co-administration of prednisolone + 5αRI on fasting glucose or insulin levels, or on circulating lipids and liver chemistry. In addition, the changes observed in the composition of the fatty acid pool were similar in both groups (**Table 3-2**).

Metabolic variable	**Prednisolone n=6**	**Prednisolone + 5aRI n=13**
Ra Glucose, mg/Kg•min		
Baseline	2.55 (0.76)	2.67 (0.58)
7 days post treatment	2.62 (0.42)	3.05 (0.66)
Change over 7 days	0.07 (0.84)	0.38 (0.46)
Difference within group (p value)	0.86	0.012
EGP, mg/Kg•min		
Baseline	1.22 (1.01 to 1.42)	1.28 (0.96 to 1.4)
7 days post treatment	1.2 (1.1 to 1.38)	1.76 (1.58 to 2.2)
Change over 7 days	-0.02 (-0.45 to 0.36)	0.55 (0.05 to 1.11)
Difference within group (p value)	0.79	0.011
M value (Low insulin), mg/Kg•min		
Baseline	3.2 (2.08 to 4.14)	3.94 (2.5 to 4.83)
7 days post treatment	2.25 (1.63 to 3.21)	2.27 (1.85 to 2.64)
Change over 7 days	-0.53 (1.3)	-1.37 (1.82)
Difference within group (p value)	0.37	0.011
M value (High insulin), mg/Kg•min		
Baseline	11.51 (2.75)	10.93 (3.84)
7 days post treatment	12.01 (4.23)	9.79 (3.16)
Change over 7 days	0.49 (2.71)	-1.14 (3.32)
Difference within group (p value)	0.71	0.24
M/I value (Low insulin), mg/Kg•min per pmol/L		
Baseline	0.027 (0.018 to 0.032)	0.022 (0.015 to 0.035)
7 days post treatment	0.016 (0.008 to 0.022)	0.015 (0.012 to 0.02)
Change over 7 days	-0.01 (0.007)	-0.01 (0.012)
Difference within group (p value)	0.02	0.013
M/I value (High insulin), mg/Kg•min per pmol/L		
Baseline	0.027 (0.013)	0.027 (0.014)
7 days post treatment	0.045 (0.034)	0.026 (0.012)
Change over 7 days	0.01 (-0.002 to 0.04)	-0.004 (-0.0 to 0.006)
Difference within group (p value)	0.16	0.72
Glucose disposal (Low insulin), mg/Kg•min		
Baseline	2.54 (1.42)	2.87 (1.7)
7 days post treatment	1.77 (1.24)	2.05 (1.23)
Change over 7 days	-0.75 (-0.91 to -0.46)	-0.47 (-1.05 to -0.03)
Difference within group (p value)	0.03	0.08
Glucose disposal (High insulin), mg/Kg•min		
Baseline	11.02 (4.5)	8.81 (4.01)
7 days post treatment	10.43 (4.8)	8.45 (3.84)
Change over 7 days	0.01 (-2.2 to 1.62)	-0.43 (-0.85 to 0.5)
Difference within group (p value)	0.73	0.77

13-CO2, Breath (Low insulin) AUC, mmol/hr/kg		
Baseline	0.043 (0.041 to 0.044)	0.042 (0.039 to 0.045)
7 days post treatment	0.036 (0.035 to 0.049)	0.036 (0.034 to 0.039)
Change over 7 days	-0.002 (0.012)	-0.007 (0.007)
Difference within group (p value)	0.79	0.0046
13-CO2, Breath (High insulin) AUC, mmol/hr/kg		
Baseline	0.073 (0.006)	0.07 (0.012)
7 days post treatment	0.056 (0.016)	0.06 (0.008)
Change over 7 days	-0.018 (0.021)	-0.01 (0.008)
Difference within group (p value)	0.13	0.0005
NEFA (Basal), µmol/L		
Baseline	490.3 (129.8)	405.8 (109.3)
7 days post treatment	393.5 (164.9)	465.9 (141.2)
Change over 7 days	-96.8 (156.4)	60.1 (162.9)
Difference within group (p value)	0.19	0.21
NEFA (Low insulin), µmol/L		
Baseline	16.5 (12.2 to 23.4)	44 (24 to 65.7)
7 days post treatment	29.5 (11.2 to 45.8)	91.8 (42.6 to 114.4)
Change over 7 days	5.63 (-2.33 to 13)*	16.11 (6.3 to 50.3)*
Difference within group (p value)	0.81	0.0039
NEFA (High insulin), µmol/L		
Baseline	14.7 (3.2 to 21.7)	18.4 (12.3 to 26.6)
7 days post treatment	17.1 (12.1 to 17.2)	18 (12.3 to 29)
Change over 7 days	2.1 (-2.6 to 3.1)	-1.3 (-3.1 to 2.5)
Difference within group (p value)	0.5	0.72
Glycerol (Basal), µmol/L		
Baseline	33 (7.6)	27.2 (6.9)
7 days post treatment	29.9 (10.3)	29.2 (9.3)
Change over 7 days	-3.2 (11.3)	2 (13.3)
Difference within group (p value)	0.52	0.6
Glycerol (Low insulin), µmol/L		
Baseline	8.2 (3.8)	7.1 (3.1)
7 days post treatment	9.9 (3.6)	10.8 (4)
Change over 7 days	1.8 (0.8)	3.7 (4.3)
Difference within group (p value)	0.0024	0.0084
Glycerol (High insulin), µmol/L		
Baseline	6.9 (3.2)	6 (2.1)
7 days post treatment	7.1 (2)	7.4 (3.6)
Change over 7 days	0.8 (0.7 to 1.1)	0.9 (-0.4 to 2)
Difference within group (p value)	0.74	0.17
OHB (Basal), µmol/L		
Baseline	132 (57.5 to 193.2)	56.8 (43.7 to 68.1)
7 days post treatment	63.6 (41.2 to 79.6)	61.2 (49.7 to 97.1)

Change over 7 days	-41.7 (107.3)	18.7 (73)
Difference within group (p value)	0.44	0.52
OHB (Low insulin), µmol/L		
Baseline	15.9 (6.5)	19.9 (7.2)
7 days post treatment	16.7 (4.5)	25.6 (7.5)
Change over 7 days	0.8 (5)	5.7 (7.4)
Difference within group (p value)	0.7	0.02
OHB (High insulin), µmol/L		
Baseline	9 (2.8)	13.6 (3.4)
7 days post treatment	10 (4.1)	13.6 (3.2)
Change over 7 days	1 (5.1)	0 (2.9)
Difference within group (p value)	0.67	0.97
TAG (Basal), µmol/L		
Baseline	544.9 (435.6 to 794.3)	711.5 (510.3 to 1071.8)
7 days post treatment	453.2 (406.1 to 503.8)	727.4 (547.6 to 864.8)
Change over 7 days	-91.9 (207.3)	-37.5 (292.4)
Difference within group (p value)	0.44	0.65
TAG (Low insulin), µmol/L		
Baseline	312 (287.8 to 336.7)	608.6 (383.3 to 883.6)
7 days post treatment	304.6 (296.8 to 314.6)	487.3 (363.8 to 555.6)
Change over 7 days	55.3 (121.4)	-140.5 (239)
Difference within group (p value)	0.31	0.094
TAG (High insulin), µmol/L		
Baseline	255.6 (210.5 to 511.7)	482.6 (339.6 to 736.5)
7 days post treatment	254.1 (202.8 to 342.3)	360.5 (307.5 to 428.2)
Change over 7 days	29.3 (232)	-175.6 (171.9)
Difference within group (p value)	>0.99	0.0081
Ra Palmitate (Basal), mg/Kg•min		
Baseline	1.66 (1.62 to 2.5)	1.64 (1.49 to 1.81)
7 days post treatment	1.75 (1.73 to 1.84)	1.7 (1.57 to 1.96)
Change over 7 days	-0.25 (0.72)	0.25 (0.71)
Difference within group (p value)	0.48	0.24
Ra Palmitate (Low insulin), mg/Kg•min		
Baseline	0.55 (0.54 to 0.67)	0.56 (0.47 to 0.7)
7 days post treatment	0.66 (0.58 to 0.71)	0.68 (0.48 to 0.75)
Change over 7 days	0.04 (-0.21 to 0.04)	0.11 (-0.01 to 0.25)
Difference within group (p value)	0.72	0.083
Ra Palmitate (High insulin), mg/Kg•min		
Baseline	0.53 (0.45 to 0.59)	0.44 (0.37 to 0.59)
7 days post treatment	0.46 (0.4 to 0.53)	0.45 (0.35 to 0.48)
Change over 7 days	-0.05 (0.08)	0.04 (0.23)
Difference within group (p value)	0.29	0.78

Fasting glucose, mmol/L		
Baseline	4.8 (0.5)	4.5 (0.4)
7 days post treatment	5.1 (0.7)	4.7 (0.4)
Change over 7 days	0.27 (0.37)	0.12 (0.44)
Difference within group (p value)	0.14	0.37
Fasting Insulin, pmol/L		
Baseline	18.22 (13.6 to 24.99)	23.62 (19.9 to 40.57)
7 days post treatment	29.36 (18.7 to 43.93)	26.28 (23.8 to 28.89)
Change over 7 days	12.86 (21.44)	-3.98 (18.66)
Difference within group (p value)	0.32	0.47
Adipose interstitial fluid - Glycerol (Basal) AUC, µmol/L•hr		
Baseline	216 (187.5 to 261)	252.4 (201.4 to 346.7)
7 days post treatment	199.5 (186.3 to 269.5)	231.9 (184.4 to 242.3)
Change over 7 days	14.4 (63.9)	-100.7 (216.4)
Difference within group (p value)	0.64	0.32
Adipose interstitial fluid - Glycerol (Low insulin) AUC, µmol/L•hr		
Baseline	121.5 (65.5 to 124.3)	174 (136.3 to 257.6)
7 days post treatment	109 (106.5 to 157)	176.3 (98 to 262.8)
Change over 7 days	27.7 (46.1)	-0.5 (103.7)
Difference within group (p value)	0.31	0.989
Adipose interstitial fluid - Glycerol (High insulin) AUC, µmol/L•hr		
Baseline	73 (65.5 to 79)	99.3 (77.8 to 145.4)
7 days post treatment	71 (54 to 146.8)	132 (73.8 to 183.9)
Change over 7 days	30.8 (58)	-3.6 (89.2)
Difference within group (p value)	0.3	>0.99
Adipose interstitial fluid - Pyruvate (Basal) AUC, µmol/L•hr		
Baseline	137.8 (131.5 to 141.3)	126.5 (110.8 to 150.8)
7 days post treatment	102.3 (66 to 120.3)	135.9 (94.3 to 151.5)
Change over 7 days	-23.3 (-35.5 to -16.3)	16.5 (-43.3 to 35.2)
Difference within group (p value)	0.63	0.67
Adipose interstitial fluid - Pyruvate (Low insulin) AUC, µmol/L•hr		
Baseline	116.2 (38.7)	144.7 (55.9)
7 days post treatment	136 (44.5)	117.3 (71.1)
Change over 7 days	19.8 (24.8)	-27.4 (89.3)
Difference within group (p value)	0.15	0.33
Adipose interstitial fluid - Pyruvate (High insulin) AUC, µmol/L•hr		
Baseline	100 (84.5 to 135.3)	111.3 (76 to 185.4)
7 days post treatment	101.5 (73.3 to 111.5)	89.3 (63.6 to 146.1)
Change over 7 days	-4.5 (66.3)	-4.8 (71.2)
Difference within group (p value)	0.89	0.97
Adipose interstitial fluid - Lactate (Basal) AUC, mmol/L•hr		
Baseline	1.5 (1.3 to 1.8)	1.4 (1 to 1.6)
7 days post treatment	1.2 (1.2 to 2.3)	1.5 (1.1 to 1.6)

Change over 7 days	0.3 (1.9)	-0.2 (1.4)
Difference within group (p value)	0.76	>0.99
Adipose interstitial fluid - Lactate (Low insulin) AUC, mmol/L•hr		
Baseline	1.6 (1.6 to 1.9)	1.8 (1.3 to 3.3)
7 days post treatment	1.9 (1.7 to 2.7)	1.5 (1 to 2.3)
Change over 7 days	-0.6 (3.4)	-0.7 (2.3)
Difference within group (p value)	>0.99	0.35
Adipose interstitial fluid - Lactate (High insulin) AUC, mmol/L•hr		
Baseline	2.4 (2.1 to 2.6)	2.3 (1.3 to 3.1)
7 days post treatment	1.6 (1.3 to 2.4)	1.4 (0.8 to 2.7)
Change over 7 days	-1.46 (2.44)	-0.66 (2.15)
Difference within group (p value)	0.25	0.38
Adipose interstitial fluid - Glucose (Basal) AUC, mmol/L•hr		
Baseline	4.1 (4.1 to 4.8)	4.3 (3.6 to 4.8)
7 days post treatment	3.8 (3.2 to 4.5)	4.2 (3.7 to 4.8)
Change over 7 days	-0.21 (1.6)	0.16 (1.22)
Difference within group (p value)	0.78	>0.99
Adipose interstitial fluid - Glucose (Low insulin) AUC, mmol/L•hr		
Baseline	3.8 (3.4 to 4)	3.5 (2.9 to 3.7)
7 days post treatment	3.8 (3.7 to 4.6)	3.3 (2.2 to 3.9)
Change over 7 days	0.47 (2.52)	-0.21 (1.6)
Difference within group (p value)	>0.99	0.67
Adipose interstitial fluid - Glucose (High insulin) AUC, mmol/L•hr		
Baseline	3.9 (2.5 to 4.4)	3.2 (2.6 to 4.5)
7 days post treatment	3.6 (3.1 to 4.7)	2.8 (2.2 to 3.2)
Change over 7 days	-0.06 (2.4)	-0.6 (1.49)
Difference within group (p value)	0.25	0.21
Palmitic acid 16:00 (Basal), %		
Baseline	26 (1.1)	27.6 (3.4)
7 days post treatment	25.8 (1.5)	27.7 (2.9)
Change over 7 days	-0.1 (1.5)	0.1 (2.5)
Difference within group (p value)	0.83	0.85
Palmitic acid 16:00 (Low insulin), %		
Baseline	32 (8.2)	27.5 (4.5)
7 days post treatment	28 (2.9)	26.5 (3.5)
Change over 7 days	-4.1 (6.9)	-1.1 (3)
Difference within group (p value)	0.21	0.22
Palmitic acid 16:00 (High insulin), %		
Baseline	31.3 (11.6)	29 (5.1)
7 days post treatment	30.7 (32.9)	29.2 (4.5)
Change over 7 days	0.4 (-0.8 to 2.5)	0.1 (-3.1 to 3.1)
Difference within group (p value)	0.52	0.91

Stearic acid 18:00 (Basal), %		
Baseline	11.8 (1.2)	12.7 (1.9)
7 days post treatment	12.5 (1.8)	12.2 (2)
Change over 7 days	0.7 (1.6)	-0.5 (2)
Difference within group (p value)	0.31	0.35
Stearic acid 18:00 (Low insulin), %		
Baseline	24.5 (22.8 to 25.5)	5.2 (2.1 to 6.8)
7 days post treatment	19.3 (15.9 to 22.5)	18 (15.5 to 20.1)
Change over 7 days	-1.6 (-6.3 to -0.6)	-2.9 (-5.1 to -0.6)
Difference within group (p value)	0.03	0.02
Stearic acid 18:00 (High insulin), %		
Baseline	23.1 (19.9 to 26)	26 (22.3 to 29.6)
7 days post treatment	21.6 (19.7 to 25.2)	24 (22.3 to 27.3)
Change over 7 days	0.9 (4.1)	-0.3 (4.7)
Difference within group (p value)	0.61	0.54
Oleic acid 18: 1n-9 (Basal), %		
Baseline	44.5 (43 to 45.2)	43.9 (37.1 to 45.2)
7 days post treatment	42.6 (41.6 to 44.2)	43.6 (40.2 to 44.1)
Change over 7 days	-1 (-3.1 to -0.3)	-0.3 (-3.6 to 4.5)
Difference within group (p value)	0.16	0.82
Oleic acid 18: 1n-9 (Low insulin), %		
Baseline	21.6 (9.9)	26.9 (9.1)
7 days post treatment	28.3 (4.1)	31.6 (7.2)
Change over 7 days	3.1 (-0.7 to 5.8)	5.2 (2.1 to 6.8)
Difference within group (p value)	0.25	0.008
Oleic acid 18: 1n-9 (High insulin), %		
Baseline	18.3 (7.1)	20.5 (6.4)
7 days post treatment	21.1 (5.2)	20.9 (6.6)
Change over 7 days	2.8 (5.4)	0.4 (2.5)
Difference within group (p value)	0.26	0.63
Linoleic acid 18: 2n-6 (Basal), %		
Baseline	11.7 (11.3 to 12.6)	12.3 (10.4 to 14)
7 days post treatment	12.1 (10.8 to 13.1)	11.8 (10.2 to 13.3)
Change over 7 days	0.2 (-0.1 to 1.3)	-0.7 (-1.4 to 0)
Difference within group (p value)	0.44	0.25
Linoleic acid 18: 2n-6 (Low insulin), %		
Baseline	13.2 (11.6 to 14.6)	13.1 (11.4 to 16.5)
7 days post treatment	14.1 (13.5 to 15.5)	13.5 (11.6 to 14.5)
Change over 7 days	0.7 (0.2 to 2.7)	-0.6 (-3.1 to -0.1)
Difference within group (p value)	0.31	0.1
Linoleic acid 18: 2n-6 (High insulin), %		
Baseline	10.9 (6.1 to 13.7)	11.2 (9 to 20.6)
7 days post treatment	14.1 (11.3 to 15.2)	12.2 (11 to 14.2)

Change over 7 days	1.5 (0.5 to 2.4)	0 (-1.2 to 1)
Difference within group (p value)	0.29	>0.99

Table 3-2 *The effect of prednisolone and co-administration of prednisolone and a 5αRI on glucose and lipid metabolism during a two-step hyperinsulinaemic euglycaemic clamp. Data are mean (SD) or median (IQR). *P <0.05, difference in change over 7 days between the two groups.*

3.3.2 Hepatic insulin sensitivity

Basal Ra glucose was not altered by treatment with prednisolone alone. However, when combined with 5αRIs, Ra glucose increased significantly; the absolute change between the two groups was not significant (p=0.30) (**Table 3-2**, **Figure 3.3-2** A and B). EGP rate was unchanged by prednisolone treatment, but following 5αRI co-administration EGP significantly increased, consistent with worsening hepatic insulin sensitivity (**Table 3-2**, **Figure 3.3-2** C and D). The absolute change between the two groups was not statistically significant (p=0.15).

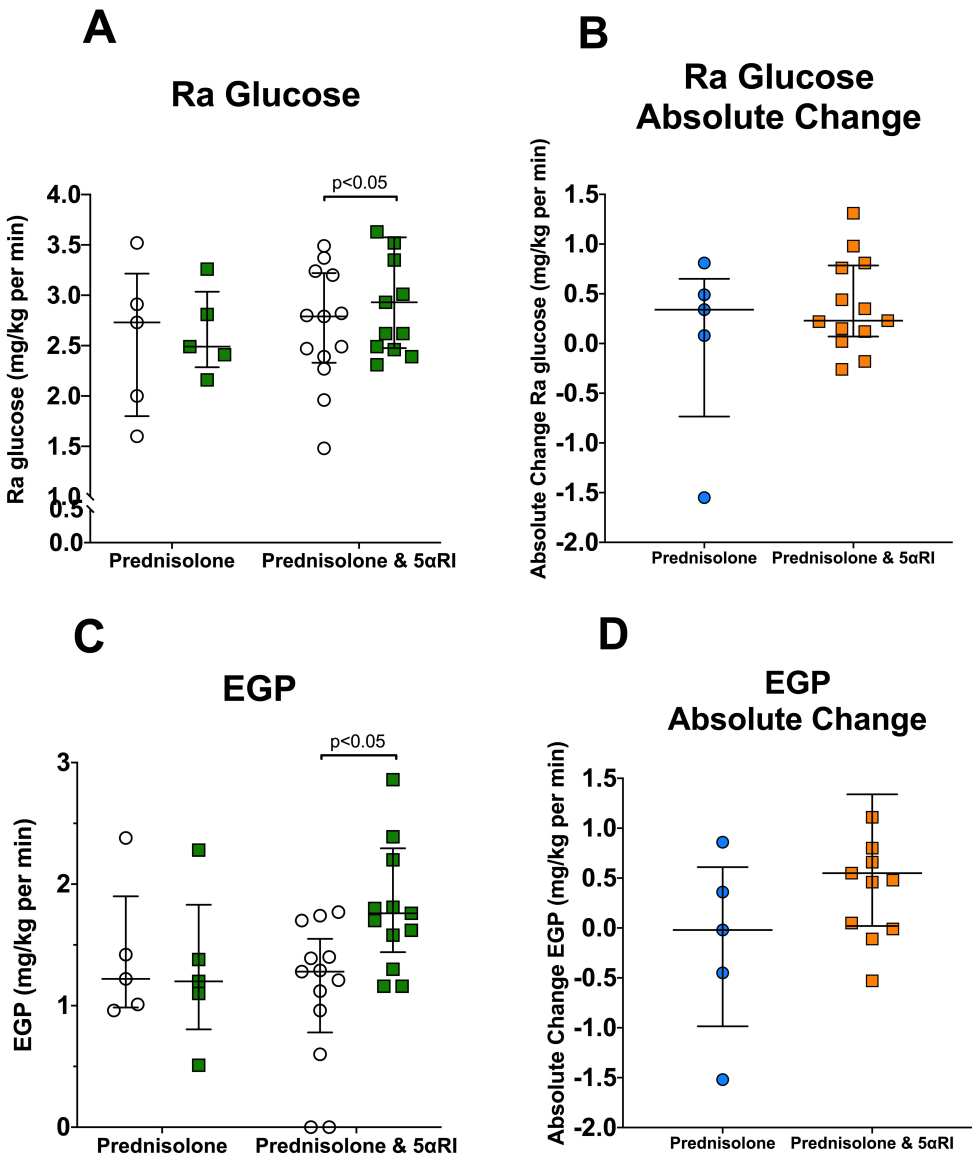

Figure 3.3-2 *The effect of prednisolone and co-administration with a 5αRI on glucose production (Ra Glucose) (A and B) and endogenous glucose production (EGP) rate (C and D), during a two-step hyperinsulinaemic euglycaemic clamp. Absolute change refers to the difference between pre- and post-treatment values (B and D). Data are medians and error bars are IQR. Datapoints represent individual patients. White circles represent pre-treatment levels and green squares post-treatment levels (7 days), blue circles are prednisolone alone and orange squares, prednisolone + 5αRI.*

3.3.3 Peripheral insulin resistance

Prednisolone alone had no impact on the M-value during the low- or high-dose insulin infusion. However, when combined with a 5αRI, under low-dose insulin infusion it decreased significantly (**Table 3-2**, **Figure 3.3-3** A and B).

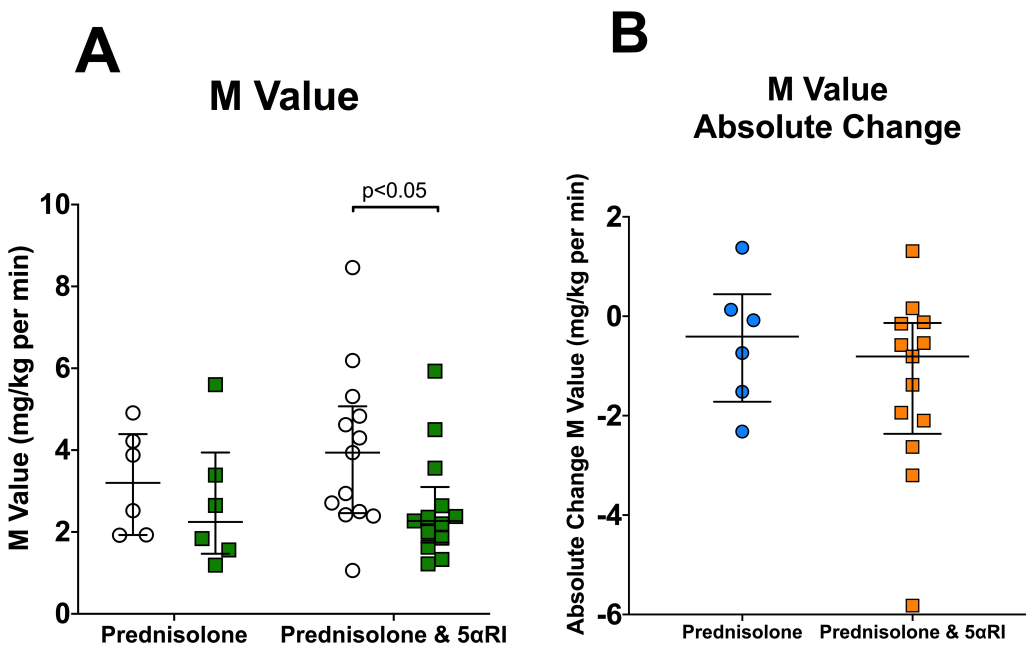

Figure 3.3-3 *The effect of prednisolone and co-administration with a 5αRI on the M-value during the low-dose insulin step of the two-step hyperinsulinaemic euglycaemic clamp. Absolute change refers to the difference between pre- and post-treatment values (B). Data are medians and error bars are IQR. Datapoints represent individual patients. White circles represent pre-treatment levels and green squares post-treatment levels (7 days), blue circles are prednisolone alone and orange squares, prednisolone + 5αRI.*

Both prednisolone alone and with 5αRI, the M/I-value was decreased during low-dose insulin but remained the same during high-dose insulin (**Table 3-2**). Gd was decreased by prednisolone alone, during low-dose insulin. Although the magnitude in reduction of Gd with prednisolone + 5αRI was similar to prednisolone alone, this did not reach statistical significance (p=0.080) (**Table 3-2**). Gd did not change during high-dose insulin in either group. There were no differences in the absolute changes between the groups (**Table 3-2**).

3.3.4 Glucose oxidation

$^{13}CO_2$ production from the infused [U-^{13}C]-glucose was used as a marker of glucose uptake and subsequent oxidation. Co-administration of prednisolone + 5αRI (but not

prednisolone alone), decreased glucose oxidation across the 2-step clamp (both low- and high-dose insulin phases) (**Table 3-2**) (**Figure 3.3-4** A and C). The absolute change between the two groups, under both low- and high-dose insulin phases, was not different (**Table 3-2**) (**Figure 3.3-4** B and D).

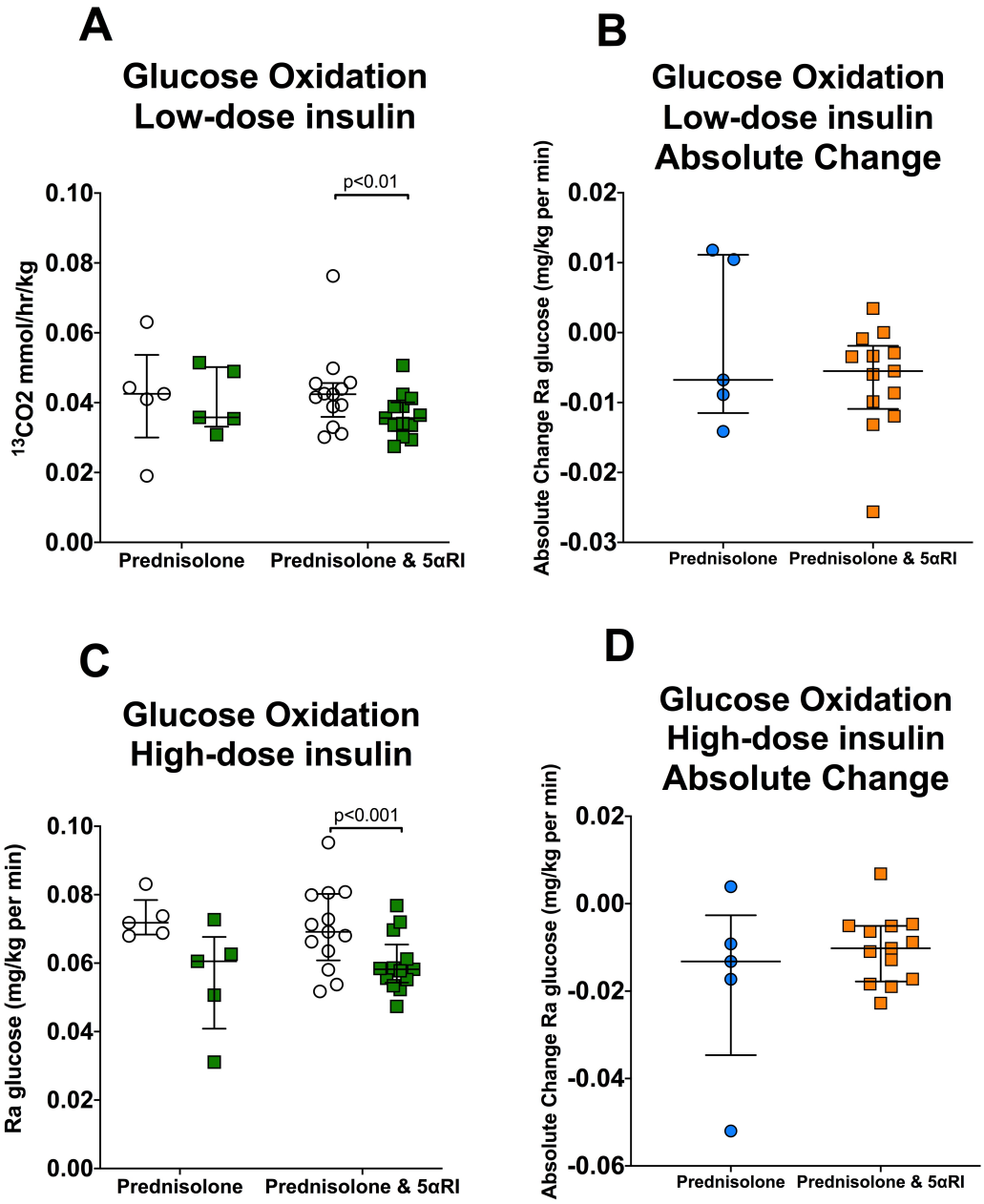

Figure 3.3-4 *The effect of prednisolone and co-administration with a 5αRI on glucose oxidation during the low-dose insulin step (A and B) and the high-dose insulin step (C and D) of the two-step hyperinsulinaemic euglycaemic clamp. Absolute change refers to the difference between pre- and post-treatment values (B and D). Data are medians and error*

bars are IQR. Datapoints represent individual patients. White circles represent pre-treatment levels and green squares post-treatment levels (7 days), blue circles are prednisolone alone and orange squares, prednisolone + 5αRI.

3.3.5 Adipose tissue insulin sensitivity

Prednisolone alone had no impact on insulin-mediated suppression of circulating NEFA levels during the low- or high-dose insulin infusion. However, when combined with a 5αRI, there was a significant reduction in the ability of low-dose insulin (but not high-dose insulin) to suppress circulating NEFA levels (**Table 3-2**, **Figure 3.3-5** A, B and C).

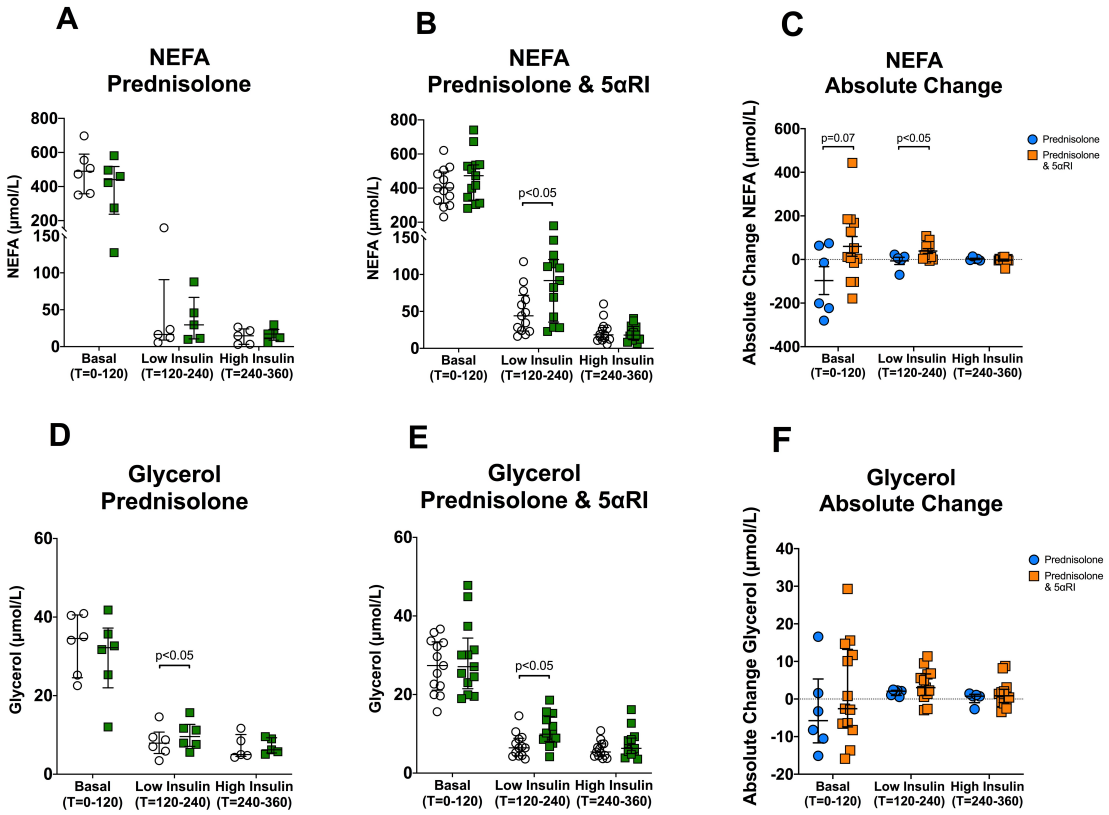

Figure 3.3-5 *The effect of prednisolone and co-administration with a 5αRI on circulating non-esterified fatty acids (NEFA) (A, B and C) and glycerol (D, E and F) levels during a two-step hyperinsulinaemic euglycaemic clamp. Absolute change refers to the difference between pre- and post-treatment values (C and F). Data are medians and error bars are IQR. Datapoints represent individual patients. White circles represent pre-treatment levels and green squares post-treatment levels (7 days), blue circles are prednisolone alone and orange squares, prednisolone + 5αRI.*

Prednisolone alone, as well as prednisolone + 5αRI were equally effective in impairing the ability of insulin to supress circulating glycerol under low-, but not high-dose insulin infusions. There was no significant difference in the absolute change between the two groups across the clamp (**Table 3-2**, **Figure 3.3-5** D, E and F).

Adipose tissue lipolysis (as measured using [2,2-$^{2}H_2$]-palmitate) was decreased by insulin (both low- and high-dose), but there was no impact of prednisolone or prednisolone + 5αRI treatment (**Table 3-2**). Insulin decreased fatty acid oxidation as measured by circulating levels of OHB. Prednisolone had no impact on the ability of insulin to suppress OHB levels, but when co-administered with a 5αRI, insulin-mediated suppression of OHB was impaired (**Table 3-2**, **Figure 3.3-6** A and B). The absolute change between the two groups was different but did not reach statistical significance (p=0.17) (**Table 3-2**, **Figure 3.3-6** C). There were no differences following high dose insulin infusion (**Table 3-2**).

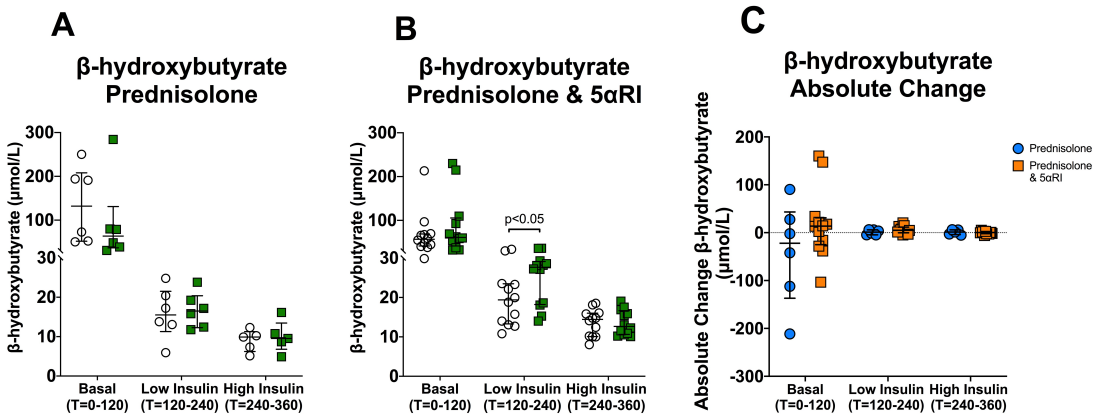

Figure 3.3-6 *The effect of prednisolone and co-administration with a 5αRI on circulating β-hydroxybutyrate (OHB) levels (A, B and C) during a two-step hyperinsulinaemic euglycaemic clamp. Absolute change refers to the difference between pre- and post-treatment values (C).*

Data are medians and error bars are IQR. Datapoints represent individual patients. White circles represent pre-treatment levels and green squares post-treatment levels (7 days), blue circles are prednisolone alone and orange squares, prednisolone + 5αRI.

Adipose tissue microdialysis was used to specifically examine the impact of treatment upon subcutaneous adipose tissue. Insulin decreased adipose tissue interstitial glycerol levels in a dose-dependent manner (**Table 3-2**). However, neither prednisolone alone, nor prednisolone + 5αRI had any impact on subcutaneous adipose interstitial fluid levels of glycerol, glucose, pyruvate, and lactate or their response to low- and high-dose insulin infusion (**Table 3-2**).

3.3.6 Subcutaneous adipose tissue gene expression

There were no changes to the expression of ACACA, FASN, GILZ, LIPE, LPL, PNPLA2 and SGK1 genes in subcutaneous adipose tissue following prednisolone treatment (**Table 3-3**), as tested by qPCR. There was a significant increase was in the FASN gene, which promotes lipogenesis, following co-administration with 5αRI, indicating that insulin action is compromised. There were no other significant differences in gene expression were observed in this group.

	Prednisolone			**Prednisolone + 5aRI**		
Gene	*Before*	*After*	*P value*	*Before*	*After*	*P value*
ACACA	0.42 (0.12)	0.45 (0.13)	0.62	0.51 (0.26)	0.55 (0.4)	0.52
FASN	0.42 (0.22)	0.65 (0.24)	0.08	0.57 (0.31)	0.73 (0.45)	0.04*
GILZ	0.85 (0.38)	1.06 (0.49)	0.4	0.76 (0.27)	0.75 (0.33)	0.91
LIPE	0.64 (0.32)	0.45 (0.38)	0.13	0.52 (0.31)	0.7 (0.54)	0.16
LPL	0.88 (0.11)	0.85 (0.28)	0.78	0.89 (0.22)	0.86 (0.21)	0.58
PNPLA2	0.86 (0.23)	0.72 (0.26)	0.11	0.9 (0.45)	0.97 (0.41)	0.51
SGK1	0.88 (0.11)	0.85 (0.28)	0.78	0.89 (0.22)	0.86 (0.21)	0.58

Table 3-3 *The effect of prednisolone and co-administration with a 5αRI on gene expression in subcutaneous adipose tissue. Data are presented as mean (SD) in arbitrary units. *P<0.05*

RNA sequencing analysis identified only 11 genes (PLA2G2A, ETNK2, MALL, EDN1, SOX7, FAM166B, LINC00844, ARNTL, KRT1, NFKBIA, GADD45B) that were regulated by prednisolone treatment, several of which are recognised GC-targets (including endothelin 1 (EDN1), aryl hydrocarbon receptor nuclear translocator like (ARNTL), NFKB inhibitor alpha (NFKBIA) and growth arrest and DNA damage inducible beta (GADD45B)) (230-233). The expression of only a single gene changed following prednisolone + 5αRI treatment (ribosomal protein L41 pseudogene 1 (RPL41P1)).

3.3.7 Finasteride and dutasteride effect on the metabolic action of prednisolone

A *post-hoc* subgroup analysis was used to compare the administration of either finasteride or dutasteride. There were no differences in the fasting basal metabolic parameters between the subgroups. Prednisolone levels were similar in those individuals treated with either prednisolone + finasteride or prednisolone + dutasteride (806 (174) vs. 709 (243) nmol/L, p=0.89). In both cases, levels were higher than in participants treated with prednisolone alone (482 (236) vs. 806 (174) vs. 709 (243) nmol/L, p=0.046).

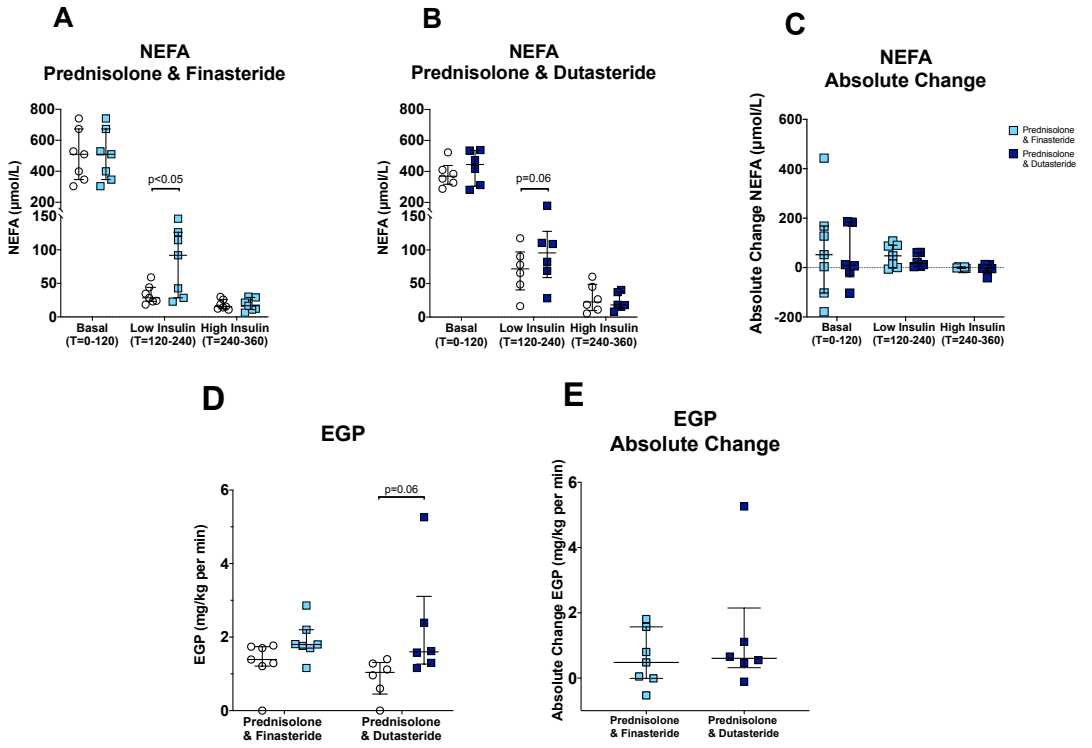

Figure 3.3-7 *The effect of co-administration of prednisolone with finasteride or dutasteride on circulating non-esterified fatty acids (NEFA) (A, B and C) levels across a 2-step hyperinsulinaemic euglycaemic clamp and endogenous glucose production (EGP) (D and E) during the low-dose insulin phase of a 2-step hyperinsulinaemic euglycaemic clamp. Absolute change refers to the difference between pre- and post-treatment values. Data are medians and error bars are IQR. Datapoints represent individual patients. White circles represent pre-treatment levels, light grey squares are post-treatment (7 days) finasteride + prednisolone and dark grey squares, post-treatment (7 days) with dutasteride + prednisolone.*

The low-dose insulin mediated suppression of NEFA was similar in individuals treated with finasteride + prednisolone ($p<0.05$) and dutasteride + prednisolone ($p=0.058$); there was no significant difference between the groups (**Figure 3.3-7** A, B and C). Changes in EGP were similar in individuals treated with either finasteride or dutasteride and there was no significant difference between the groups (**Figure 3.3-7** D and E).

Interestingly, the changes in glycerol, OHB, M-value and Gd under high-dose insulin were more marked in individuals treated with finasteride (**Table 3-4**). Changes in

other metabolic variables were not different between the two groups and are summarized in **Table 3-4**.

Metabolic variable	**Prednisolone + Dutasteride**	**Prednisolone + Finasteride**
Ra Glucose, mg/Kg•min		
Baseline	2.48 (2.41 to 2.72)	2.82 (2.53 to 3.22)
7 days post treatment	2.55 (2.47 to 3.73)	3.01 (2.78 to 3.44)
Change over 7 days	0.36 (0.49)	0.26 (0.33)
Difference within group (p value)	0.09	0.08
EGP, mg/Kg•min		
Baseline	1.04 (0.69 to 1.24)	1.39 (1.25 to 1.72)
7 days post treatment	1.6 (1.37 to 2.2)	1.8 (1.73 to 2)
Change over 7 days	0.54 (0.44)	0.6 (0.86)
Difference within group (p value)	0.06	0.16
M value (Low insulin), mg/Kg•min		
Baseline	3.87 (2.4 to 5.97)	3.94 (2.83 to 4.46)
7 days post treatment	2.46 (1.96 to 3.33)	2.2 (1.82 to 2.37)
Change over 7 days	-1.63 (2.27)	-1.14 (1.48)
Difference within group (p value)	0.14	0.08
M value (High insulin), mg/Kg•min		
Baseline	8.65 (4.36)	12.88 (2.01)
7 days post treatment	9.61 (3.19)	9.94 (3.39)
Change over 7 days	1.42 (2.16)*	-2.94 (3.11)*
Difference within group (p value)	0.34	0.047
M/I value (Low insulin), mg/Kg•min per pmol/L		
Baseline	0.028 (0.014 to 0.043)	0.022 (0.02 to 0.03)
7 days post treatment	0.016 (0.009 to 0.019)	0.015 (0.012 to 0.018)
Change over 7 days	-0.014 (0.014)	-0.006 (0.01)
Difference within group (p value)	0.06	0.16
M/I value (High insulin), mg/Kg•min per pmol/L		
Baseline	0.019 (0.012)	0.034 (0.012)
7 days post treatment	0.023 (0.008)	0.028 (0.015)
Change over 7 days	0.006 (0.004 to 0.013)	-0.008 (-0.01 to -0.005)
Difference within group (p value)	0.26	0.1
Glucose disposal (Low insulin), mg/Kg•min		
Baseline	3.06 (2.37)	2.71 (1.03)
7 days post treatment	2.16 (1.28)	1.95 (1.27)
Change over 7 days	-0.24 (-0.43 to -0.03)	-0.7 (-1.21 to 0.13)
Difference within group (p value)	0.28	0.22

Glucose disposal (High insulin), mg/Kg•min		
Baseline	6.49 (3.45)	10.8 (3.5)
7 days post treatment	8.65 (4.76)	8.27 (3.23)
Change over 7 days	0.49 (0.03 to 1.39)*	-0.8 (-3.51 to -0.46)*
Difference within group (p value)	0.25	0.11
13-CO2, Breath (Low insulin) AUC, mmol/hr/kg		
Baseline	0.043 (0.04 to 0.048)	0.042 (0.032 to 0.044)
7 days post treatment	0.039 (0.037 to 0.041)	0.034 (0.03 to 0.035)
Change over 7 days	-0.008 (0.01)	-0.005 (0.006)
Difference within group (p value)	0.06	0.05
13-CO2, Breath (High insulin) AUC, mmol/hr/kg		
Baseline	0.076 (0.012)	0.065 (0.011)
7 days post treatment	0.064 (0.009)	0.056 (0.007)
Change over 7 days	-0.01 (0.006)	-0.009 (0.009)
Difference within group (p value)	0.009	0.036
NEFA (Basal), µmol/L		
Baseline	381.1 (81.7)	427 (131.1)
7 days post treatment	425.9 (110)	500.2 (163.9)
Change over 7 days	44.8 (115.8)	73.2 (203.6)
Difference within group (p value)	0.39	0.38
NEFA (Low insulin), µmol/L		
Baseline	69.3 (34.8)	33.1 (14.2)
7 days post treatment	96.3 (50.6)	81.8 (50.3)
Change over 7 days	20.1 (23.5)	48.7 (47.1)
Difference within group (p value)	0.06	0.03
NEFA (High insulin), µmol/L		
Baseline	27.8 (21)	18.2 (7.2)
7 days post treatment	23 (12.8)	18.2 (9.1)
Change over 7 days	-5.2 (21.8)	0 (3)
Difference within group (p value)	0.57	0.99
Glycerol (Basal), µmol/L		
Baseline	25.2 (4.9)	29 (8.2)
7 days post treatment	26.6 (6.4)	31.5 (11.1)
Change over 7 days	1.3 (9.2)	2.6 (16.7)
Difference within group (p value)	0.74	0.7
Glycerol (Low insulin), µmol/L		
Baseline	6.6 (5.5 to 7.3)	6.4 (4.3 to 8.9)
7 days post treatment	9.5 (8.7 to 11.5)	9.9 (8.5 to 15.4)
Change over 7 days	2.5 (3.2)	4.8 (5)
Difference within group (p value)	0.12	0.04
Glycerol (High insulin), µmol/L		
Baseline	6.34 (2.58)	5.7 (1.8)
7 days post treatment	6.57 (1.52)	8.2 (4.8)

Change over 7 days	0.2 (2)	2.5 (4.5)
Difference within group (p value)	0.76	0.2
OHB (Basal), µmol/L		
Baseline	60.3 (42.3 to 67.1)	53.8 (45.8 to 66.9)
7 days post treatment	64.4 (43.1 to 99.5)	60.4 (54.9 to 85.3)
Change over 7 days	9 (81.7)	28.5 (69.5)
Difference within group (p value)	0.84	0.56
OHB (Low insulin), µmol/L		
Baseline	18.8 (13.3 to 28.7)	19.4 (16.5 to 21.6)
7 days post treatment	27.7 (20.8 to 28.5)	27.7 (20.3 to 34.2)
Change over 7 days	3 (2.8 to 7)	8.4 (7.4)
Difference within group (p value)	0.44	0.04
OHB (High insulin), µmol/L		
Baseline	12.23 (3.71)	14.9 (2.8)
7 days post treatment	13.11 (2.9)	14.1 (3.7)
Change over 7 days	0.7 (2.1)	-0.8 (3.7)
Difference within group (p value)	0.32	0.61
Ra Palmitate (Basal), mg/Kg•min		
Baseline	1.53 (1.24 to 1.74)	1.66 (1.56 to 1.89)
7 days post treatment	1.59 (1.44 to 1.68)	1.96 (1.68 to 2.12)
Change over 7 days	-0.05 (0.3)	0.41 (0.9)
Difference within group (p value)	0.73	0.2
Ra Palmitate (Low insulin), mg/Kg•min		
Baseline	0.52 (0.47 to 0.6)	0.56 (0.48 to 0.73)
7 days post treatment	0.68 (0.53 to 0.7)	0.75 (0.54 to 1.06)
Change over 7 days	0.01 (-0.01 to 0.11)	0.25 (-0.01 to 0.41)
Difference within group (p value)	0.69	0.16
Ra Palmitate (High insulin), mg/Kg•min		
Baseline	0.37 (0.31 to 0.43)	0.59 (0.48 to 0.69)
7 days post treatment	0.44 (0.35 to 0.46)	0.48 (0.35 to 0.8)
Change over 7 days	0 (0.07)	-0.03 (-0.16 to 0.22)
Difference within group (p value)	0.81	0.67

Table 3-4 *The effect of prednisolone and co-administration of prednisolone and a 5αRI on glucose and lipid metabolism during a two-step hyperinsulinaemic euglycaemic clamp. Data are mean (SD) or median (IQR). *P <0.05, difference in change over 7 days between the two groups.*

3.4 Discussion

In this proof-of-concept, experimental medicine study, we have shown that the metabolic impact of prednisolone (10mg daily) for 7 days is relatively modest.

However, when co-administered with a 5αRI, circulating prednisolone levels are increased and the adverse metabolic effects of prednisolone on peripheral, hepatic and adipose tissue insulin sensitivity are augmented. Whilst in the acute phases of immune and inflammatory conditions, dose of prednisolone higher than 10mg are often used, longer-term maintenance doses are often lower and therefore co-administration of drugs that can impact on prednisolone metabolism may well have a clinical impact. Given that combined administration is not infrequent either in men with BPH or in women with PCOS, these data have broad clinical implications.

Previous studies have examined the metabolic effects of short-term isolated GC treatment, including both prednisolone and hydrocortisone. High doses (30-75mg) of prednisolone for 1-15 days' duration causes pancreatic β-cell dysfunction and reduced glucose tolerance (44, 234). In healthy male volunteers, treatment with low (7.5mg) and high (30mg) dose prednisolone for 2 weeks decreased the ability of insulin to suppress EGP and lipolysis, and high- (but not low-) dose treatment decreased glucose disposal and increased fasting insulin levels (235, 236). In patients with inflammatory rheumatologic disease, a 7-10-day course of prednisolone (6mg) increased basal EGP, reduced glucose disposal and increased peripheral insulin resistance (237, 238). These data are consistent with the current study, although the magnitude of effect that we observed with prednisolone treatment alone was less than in the published studies and this is likely to reflect the fact that this was a shorter treatment duration (1-week). Both dose, and duration are important and we have shown that acute administration of high-dose of intravenous hydrocortisone (0.2 mg/kg•hr) increases EGP, limits glucose disposal and induces systemic insulin resistance (239).

The role of 5αRs in the regulation of metabolic phenotype is still not entirely understood. Cross-sectional observation studies provided the first evidence of dysregulation of 5αR activity, demonstrating increased activity with weight gain and insulin resistance and reduced activity with weight loss (201-203). In rodent models, 5αR1 KO male mice are more prone to the development of glucose intolerance as well as hepatosteatosis and liver fibrosis (198, 199). It is important to note however, that mice (contrasting with humans) do not express 5αR2 in the liver and therefore direct extrapolation to clinical studies cannot be made.

Very few translational, interventional clinical studies have been performed. A retrospective clinical analysis has suggested that long-tern dutasteride treatment is associated with hyperglycaemia and adverse circuiting lipid profiles (240). In smaller mechanistic studies, isolated treatment with dutasteride alone have demonstrated increased skeletal muscle and hepatic insulin resistance and increased hepatic triglyceride content (208, 213). Finasteride was without effect, suggestive of a specific role for 5αR1. More recently, data have been published suggesting an increased risk of incident T2DM associated with both dutasteride and finasteride (214) although the analysis did not examine the impact of co-prescription of these medications with GCs.

Building on the established role of the 5αRs in glucocorticoid metabolism (241), the aim of the current study was to test the impact of co-administration of prednisolone and 5αRIs. We have previously shown that both finasteride (5mg daily) and dutasteride (0.5mg daily) (in the absence of exogenous GC, for a 3-week duration) have no impact on fasting glucose, fasting insulin, M-value across a 2-step

hyperinsulinaemic euglycaemic clamp, Ra glucose, M-value, Gd, circulating NEFA or Ra glycerol (213). We have therefore concluded that the changes that we observed in the prednisolone + 5αRI arm of this study are due to the combination of treatment rather than the 5αRI treatment alone. This study therefore provides the first evidence to suggest that co-administration of GC and 5αRI can precipitate the development of adverse metabolic consequences.

There are very few differences in GC metabolites when comparing individuals taking finasteride or dutasteride (213). The limited additional impact of combined 5αR1 and 2 inhibition suggests that 5αR2 may be most critical for glucocorticoid metabolism. Our data would endorse this observation; our subgroup analysis showed the impact of finasteride was similar (or indeed slightly more marked) than that of dutasteride.

There are many examples of co-prescriptions of medications altering GC half-life and availability with resultant adverse metabolic effects. In particular, ritonavir, itraconazole, erythromycin, cyclosporin and oral contraceptives have been shown to increase circulating GC levels (221, 222, 242). In contrast, drugs such as carbamazepine, phenytoin, phenobarbital, rifampicin decrease GC levels due to increased P-450 activity (221, 222, 242). In cases were these medications are co-administered with GCs dose adjustments and vigilance as to the development of adverse effects need to be considered.

There are a number of limitations to this study; the sample size is modest although does reflect the complex and sensitive nature of the investigations that were performed. We did not include a dedicated arm of participants treated with 5αRI alone

as we have already reported findings from participants treated in this way (213). Whilst it is established that 5αRs are able to metabolise prednisolone and prednisone (243), there are very limited data with respect to other synthetic GCs and therefore it may not be possible to extrapolate our findings to all prescribed steroids across all routes of administration.

In conclusion, we have demonstrated for the first time that co-administration of prednisolone with a 5αRI worsens metabolic phenotype. These data not only demonstrate the potent ability of the pre-receptor 5αR system to regulate exogenous GC action, but raise important clinical questions with respect to vigilance and surveillance for adverse effects as well as the potential need to consider dose adjustments.

4 Targeting Iatrogenic Cushing's Syndrome with 11β-hydroxysteroid dehydrogenase type 1 Inhibition (TICSI)

4.1 Introduction

As mentioned in **Chapter 3**, GC therapy is prescribed to 2-3% of the population of the United Kingdom and United States for their anti-inflammatory actions (93). Despite their therapeutic efficacy, GC use is associated with significant adverse effects including obesity, skeletal muscle myopathy, skin thinning, hypertension, osteoporosis, insulin resistance and T2DM, collectively termed '*Iatrogenic Cushing's syndrome'*. Adverse effects are not limited to chronic use; frequent short-term GC administration is associated with increased morbidity and mortality (92). Despite the health burden associated with these adverse effects, there are currently no licenced therapies that are able to ameliorate this detrimental side effect profile, without compromise to the desirable anti-inflammatory actions of GCs.

At a cellular level, the ability of GCs to bind and activate the GR, is controlled by a series of enzymes including the 11β-hydroxysteroid dehydrogenases (11β-HSD1 and 2) that interconvert active and inactive GCs (107). 11β-HSD2, is highly expressed in the kidney and rapidly inactivates cortisol to cortisone as well as synthetic prednisolone to inactive prednisone. Within metabolic tissues, including liver, skeletal muscle and adipose tissue, GCs are reactivated by 11β-HSD1, converting inactive cortisone to active cortisol as well as inactive prednisone to active prednisolone (244).

In preclinical studies, we have shown that 11β-HSD1 is critical in regulating the development of the adverse features associated with circulating GC excess. 11β-HSD1 KO mice fail to develop a classical Cushing's phenotype despite circulating GC excess (135, 245) and this is critically dependent upon adipose tissue 11β-HSD1

expression (135). Endorsing these rodent data, two patients with Cushing's were previously described, who were protected from the severe adverse effects of endogenous GC excess due to a functional deficit in 11β-HSD1 activity (96, 97).

Highly potent and selective 11β-HSD1 inhibitors have been developed, initially as a potential therapy for patients with T2DM and metabolic disease, although their beneficial effects were modest (184, 185, 246). To date, their ability to limit the adverse effects of prescribed exogenous GC therapy has not been tested. AZD4017 is a potent, competitive inhibitor of human 11β-HSD1 that is safe and well-tolerated in clinical studies (247, 248); urinary steroid metabolite analysis has shown global inhibition of 11β-HSD1 to levels similar to those observed in patients with inactivating mutations in the HSD11B1 gene (104). A recent study has suggested that AZD4017 may reduce intracranial pressure in patients with idiopathic intracranial hypertension (IIH) (248).

Taking into account both the role of 11β-HSD1 to regenerate active GC and its tissue distribution (high levels of expression in metabolic tissues e.g. liver, adipose, skeletal muscle, and low levels of expression in immune-inflammatory cells), we have hypothesised that selective and specific inhibition of 11β-HSD1 may represent an entirely novel strategy to limit the adverse effects of prescribed GCs without compromise to their anti-inflammatory actions.

Adopting an experimental medicine, proof-of-concept approach the first randomized, double-blind placebo-controlled study to test whether AZD4017 is able to limit the

adverse metabolic and bone effects of prednisolone (20mg daily for 7 days) in healthy male volunteers was performed.

4.2 Methods

4.2.1 Research strategy

In this chapter, we will evaluate the impact of the selective 11β-HSD1 inhibitor, AZD4017, in healthy volunteers taking exogenous glucocorticoids (prednisolone). 30 healthy male volunteers underwent detailed metabolic assessments to demonstrate the beneficial effect of AZD4017 upon the metabolic adverse effects of prednisolone such as glucose disposal and endogenous glucose production rates. This study also evaluated the impact of AZD4017 on the anti-inflammatory actions of prednisolone. The hypothesis tests by this study was that the adverse metabolic effects of prednisolone will be reduced by co-administration of AZD4017.

4.2.2 Statement of contributions

This study was designed by Prof Jeremy Tomlinson and implemented by myself and Dr Riccardo Pofi. Joanne Duffy and Prof Craig Webster processed serum samples to obtain prednisolone, prednisone, cortisol and cortisone levels, at the University Hospitals Birmingham NHS Foundation Trust, UK, as described in **Chapter 2**. Dr Elizabeth Bateman and Dr Ross Sadler processed serum samples to assess the immune response to VZV and PHA using an OX40 assay, at Churchill Hospital, Oxford, UK. Dr Roland Stimson run ~15% of the microdialysis samples, at the University of Edinburgh, UK, due to a machine failure. The samples were run on an identical machine, with appropriate calibration and quality checks. Dr Andre van Beek and Dr Martijn van Faassen processed the over-night urine samples to check the urinary

levels of cortisol, cortisone, THF, allo-THF and THE, at the University of Groningen, The Netherlands. The rest of the samples were processed by myself with laboratory advice by Thomas Cornfield, Dr Jonathan Hazlehurst and Dr Nikolaos Nikolaou. I received laboratory support in RNA extractions by Anastasia Arvaniti. I undertook all of the analyses, with the exception of the comparisons between changes in the two groups using non-linear generalised model which was done by Dr Ruth Coleman.

4.2.3 Clinical Protocol

The clinical protocol received full ethical approval from the East of England Cambridge East Research Ethics Committee (reference 16/EE/0550). Thirty healthy male volunteers were recruited from local advertisement and the Oxford Biobank, (reference 08/H0606/107+5).

Inclusion criteria

- Male volunteers without diabetes (HbA_{1C} < 48mmol/mol at screening)
- BMI 20-30kg/m^2
- Age 18-60 years
- BP <160/100mmHg or on stable antihypertensive therapy for >3 months
- No known hypercholesterolaemia or on stable lipid lowering therapy for >3 months
- No contraindications to AZD4017 or prednisolone treatment

Exclusion criteria

- Age <18 or >60 years
- Body mass index <20 or >30kg/m^2

- Diagnosis of diabetes (type 1 or type 2)
- Haemoglobin <120mg/dL
- Haemorrhagic disorders
- Anticoagulant treatment
- Renal impairment with eGFR <60ml/min
- Abnormal liver chemistry with AST, ALT and/or GGT and/or bilirubin >ULN
- Glucocorticoid therapy (including inhaled, topical or oral) within the last 6 months
- Concomitant anti-inflammatory medication including NSAIDs, disease modifying anti-rheumatic drugs (DMARDs) / steroid-sparing medications (e.g. methotrexate, sulphasalzine, hydroxychloroquine, azathioprine, leflunamide, biologics [anti-TNFa, IL-1ra])
- Any medical condition in the opinion of the investigator that might impact upon safety or validity of the results – recent (within 2 weeks) or active infection, known liver disease, known thyroid disease, active malignancy, existing inflammatory condition (e.g. inflammatory arthropathy, inflammatory bowel disease, autoimmune disease, connective tissue disease)
- Current evidence of alcohol abuse or a significant history of alcohol abuse, as judged by the investigator
- Contraindication to any of the study treatments or known or suspected hypersensitivity to the investigational product, compounds of the same class, other study treatments or any excipients
- Unwilling, or unable, to give informed consent
- Participation in another IMP trial / study within the past 6 months

The clinical study comprised of 6 study visits which are presented in **Figure 4.2-1** as a schematic summary of the investigations performed.

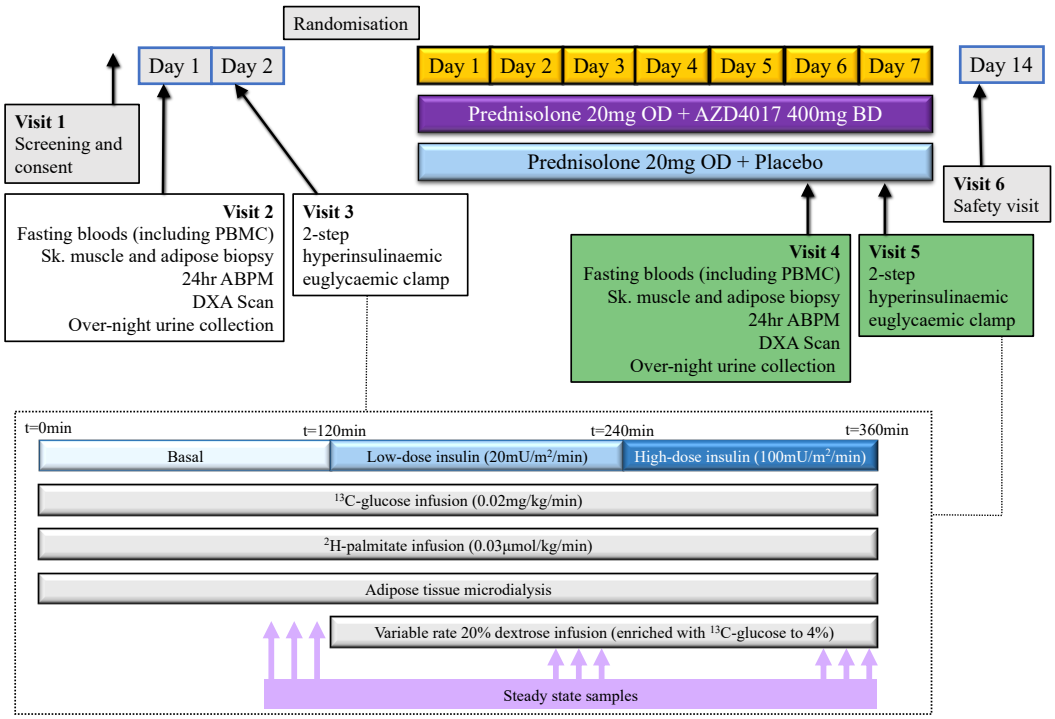

Figure 4.2-1 *TICSI Study design Participants were screened and consented at Visit 1. At Visit 2, they had fasting bloods, skeletal muscle and adipose tissue biopsies, DEXA scan, were given a sample bottle to collect over-night urine and were fitted with a 24 hr ambulatory blood pressure monitor. At Visit 3, they underwent 2-step hyperinsulinaemic euglycaemic clamp and they were randomized to receive prednisolone 20mg OD and AZD4017 400mg BD for 7 days or prednisolone 20mg OD and placebo for 7 days. At Visit 4, they underwent identical assessments to those described at Visit 2 and at Visit 5, the 2-step hyperinsulinaemic euglycaemic clamp was repeated.*

Study visits

Visit 1 (Screening and consent):

Participants were screened for eligibility and baseline assessments were done which included:

- Height and weight measurements

- Blood tests: full blood count, urea, creatinine, electrolytes and eGFR, AST, ALT, γGT, bilirubin, ALP, albumin, glycated haemoglobin, TSH, free T4, hepatitis B, C and HIV serology
- Blood pressure

Visit 2 (Pre-treatment Day 1) (within 3 weeks of Visit 1):

The participants attended the Clinical Research Unit (CRU), at Oxford Centre for Diabetes, Endocrinology and Metabolism (OCDEM), Churchill Hospital (Oxford, UK) at 8:00 AM following a 12 hour fast.

Fasting blood tests were taken which included:

- Urea, creatinine, electrolytes and eGFR, AST, ALT, γGT, bilirubin, ALP, albumin, creatinine kinase, TSH and free T4
- ACTH, cortisol, DHEAS, androstenedione, testosterone, sex hormone binding globulin
- Lipid profiles (total cholesterol, triglyceride, HDL cholesterol)
- Markers of bone turnover (osteocalcin)
- Isolation of peripheral blood mononuclear cells (for assessment of inflammatory response)

Subcutaneous adipose tissue biopsy was taken using a Pro-MagTM Ultra Biopsy 14g needle, a 20ml syringe and 100ml of 0.9% saline inserted into the abdominal subcutaneous tissue and adipocytes were aspirated using a negative pressure achieved with the needle and syringe. The skin had been cleaned and a local anaesthetic (3.5ml of 1% lidocaine) had been injected. Approximately 1g of tissue was taken and placed into liquid nitrogen.

Skeletal muscle biopsy was taken from the lateral part of the vastus lateralis muscle. Similarly to the adipose tissue biopsy method, the skin was cleaned and local anaesthetic was injected (3ml of 1% lidocaine). The skin was punctured with a 12g needle to allow entry of the biopsy needle. The spring-loaded gun device was then inserted vertically through the muscle fascia and into the muscle. The spring-loaded device was fired and the biopsy was taken (approximately 200-300mg). The procedure was repeated twice to ensure that adequate tissue samples were collected.
The participants then underwent a dual energy X-ray absorptiometry (DEXA) scan to assess total and regional lean and fat mass. Prior to leaving, they had a 24hour ambulatory blood pressure monitor fitted and were provided with a container to collect overnight urine for urinary steroid metabolite analysis.

Visit 3 (Pre-treatment Day 2):

The participants attended the CRU at 9:00 AM following a 12 hour fast. On this visit, an adipose tissue microdialysis catheter (CMA Microdialysis, Solna, Sweden) was inserted, as described in **Chapter 2**. Samples were taken every 30 minutes during the two-step hyperinsulinaemic euglycaemic clamp. Microdialysate fractions were analyzed by automated analyzer (ISCUS flex) for glycerol, glucose, lactate and pyruvate. Immediately prior to the clamp procedure, indirect calorimetry was taken using a transparent hood for 15 minutes to measure resting energy expenditure and respiratory quotient, in a similar manner as described in **Chapter 3**. The 2-step hyperinsulinaemic euglycaemic clamp was then performed, as described in **Chapter 2**. Throughout the clamp regular breath samples (every 30 minutes) were taken and blood samples over the course of the following 6 hours to assess the incorporation of

the stable-isotope into particles and molecules secreted by the liver and into the expired breath samples (Exetainer tubes, Labco Ltd, Bucks, UK).

At the end of this visit, the participants were randomized to receive prednisolone (20mg OD) and AZD4017 (400mg BD) for 7 days or prednisolone (20mg OD) and placebo (BD) for 7 days.

Visits 4 and 5 were scheduled within 2 weeks of visit 3 and the treatment was initiated 5 days prior to visit 4.

Visit 4 (Treatment Day 6):

Participants underwent identical assessments to those described for pre-treatment day 1 (visit 2). Volunteers took the prednisolone + AZD4017 or placebo on the morning of the investigations.

Visit 5 (Treatment Day 7):

Participants underwent identical assessments to those described for pre-treatment day 2 (visit 3). They took the prednisolone + AZD4017 or placebo on the morning of the investigations.

Visit 6 (Follow-up day 7):

7 days after the final treatment dose the participants came back for the final visit where the wounds of the biopsies were inspected and blood samples were taken to measure liver, renal and thyroid function, DHEAS, androstenedione and testosterone.

4.2.4 Osteocalcin ELISA

Serum osteocalcin was measured by commercially available enzyme-linked immunosorbent assay (ELISA) (Invitrogen, Frederick, USA). This assay uses monoclonal antibodies targeted against distinct epitopes of human osteocalcin. The plates provided were pre-coated with osteocalcin antibody (Mab1) and were loaded with sample and standard and osteocalcin antibody (Mab2) conjugated to horseradish peroxidase was also added. After incubation and washing, chromogenic solution was added and incubated. The reaction stopped following the addition of the Stop solution and the plate was read using a spectrophotometer at 450 nm. The concentration of samples was then calculated from a standard curve with a linear x-axis of the concentrations of the standards and a linear y-axis of the absorbance. The osteocalcin levels were processed using two plates and therefore the intra-assay co-efficient of variation of the osteocalcin ELISA could not be calculated.

4.2.5 OX40 assay

Heparin blood was collected from participants pre-treatment and 7 days post-treatment. Samples were processed as previously described (249). Each sample was tested for CD4+ T cell specific responses towards Phytohaemagluttinin (PHA) (Sigma-Aldrich) and varicella zoster virus (VZV) (Source-Bioscience). The number of antigen-specific CD4+ T cells was calculated for each stimulation and expressed as the relative percentage of CD25+CD134+CD4+CD3+ cells minus the equivalence analysis in unstimulated but incubated cells from the same sample. Values pre- and post-treatment were compared to determine a delta-change percentage of antigen specific CD4+ T cells.

4.2.6 Urinary steroid metabolites

Total urinary cortisol, cortisone, THF, allo-THF, and THE were measured by using a validated high-performance liquid chromatography tandem-mass spectrometry (LC-MS/MS) assay (250). For THE, THF, and allo-THF, the LC-MS/MS method was compared with a GC-MS/MS method and found the following correlations: THE r2 =0.99, THF r2 = 0.97, and allo-THF r2 =0.94 for 40 urines (251).

For all components, appropriate internal standards were added and the mixtures were incubated with an enzyme solution consisting of sulfatases and β-glucuronidases, to ensure hydrolysis of cortisol and the metabolites from their sulphated and glucuronidated forms. Internal standards that were used were cortisol-^{13}C3, cortisone-D7, THE-D5, THF-D5, and allo-THF-D5. Subsequently, the analytes were extracted using a Supported Liquid Extraction technique. Finally, separation and detection were performed by use of a Phenomenex Luna Phenyl-Hexyl column (particle size 3 μm, 2.0 mm internal diameter by 150 mm; Waters) and a XEVO TQ-s tandem mass spectrometer operated in negative electrospray ionization mode (Waters). Intra- and inter-assay variation coefficients were <5.7% and <9.8%, respectively.

4.2.7 Statistical analysis

The sample size required to detect a 20% Gd reduction with 80% power and a type I error of 0.05 was calculated to be 13 per group. Allowing for a potential dropout rate of 20%, 32 was the recruitment target for the study. Data are presented as mean (SD) or median (IQR) as appropriate. Generalised non-linear models were employed for comparison of change pre- and post-treatment visit measurements between the two groups for both primary and secondary endpoints. The model response (outcome) was

defined as the absolute change between visits and the model estimate (effect size) was adjusted for baseline (pre-treatment) value. Within group changes were determined using paired t-tests or Wilcoxon test according to the distribution of data, which was assessed by Shapiro-wilk test. These analyses were carried out using the per-protocol population tested at a significance level of 0.05. No adjustments were made for multiple testing.

Analyses were performed using SAS v9.4 (SAS Institute, Cary NC) and GraphPad Prism 8 software package (GraphPad Software, La Jolla, CA) for MacOS. All recruited participants were included in the safety analysis and all participants who completed the study as per protocol were included in the primary analysis.

4.3 Results

4.3.1 Demographics and clinical characteristics of the participants

42 participants were assessed for recruitment into the study; 10 failed the screening process and subsequently 32 participants were enrolled and randomized. The randomization schedule was drawn up by Almac group, who packaged and labelled AZD4017/placebo on behalf of AstraZeneca. Randomization was in blocks of 4 volunteers (2 AZD4017 and 2 to placebo). 16 participants were assigned to AZD4017 (400mg BD) plus prednisolone (20mg OD) and 16 to placebo plus prednisolone (20mg OD) (**Figure 4.3-1**). One participant from the AZD4017-treated group was excluded due to <85% compliance with study medication and one participant from the placebo-treated group was excluded for repeated failure to fast before study procedure. The participant baseline demographics and biochemical characteristics are shown in **Table 4-1**.

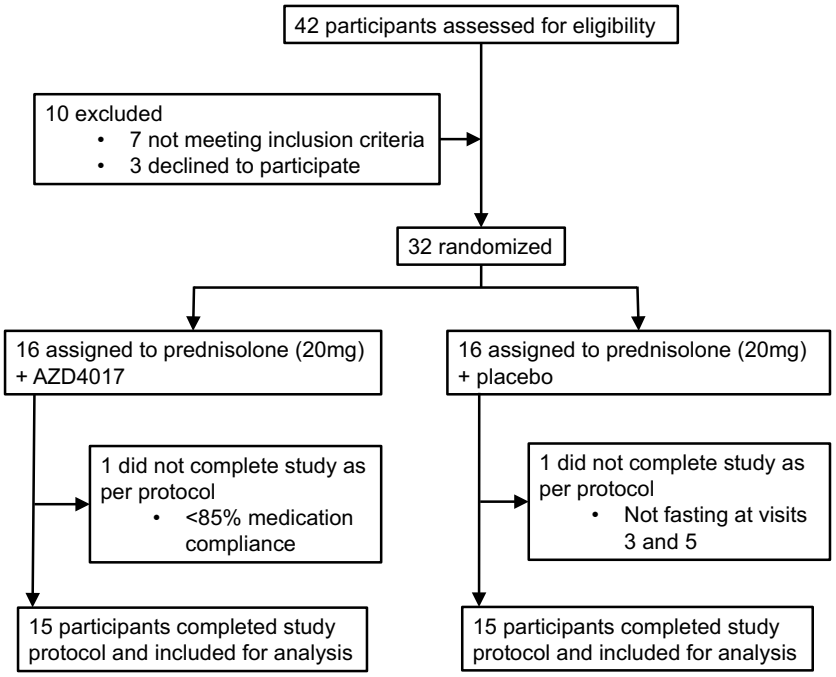

Figure 4.3-1 *TICSI Trial profile*

Clinical/metabolic variable	**AZD4017 (n=15)**	**Placebo (n=15)**	***P* value**
Age, yr	36.5 (11.0)	39.0 (12.7)	0.56
Weight, kg	79.9 (8.7)	83.1 (8.5)	0.32
BMI, kg/m^2	24.5 (2.5)	25.8 (2.0)	0.13
SBP, mm Hg	135.7 (10.6)	138.3 (14.4)	0.58
DBP, mm Hg	78.5 (9.8)	79.6 (11.4)	0.77
HbA1c, mmol/mol	34.0 (32.0 to 37.0)	35.0 (33.0 to 36.0)	0.49
Fasting glucose, mmol/L	4.6 (4.3 to 5.5)	4.9 (4.4 to 5.1)	0.89
Fasting insulin, mU/L	3.13 (1.79 to 6.60)	2.84 (1.36 to 5.17)	0.47
HDL cholesterol, mmol/L	1.3 (0.3)	1.3 (0.3)	0.99
Total cholesterol, mmol/L	5.0 (1.2)	4.6 (0.9)	0.26
AST, IU/L	21.3 (4.5)	21.6 (6.7)	0.9
Bilirubin, mmol/L	15.3 (5.3)	15.0 (5.6)	0.89
ALT, IU/L	21.0 (5.2)	18.8 (5.5)	0.27
ALP, IU/L	52.9 (8.9)	57.3 (11.5)	0.25

Albumin, g/L	39.5 (2.6)	38.5 (2.3)	0.28
TSH, mIU/L	1.4 (1.3 to 1.8)	1.5 (1.0 to 1.9)	0.69
Androstenedione, nmol/L	8.4 (5.9 to 9.4)	6.4 (5.3 to 8.1)	0.07
DHEAS, umol/L	11.2 (5.5 to 15.1)	6.7 (4.2 to 12.2)	0.25
SHBG, nmol/L	33.4 (16.5)	35.6 (15.9)	0.71
Testosterone, nmol/L	18.4 (15.0 to 23.1)	18.7 (13.6 to 22.0)	0.75
ACTH, ng/L	21.9 (18.1 to 52.9)	30.5 (16.9 to 54.6)	0.91
Cortisol, nmol/L	372.7 (117.2)	385.7 (77.1)	0.72

Table 4-1 *The demographic and biochemical profiles of the participants. Data are presented as mean (SD) or median (IQR).*

At baseline, circulating cortisol, cortisone and ACTH levels were not different between the two groups (**Table 4-1**). Whilst post-treatment circulating cortisol levels were similar (91 (54 to 127) vs. 61 (36 to 150) nmol/L, p=0·55, AZD4017 vs. placebo), cortisone levels were significantly higher in the AZD4017-treated group (46.5 (35.8 to 55.9) vs. 20.0 (20.0 to 41.4) nmol/L, p=0.004, AZD4017 vs. placebo). Post-treatment, ACTH levels decreased in the placebo (30.5 (16.9 to 54.6) vs. 11.7 (5.2 to 26.2) ng/L, p=0.030) but not in the AZD4017-treated group (21.9 (18.1 to 52.9) vs. 20.4 (9.0 to 42.4) ng/L, p=0.22).

After 7 days of treatment, circulating prednisolone levels were similar in the AZD4017 and placebo-treated groups (650 (282) vs. 722 (429) nmol/L, p=0.63, AZD4017 vs. placebo). Similarly, there were no differences in circulating prednisone levels (142 (62) vs. 103 (52) nmol/L, p=0.11, AZD4017 vs. placebo) or the prednisolone/prednisone ratio (4.89 (2.48) vs. 6.33 (3.11), p=0.22, AZD4017 vs. placebo).

Metabolic variable	AZD4017 + Prednisolone n=15	Placebo + Prednisolone n=15	Between group p value
Glucose disposal (low insulin) (mg/Kg•min)			
Baseline	4.59 (1.98)	4.61 (2.28)	
7 days post treatment	4 (2.65)	3.06 (1.48)	
Change over 7 days	-0.81 (-1.91 to -0.28)	-1.35 (-2.43 to -0.26)	0.17
Difference within group (p value)	0.32	0.009	
Glucose disposal (high insulin) (mg/Kg•min)			
Baseline	13.13 (3.67)	12.72 (3.73)	
7 days post treatment	10.97 (3.26)	9.83 (2.33)	
Change over 7 days	-2.16 (2.89)	-2.88 (2.91)	0.26
Difference within group (p value)	0.012	0.0018	
M value (Low insulin) (mg/Kg•min)			
Baseline	5.42 (3.33 to 6.51)	4.47 (3.31 to 6.61)	
7 days post treatment	3.75 (1.99 to 5.05)	2.95 (2.35 to 3.96)	
Change over 7 days	-1.06 (2.29)	-1.69 (1.93)	0.32
Difference within group (p value)	0.064	0.0044	
M value (High insulin) (mg/Kg•min)			
Baseline	13.38 (2.87)	13.22 (3.55)	
7 days post treatment	11.42 (3.4)	10.17 (2.23)	
Change over 7 days	-1.96 (3.19)	-3.05 (2.6)	0.38
Difference within group (p value)	0.032	0.00046	
M/I value (Low insulin) (mg/Kg•min per mU/mL)			
Baseline	28.11 (16.58 to 37)	30.98 (18.72 to 35.45)	
7 days post treatment	17.19 (6.83 to 28.01)	14.41 (9.56 to 18.04)	
Change over 7 days	-2.67 (17.48)	-10.6 (10.33)	0.15
Difference within group (p value)	0.63	0.0014	
M/I value (High insulin) (mg/Kg•min per mU/mL)			
Baseline	13.26 (10.01 to 15.2)	15.44 (11.07 to 18.66)	
7 days post treatment	14.71 (8.84 to 16.68)	9.87 (7.41 to 11.99)	
Change over 7 days	-0.51 (-3.76 to 2.53)	-3.72 (-7.25 to -0.98)	0.17
Difference within group (p value)	0.71	0.0049	
Ra Glucose (mg/Kg•min)			
Baseline	1.34 (1.23 to 1.47)	1.35 (1.26 to 1.44)	
7 days post treatment	1.44 (1.34 to 1.47)	1.42 (1.35 to 1.47)	
Change over 7 days	0.08 (-0.02 to 0.12)	0.06 (-0.02 to 0.13)	0.55
Difference within group (p value)	0.048	0.051	

EGP (mg/Kg•min)			
Baseline	0.66 (0.61 to 0.78)	0.68 (0.55 to 0.87)	
7 days post treatment	0.81 (0.71 to 0.94)	1 (0.97 to 1.17)	
Change over 7 days	0.16 (-0.03 to 0.29)	0.35 (0.12 to 0.49)	0.11
Difference within group (p value)	0.016	0.013	
13-CO2 Breath (Basal) AUC (mmol/hr/Kg)			
Baseline	0.023 (0.021 to 0.028)	0.024 (0.022 to 0.026)	
7 days post treatment	0.021 (0.019 to 0.024)	0.024 (0.021 to 0.026)	
Change over 7 days	-0.002 (-0.004 to -0.001)	-0.001 (-0.003 to 0)	0.42
Difference within group (p value)	0.0003	0.15	
13-CO2 Breath (Low insulin) AUC (mmol/hr/Kg)			
Baseline	0.032 (0.029 to 0.035)	0.033 (0.03 to 0.036)	
7 days post treatment	0.029 (0.025 to 0.032)	0.028 (0.026 to 0.028)	
Change over 7 days	-0.003 (0.004)	-0.006 (0.004)	0.2
Difference within group (p value)	0.013	0.0006	
13-CO2 Breath (High insulin) AUC (mmol/hr/Kg)			
Baseline	0.084 (0.078 to 0.09)	0.081 (0.074 to 0.094)	
7 days post treatment	0.077 (0.067 to 0.085)	0.072 (0.066 to 0.08)	
Change over 7 days	-0.006 (0.011)	-0.009 (0.016)	0.68
Difference within group (p value)	0.048	0.057	
Fasting glucose (mmol/L)			
Baseline	4.6 (4.4 to 5.4)	4.9 (4.5 to 5.1)	
7 days post treatment	4.9 (4.7 to 5.6)	4.9 (4.8 to 5.1)	
Change over 7 days	0.26 (0.33)	0.11 (0.47)	0.24
Difference within group (p value)	0.0095	0.37	
Fasting Insulin (mU/L)			
Baseline	3.13 (1.8 to 6.18)	2.84 (1.4 to 4.88)	
7 days post treatment	2.28 (1.2 to 5.32)	3.77 (2.2 to 5.01)	
Change over 7 days	-0.2 (2.94)	0.48 (1.99)	0.63
Difference within group (p value)	0.89	0.36	

Table 4-2 *The effect of AZD4017 + prednisolone and placebo + prednisolone on glucose metabolism during a two-step hyperinsulinaemic euglycaemic clamp. Data are mean (SD) or median (IQR).*

Prior to treatment, the urinary (allo-THF+THF)/THE ratio (indicative of 11β-HSD1 activity) was similar in both groups (0.85 (0.19) vs. 1.04 (0.37), p=0.08, AZD4017

vs. placebo). Consistent with 11β-HSD1 inhibition, after 7 days of treatment, the (allo-THF+THF)/THE ratio was significantly lower in the AZD4017 group (0.068 (0.059 to 0.086) vs. 0.99 (0.87 to 1.25), p<0.0001, AZD4017 vs. placebo). The urinary cortisol/cortisone (reflecting 11β-HSD2 activity) ratio was similar in both groups at baseline and did not change following treatment (0.64 (0.57 to 0.76) vs. 0.71 (0.55 to 0.82), p=0·62, AZD4017 vs. placebo).

Fasting glucose increased in the prednisolone + AZD4017, but not the placebo-treated group. Fasting insulin levels did not change in either group (**Table 4-2**).

4.3.2 Hepatic insulin sensitivity

In both groups, Ra Glucose and EGP increased after 7 days of treatment; there were no significant differences between the groups (**Table 4-2**, **Figure 4.3-2** A-D).

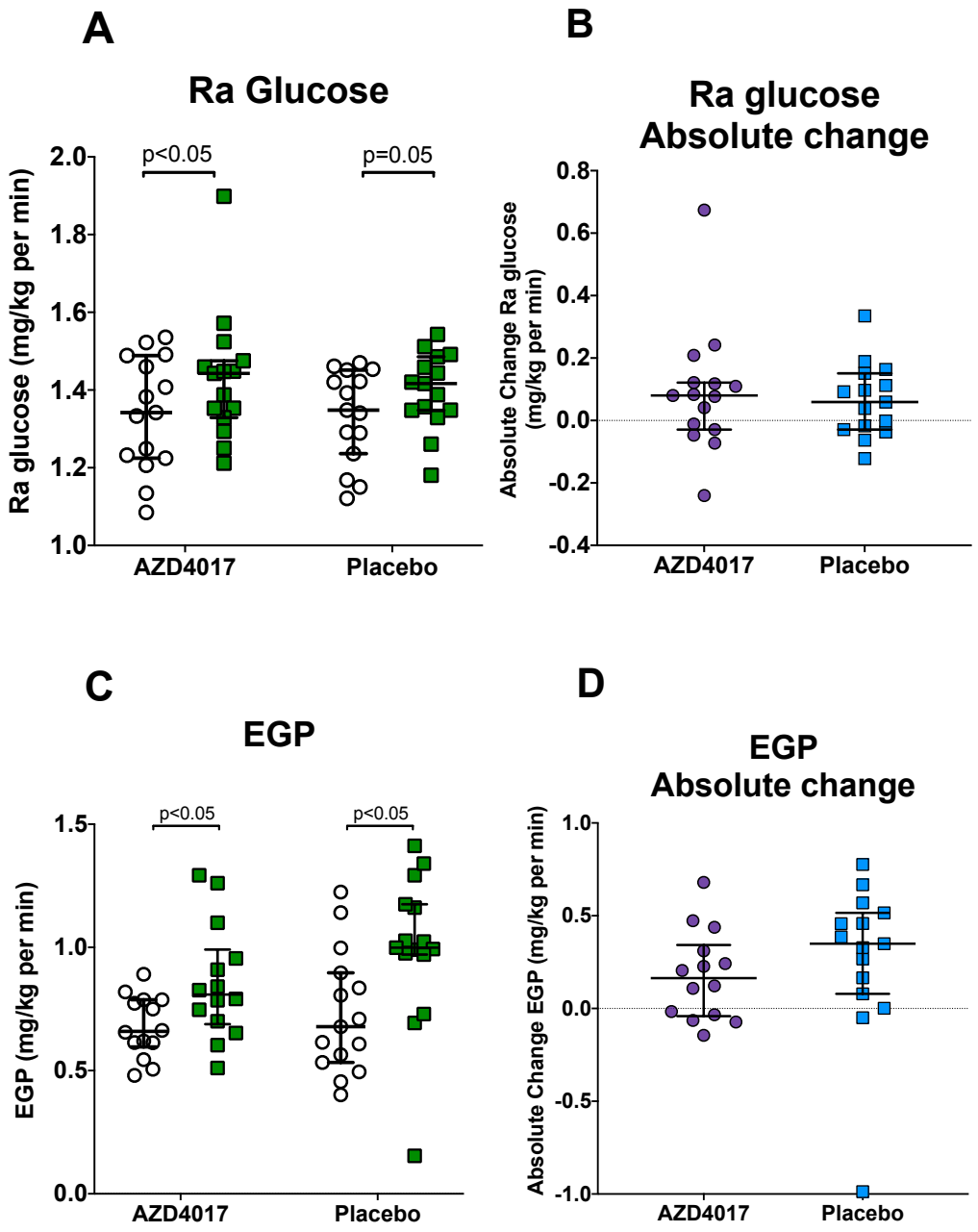

Figure 4.3-2 *The effect of prednisolone + AZD4017 and prednisolone + placebo on Ra glucose (A and B) and endogenous glucose production (EGP) (C and D) during a two-step hyperinsulinaemic euglycaemic clamp. Absolute change refers to the difference between pre- and post-treatment values (B and D). Data are medians and error bars are IQR. Datapoints represent individual patients. White circles represent pre-treatment levels and green squares post-treatment levels (7 days), purple circles are AZD4017 and blue squares, placebo.*

4.3.3 Peripheral insulin resistance

The primary endpoint of the study (change in stable isotope-measured Gd (low insulin) after 7 days of treatment), was not different between the two groups (-0.81 (-1.91 to -0.28) vs. -1.35 (-2.43 to -0.26), p=0.17, AZD4017 vs. placebo). However, treatment with prednisolone + placebo significantly reduced Gd under low-dose insulin infusion (4.61 (2.28) vs. 3.06 (1.48) mg/kg•min, p=0.0090, pre- vs. post-treatment), whereas co-administration of prednisolone with AZD4017 had no effect (4.59 (1.98) vs. 4.00 (2.65) mg/kg•min, p=0.32, pre- vs. post-treatment) (**Table 4-2**). Similarly, glucose utilization (corrected for circulating insulin levels, M/I-value) decreased following treatment with prednisolone + placebo during both low- and high-dose insulin infusions **Table 4-2**). In contrast, there was no change in M/I-value (low- or high-dose insulin) in prednisolone + AZD4017 treated group (**Figure 4.3-3**, **Table 4-2**): The absolute changes in Gd or M/I-value were not significantly different between the two arms of the study (**Figure 4.3-3** B and D, **Table 4-2**).

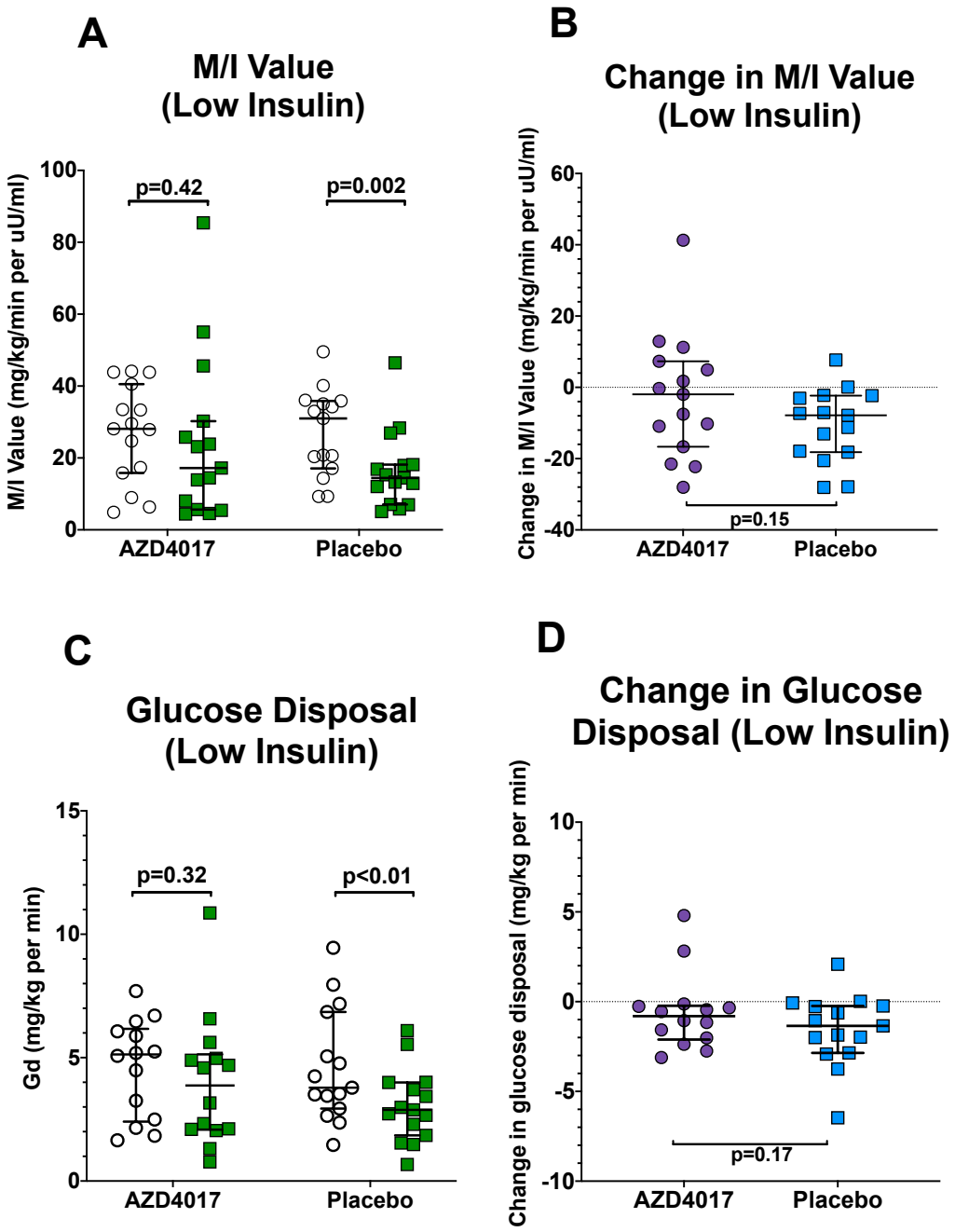

Figure 4.3-3 *The effect of prednisolone + AZD4017 and prednisolone + placebo on the M/I value (A and B) and glucose disposal (Gd) (C and D) during the low-dose insulin step of the two-step hyperinsulinaemic euglycaemic clamp. Absolute change refers to the difference between pre- and post-treatment values (B and D). Data are medians and error bars are IQR. Datapoints represent individual patients. White circles represent pre-treatment levels and green squares post-treatment levels (7 days), purple circles are AZD4017 and blue squares, placebo.*

4.3.4 Glucose oxidation

As mentioned in **Chapter 3**, $^{13}CO_2$ production from the infused [U-^{13}C]-glucose was used as a marker of glucose uptake and subsequent oxidation. Co-administration of prednisolone + AZD4017 significantly decreased glucose oxidation across the 2-step clamp (both low- and high-dose insulin phases) but there was a more significant decrease following prednisolone + placebo ($p<0.001$) under low-dose insulin (**Table 4-2Table 2-1**) (**Figure 4.3-4** A and C). There was no significant change under high-dose insulin conditions in the prednisolone + placebo group. The absolute change between the two groups, under both low- and high-dose insulin phases, was not different (**Table 4-2**) (**Figure 4.3-4** B and D).

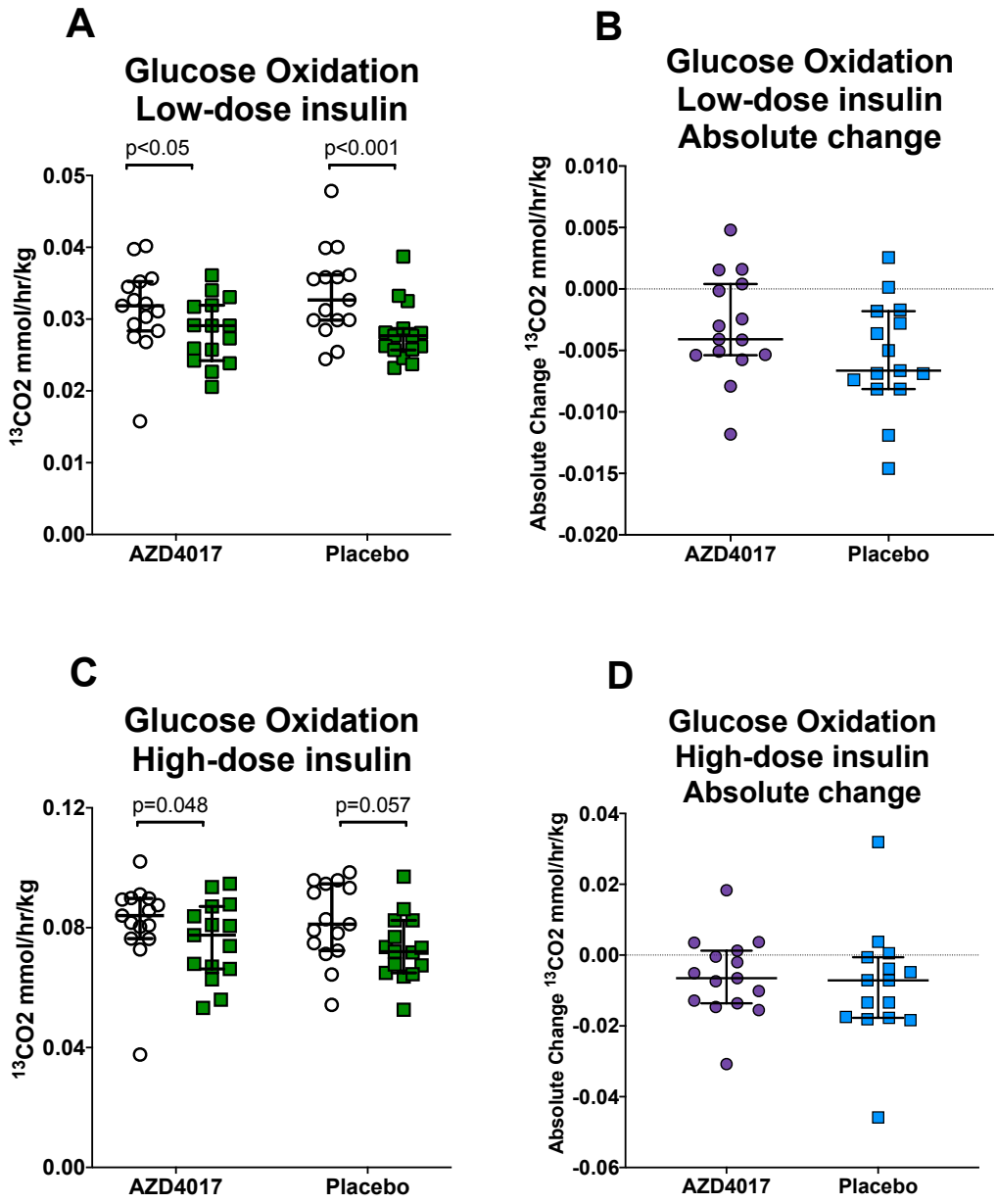

Figure 4.3-4 *The effect of prednisolone + AZD4017 and prednisolone + placebo on glucose oxidation during the low-dose insulin step (A and B) and the high-dose insulin step (C and D) of the two-step hyperinsulinaemic euglycaemic clamp. Absolute change refers to the difference between pre- and post-treatment values (B and D). Data are medians and error bars are IQR. Datapoints represent individual patients. White circles represent pre-treatment levels and green squares post-treatment levels (7 days) purple circles are AZD4017 and blue squares, placebo.*

Metabolic variable	AZD4017 + Prednisolone n=15	Placebo + Prednisolone n=15	Between group p value
NEFA (Basal) (µmol/L)			
Baseline	309.9 (257.9 to 423.1)	278.9 (243.2 to 433.1)	
7 days post treatment	452.1 (266.9 to 667.8)	452.7 (294.9 to 629.9)	
Change over 7 days	-4.6 (-93.4 to 241.2)	129.2 (-5.1 to 196.9)	0.72
Difference within group (p value)	0.36	0.073	
NEFA (Low insulin) (µmol/L)			
Baseline	71.9 (54.7 to 125.3)	83.7 (52.7 to 141.3)	
7 days post treatment	155 (62.5 to 216.8)	129.3 (98.2 to 299.6)	
Change over 7 days	2.4 (-4.1 to 69.5)	33.2 (21.3 to 71.4)	0.25
Difference within group (p value)	0.36	0.073	
NEFA (High insulin) (µmol/L)			
Baseline	57.9 (35.4 to 135.1)	54.3 (42.3 to 139.2)	
7 days post treatment	57.2 (38.2 to 95.8)	68.3 (46.3 to 218.6)	
Change over 7 days	1.2 (-9.5 to 43.4)	16.3 (2.1 to 55.8)	0.66
Difference within group (p value)	0.6	0.022	
Glycerol (Basal) (µmol/L)			
Baseline	22.6 (16.2 to 26.8)	20 (17.8 to 24.8)	
7 days post treatment	25.8 (20.1 to 31.5)	27.2 (20 to 35.2)	
Change over 7 days	3.3 (10.3)	8.3 (9.9)	0.39
Difference within group (p value)	0.36	0.0056	
Glycerol (Low insulin) (µmol/L)			
Baseline	8.7 (5)	7.6 (3)	
7 days post treatment	10.5 (6.3)	12.3 (3.5)	
Change over 7 days	1.5 (0.4 to 2.7)	4.1 (3.3 to 6)	0.11
Difference within group (p value)	0.21	<0.0001	
Glycerol (High insulin) (µmol/L)			
Baseline	5.8 (4.6 to 10.9)	6.8 (4.7 to 8.6)	
7 days post treatment	6.3 (5.2 to 11.2)	9.5 (8.4 to 14.6)	
Change over 7 days	0.2 (-1.2 to 1.1)	2.8 (1.9 to 4.9)	0.089
Difference within group (p value)	0.93	0.00016	
OHB (Basal) (µmol/L)			
Baseline	59.4 (35.5 to 93.8)	39 (29 to 83.8)	
7 days post treatment	40.8 (33.8 to 123.1)	45.9 (31.4 to 82)	
Change over 7 days	1.1 (-24.3 to 20.1)	1.1 (-8.9 to 12.8)	0.28
Difference within group (p value)	0.99	0.95	

OHB (Low insulin) (µmol/L)			
Baseline	17 (11.4 to 27.8)	15.8 (11.2 to 22.2)	
7 days post treatment	16.7 (7.8 to 28)	18.8 (13.3 to 25.4)	
Change over 7 days	-0.5 (-3.7 to 2.9)	4.6 (0.4 to 6.8)	0.64
Difference within group (p value)	0.7	0.13	
OHB (High insulin) (µmol/L)			
Baseline	9.7 (7.8 to 16.8)	12.2 (7 to 17.9)	
7 days post treatment	10.4 (6.8 to 14.7)	14.9 (8.4 to 23.5)	
Change over 7 days	-1.8 (3.8)	3.3 (6.3)	0.016
Difference within group (p value)	0.24	0.049	
TAG (Basal) (µmol/L)			
Baseline	370.2 (339.2 to 610)	365.1 (302.5 to 597.9)	
7 days post treatment	374 (313.7 to 493)	590.9 (526.3 to 879.9)	
Change over 7 days	-50 (198.4)	258.2 (240.7)	0.001
Difference within group (p value)	0.35	0.004	
TAG (Low insulin) (µmol/L)			
Baseline	306.2 (250.8 to 539.8)	260.3 (213.7 to 477.8)	
7 days post treatment	259.2 (172.4 to 362.2)	386.1 (281.4 to 534.9)	
Change over 7 days	-46.9 (-134.9 to 3.5)	125.8 (18 to 155.9)	0.0014
Difference within group (p value)	0.026	0.018	
TAG (High insulin) (µmol/L)			
Baseline	233.3 (188.5 to 448.9)	179.5 (157.9 to 428.1)	
7 days post treatment	182.4 (151.9 to 240.7)	248.9 (204.5 to 380.7)	
Change over 7 days	-40.7 (-190.5 to 2.4)	58.1 (-6.9 to 90.2)	0.0069
Difference within group (p value)	0.026	0.15	
Ra Palmitate (Basal) (mg/kg•min)			
Baseline	1.9 (0.46)	1.93 (0.69)	
7 days post treatment	1.99 (0.78)	1.82 (0.59)	
Change over 7 days	0.1 (0.86)	-0.12 (0.69)	0.51
Difference within group (p value)	0.71	0.57	
Ra Palmitate (Low insulin) (mg/kg•min)			
Baseline	0.66 (0.56 to 0.94)	0.67 (0.47 to 0.98)	
7 days post treatment	0.81 (0.69 to 1.16)	0.81 (0.71 to 0.95)	
Change over 7 days	0.1 (-0.05 to 0.41)	0.16 (-0.15 to 0.32)	0.62
Difference within group (p value)	0.32	0.52	
Ra Palmitate (High insulin) (mg/kg•min)			
Baseline	0.77 (0.68 to 0.97)	0.67 (0.5 to 1.06)	
7 days post treatment	0.6 (0.51 to 0.86)	0.64 (0.55 to 0.82)	
Change over 7 days	-0.17 (-0.44 to -0.03)	-0.03 (-0.22 to 0.15)	0.31

Difference within group (p value)	0.024	0.79	
Adipose interstitial fluid - Glycerol (Basal) (µmol/L•hr)			
Baseline	219.5 (171.6 to 281.4)	250.3 (205 to 266.8)	
7 days post treatment	266.1 (222.2 to 307.1)	265 (202.8 to 316.8)	
Change over 7 days	47.8 (-9.8 to 77.9)	30.3 (-60 to 101.5)	0.3
Difference within group (p value)	0.38	0.47	
Adipose interstitial fluid - Glycerol (Low insulin) (µmol/L•hr)			
Baseline	132.3 (85.1 to 163.5)	114 (87.3 to 142.3)	
7 days post treatment	178.8 (79 to 272.8)	165.5 (138 to 228)	
Change over 7 days	36.6 (71)	87.3 (109.3)	0.38
Difference within group (p value)	0.28	0.011	
Adipose interstitial fluid - Glycerol (High insulin) (µmol/L•hr)			
Baseline	84.6 (16.8)	72.4 (8.5)	
7 days post treatment	110.5 (19.7)	141.6 (15.1)	
Change over 7 days	-3.9 (-15.4 to 46.8)	71.8 (28.1 to 109.3)	0.16
Difference within group (p value)	0.22	0.0013	
Adipose interstitial fluid - Pyruvate (Basal) (µmol/L•hr)			
Baseline	115.4 (8.9)	124.1 (8.5)	
7 days post treatment	138.6 (16.2)	135.4 (11.9)	
Change over 7 days	23.2 (50)	11.3 (52)	0.56
Difference within group (p value)	0.11	0.41	
Adipose interstitial fluid - Pyruvate (Low insulin) (µmol/L•hr)			
Baseline	140.1 (9.7)	144.7 (10)	
7 days post treatment	158.1 (17.4)	165.6 (9.7)	
Change over 7 days	18 (54.9)	20.8 (58.3)	0.83
Difference within group (p value)	0.26	0.19	
Adipose interstitial fluid - Pyruvate (High insulin) (µmol/L•hr)			
Baseline	135.4 (10.5)	143.9 (12.1)	
7 days post treatment	143.1 (12.1)	140.6 (7.8)	
Change over 7 days	7.7 (49.4)	-3.3 (53.7)	0.38
Difference within group (p value)	0.57	0.82	
Adipose interstitial fluid - Lactate (Basal) (mmol/L•hr)			
Baseline	1.2 (0.9 to 1.7)	1.28 (1.2 to 1.4)	
7 days post treatment	1.56 (1.1 to 1.9)	1.73 (1.3 to 2.2)	
Change over 7 days	0.4 (0.8)	0.4 (0.8)	0.88
Difference within group (p value)	0.12	0.057	
Adipose interstitial fluid - Lactate (Low insulin) (mmol/L•hr)			
Baseline	2.7 (2.2 to 3.1)	1.88 (0.9 to 2.3)	

7 days post treatment	2.25 (1.8 to 2.8)	2.23 (1.7 to 3.1)	
Change over 7 days	-0.2 (1.7)	0.7 (1.2)	0.11
Difference within group (p value)	0.39	0.04	
Adipose interstitial fluid - Lactate (High insulin) (mmol/L•hr)			
Baseline	3.01 (1.31)	2.44 (1.23)	
7 days post treatment	2.64 (1.13)	2.6 (1.14)	
Change over 7 days	-0.38 (1.42)	0.16 (1.4)	0.31
Difference within group (p value)	0.342	0.67	
Adipose interstitial fluid - Glucose (Basal) (mmol/L•hr)			
Baseline	4.78 (5.1)	4.6 (3.8 to 5.3)	
7 days post treatment	5.21 (6.2)	4.93 (3.6 to 5.5)	
Change over 7 days	0.54 (1.46)	-0.01 (0.56)	0.25
Difference within group (p value)	0.06	0.96	
Adipose interstitial fluid - Glucose (Low insulin) (mmol/L•hr)			
Baseline	4.3 (0.75)	4.26 (1.12)	
7 days post treatment	4.98 (1.97)	4.65 (0.85)	
Change over 7 days	0.63 (1.61)	0.38 (0.9)	0.74
Difference within group (p value)	0.17	0.12	
Adipose interstitial fluid - Glucose (High insulin) (mmol/L•hr)			
Baseline	4.07 (1.42)	3.6 (1.49)	
7 days post treatment	4.66 (1.41)	4.02 (1.19)	
Change over 7 days	0.58 (1.5)	0.42 (1.27)	0.9
Difference within group (p value)	0.171	0.26	
Palmitic acid 16:00 (Basal) (%)			
Baseline	27 (24 to 27.7)	25.4 (22.1 to 26.6)	
7 days post treatment	26.7 (22.4 to 27.7)	26.9 (25.7 to 28)	
Change over 7 days	-0.4 (-1.2 to 0.3)	2.8 (3.7)	0.03
Difference within group (p value)	0.24	0.016	
Palmitic acid 16:00 (Low insulin) (%)			
Baseline	24.1 (4.6)	24.5 (2.8)	
7 days post treatment	25.5 (4.6)	25.7 (3.4)	
Change over 7 days	0.3 (-2.9 to 5.5)	1.7 (0.7 to 3.5)	0.64
Difference within group (p value)	0.43	0.31	
Palmitic acid 16:00 (High insulin) (%)			
Baseline	23.9 (21.3 to 27.7)	22.1 (21.1 to 27.2)	
7 days post treatment	20.3 (19 to 26.4)	25.2 (23.1 to 27)	
Change over 7 days	-2.7 (5.1)	1.2 (4.2)	0.063
Difference within group (p value)	0.15	0.36	

Stearic acid 18:00 (Basal) (%)			
Baseline	13.6 (2.3)	12.1 (2.7)	
7 days post treatment	12.5 (2.8)	12.5 (2.8)	
Change over 7 days	-1.1 (1.7)	0.5 (2.1)	0.086
Difference within group (p value)	0.064	0.44	
Stearic acid 18:00 (Low insulin) (%)			
Baseline	21.3 (6.7)	21.5 (4.8)	
7 days post treatment	20.9 (7.5)	16.6 (2.7)	
Change over 7 days	-0.4 (8.7)	-4.9 (5.2)	0.31
Difference within group (p value)	0.88	0.0076	
Stearic acid 18:00 (High insulin) (%)			
Baseline	24.1 (10.6)	23.5 (7.1)	
7 days post treatment	20.4 (7.9)	20.6 (5.2)	
Change over 7 days	-3.7 (10)	-2.9 (4.2)	0.68
Difference within group (p value)	0.25	0.035	
Oleic acid 18: 1n-9 (Basal) (%)			
Baseline	40.2 (2.8)	39.7 (3)	
7 days post treatment	39.5 (5.6)	39.7 (3.7)	
Change over 7 days	0.1 (-0.7 to 1.3)	0.3 (-2.5 to 1.1)	0.97
Difference within group (p value)	0.65	0.97	
Oleic acid 18: 1n-9 (Low insulin) (%)			
Baseline	27.2 (8.2)	26.5 (5.6)	
7 days post treatment	27.6 (8.4)	30.1 (4.7)	
Change over 7 days	0.4 (10.7)	3.6 (5.1)	0.21
Difference within group (p value)	0.9	0.031	
Oleic acid 18: 1n-9 (High insulin) (%)			
Baseline	24.3 (8.9)	22.1 (5.8)	
7 days post treatment	21.7 (9.3)	23.7 (5.8)	
Change over 7 days	-2.7 (11.7)	1.5 (5)	0.15
Difference within group (p value)	0.49	0.32	
Linoleic acid 18: 2n-6 (Basal) (%)			
Baseline	13 (2)	13.6 (2.8)	
7 days post treatment	13.9 (3)	12.8 (1.9)	
Change over 7 days	0.9 (2.3)	-0.8 (1.8)	0.041
Difference within group (p value)	0.21	0.16	
Linoleic acid 18: 2n-6 (Low insulin) (%)			
Baseline	12.5 (3.9)	11.1 (3.2)	
7 days post treatment	12.9 (4.2)	11.4 (2.5)	
Change over 7 days	0.5 (3.8)	0.3 (3.4)	0.71

Difference within group (p value)	0.68	0.77	
Linoleic acid 18: 2n-6 (High insulin) (%)			
Baseline	16.4 (13.2 to 16.6)	11.5 (7.6 to 13.2)	
7 days post treatment	11.9 (7.9 to 13.9)	10.2 (7.6 to 12.3)	
Change over 7 days	-1.8 (6.9)	-0.1 (2.8)	0.49
Difference within group (p value)	0.43	0.92	

Table 4-3 *The effect of AZD4017 + prednisolone and placebo + prednisolone on lipid metabolism during a two-step hyperinsulinaemic euglycaemic clamp. Data are mean (SD) or median (IQR).*

4.3.5 Adipose tissue insulin sensitivity

AZD4017 treatment prevented the prednisolone-induced increase in basal circulating TAG levels. Furthermore, across all the phases of the 2-step hyperinsulinaemic euglycaemic clamp, the changes in circulating TAG levels associated with prednisone administration, were significantly reduced by AZD4017 (**Table 4-3**, **Figure 4.3-5** A, B and C).

Similarly, as expected, prednisolone + placebo caused an increase in circulating glycerol concentrations across all stages of the 2-step clamp. When prednisolone was co-administered with AZD4017, circulating glycerol concentration did not change (**Table 4-3**, **Figure 4.3-5** D and E). Absolute changes in glycerol concentrations were significantly higher in the placebo-treated group during the low- and high-dose insulin infusion although not basally (**Table 4-3**, **Figure 4.3-5** F).

Mirroring these observations, subcutaneous adipose interstitial fluid glycerol levels measured in adipose tissue microdialysis samples, increased in the prednisolone + placebo treated group during low- and high-insulin infusions. In the prednisolone + AZD4017 treated group, there were no changes in adipose tissue interstitial glycerol

levels pre- and post-treatment. There were no significant changes in the absolute changes in glycerol concentrations between the 2 groups (**Table 4-3**, **Figure 4.3-5** G, H and I).

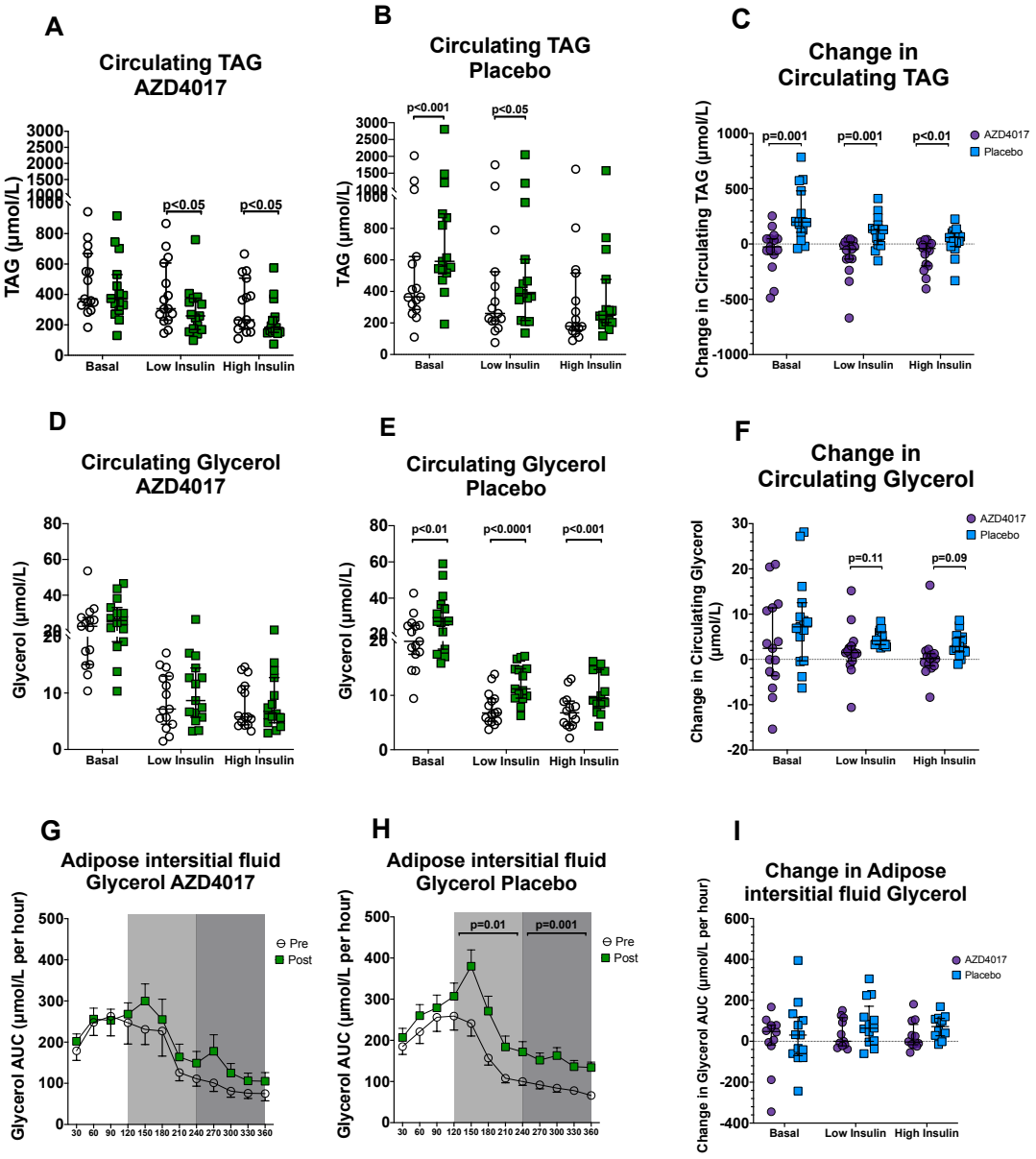

Figure 4.3-5 *The effect of prednisolone + AZD4017 and prednisolone + placebo on circulating levels of triglycerides (TAG) (A-C), glycerol (D-F) and adipose interstitial fluid levels of glycerol (G-I) during a two-step hyperinsulinaemic euglycaemic clamp. Absolute change refers to the difference between pre- and post-treatment values (C, F and I). Data are medians and error bars are IQR (A-F, I) and mean and SE (G and H). Datapoints represent individual patients. White circles represent pre-treatment levels and green squares post-treatment levels (7 days), purple circles are AZD4017 and blue squares, placebo.*

Circulating NEFA levels were suppressed during low- and high-dose insulin infusions in both groups. High-dose insulin infusion failed to suppress NEFA levels in the prednisolone + placebo group (**Table 4-3**). Ra palmitate decreased during high-dose insulin infusion following prednisolone + AZD4017 treatment, but there was no significant difference between the groups (**Table 4-3**).

OHB levels increased during high-dose insulin infusion following prednisolone + placebo treatment and there was also significant absolute change between the groups (-1.8 (3.8) vs. 3.3 (6.3), p=0.016, AZD4017 vs. placebo) (**Table 4-3**). There was a significant increase in the adipose tissue interstitial fluid levels of lactate under low-dose insulin conditions following prednisolone + placebo treatment, but was no significant difference between the groups (**Table 4-3**). There were no significant changes in the adipose tissue interstitial fluid levels of pyruvate and glucose.

The relative concentration of palmitic acid increased following prednisolone + placebo treatment during the basal phase of the clamp but there were no other changes during low- and high-dose insulin infusion (**Table 4-3**). The relative concentration of stearic acid increased during low- and high-dose insulin infusion phases following prednisolone + placebo treatment but there were no changes following prednisolone + AZD4017 treatment (**Table 4-3**). Similarly, the relative concentration of oleic acid increased during low-dose insulin infusion following prednisolone + placebo treatment but remained the same in the prednisolone + AZD4017 group (**Table 4-3**). There were no changes in the linoleic acid percentage in either group throughout the clamp (**Table 4-3**).

4.3.6 Blood pressure

Although blood pressure measurements did not change significantly within each group, the absolute change in the mean night-time diastolic blood pressure was significantly higher in the prednisolone + placebo group (0.7 (8.1) vs. 4.6 (8.6), p=0.03, AZD4017 vs. placebo) (**Figure 4.3-6**). There were no changes in the mean day-time systolic and diastolic blood pressure, mean night-time systolic blood pressure and mean 24-hour systolic and diastolic blood pressure measurements (**Table 4-4**).

Metabolic variable	AZD4017 + Prednisolone n=15	Placebo + Prednisolone n=15	Between group p value
PHA OX40 (% of CD25+CD134+)			
Baseline	59.4 (51.6 to 74.4)	63.2 (56.3 to 75)	
7 days post treatment	54.4 (41.2 to 63.2)	40.3 (27.7 to 55.8)	
Change over 7 days	-10.18 (14.35)	-21.72 (13.99)	0.046
Difference within group (p value)	0.018	0.0004	
VZV OX40 (% of CD25+CD134+)			
Baseline	1.08 (0.26 to 1.02)	1.41 (0.31 to 1.2)	
7 days post treatment	0.57 (0.13 to 0.5)	0.57 (0.17 to 0.64)	
Change over 7 days	-0.4 (-0.55 to -0.1)	-0.3 (-1.85 to 0)	0.81
Difference within group (p value)	0.016	0.011	
Osteocalcin (ng/mL)			
Baseline	7.79 (6.18 to 11.69)	9.12 (7.44 to 9.76)	
7 days post treatment	8.13 (6.8 to 10.31)	4.16 (3.46 to 5.04)	
Change over 7 days	0·00 (-3·46 to 2·18)	-3·86 (-5·78 to -2·74)	<0.0001
Difference within group (p value)	0.64	<0.0001	
Day-time blood pressure - Systolic (mm Hg)			
Baseline	125 (6.3)	127.8 (8.8)	
7 days post treatment	127.4 (8.8)	130.3 (9.8)	
Change over 7 days	2.4 (7)	2.5 (6.1)	0.66
Difference within group (p value)	0.22	0.15	
Day-time blood pressure - Diastolic (mm Hg)			
Baseline	74.6 (7.2)	79.1 (7.4)	

7 days post treatment	75.9 (7.4)	79.4 (6.8)	
Change over 7 days	1.4 (6.2)	0.3 (5.8)	0.92
Difference within group (p value)	0.42	0.86	
Night-time blood pressure - Systolic (mm Hg)			
Baseline	111.1 (7.7)	111.8 (9)	
7 days post treatment	112.1 (9.9)	116.4 (13.6)	
Change over 7 days	1 (11.5)	4.6 (10.6)	0.19
Difference within group (p value)	0.76	0.13	
Night-time blood pressure - Diastolic (mm Hg)			
Baseline	63 (61 to 64)	63.5 (60.5 to 71)	
7 days post treatment	65 (55 to 69)	68.5 (65.8 to 74.5)	
Change over 7 days	0.7 (8.1)	4.6 (8.6)	0.03
Difference within group (p value)	0.72	0.064	
24-hour blood pressure - Systolic (mm Hg)			
Baseline	119.8 (5.9)	122.1 (8.7)	
7 days post treatment	121.4 (8.8)	125.1 (10.9)	
Change over 7 days	1.5 (8.5)	3 (7.3)	0.26
Difference within group (p value)	0.52	0.15	
24-hour blood pressure - Diastolic (mm Hg)			
Baseline	70.2 (6.4)	74.3 (7)	
7 days post treatment	70.5 (6.9)	76.4 (7)	
Change over 7 days	0.4 (6.2)	2.1 (6.2)	0.12
Difference within group (p value)	0.83	0.23	
% android fat mass			
Baseline	27.6 (11)	28.8 (11)	
7 days post treatment	27.2 (11.1)	28.4 (10.8)	
Change over 7 days	-0.5 (1.7)	-0.4 (1.2)	0.89
Difference within group (p value)	0.3	0.19	
% gynoid fat mass			
Baseline	24 (6.9)	22.8 (6.1)	
7 days post treatment	24.1 (6.8)	22.7 (6.2)	
Change over 7 days	0.1 (1.2)	-0.1 (1)	0.54
Difference within group (p value)	0.78	0.56	
% fat mass			
Baseline	24.2 (7.3)	24.3 (6.6)	
7 days post treatment	24 (7.2)	24 (6.4)	
Change over 7 days	-0.3 (0.6)	-0.2 (0.9)	0.92
Difference within group (p value)	0.11	0.35	

Android tissue mass (g)			
Baseline	5708.5 (648.4)	5500 (1198.7)	
7 days post treatment	5721.3 (652.9)	5471.3 (1187)	
Change over 7 days	12.8 (187)	-28.7 (190.2)	0.58
Difference within group (p value)	0.79	0.57	
Gynoid tissue mass (g)			
Baseline	12276 (11374 to 13104)	11617 (10650 to 12868)	
7 days post treatment	12311 (11121.5 to 13415.5)	11644 (10630 to 13016.5)	
Change over 7 days	35 (-117 to 315)	-13 (-211.5 to 178.5)	0.39
Difference within group (p value)	0.42	0.59	
Total tissue mass (g)			
Baseline	79490.1 (6552.4)	74905.5 (9180.7)	
7 days post treatment	80025.6 (6703.8)	74941.9 (9344.2)	
Change over 7 days	535.5 (983.5)	36.4 (1228.1)	0.27
Difference within group (p value)	0.053	0.91	
Android fat tissue (g)			
Baseline	1613.7 (768.5)	1685.7 (933.1)	
7 days post treatment	1599.5 (763.3)	1654.1 (917.3)	
Change over 7 days	-14.2 (115.4)	-31.6 (101.3)	0.69
Difference within group (p value)	0.64	0.25	
Gynoid fat tissue (g)			
Baseline	3016.3 (978.2)	2713.7 (930.9)	
7 days post treatment	3009.5 (970.4)	2686.5 (926.9)	
Change over 7 days	-6.9 (122.6)	-27.3 (117)	0.59
Difference within group (p value)	0.83	0.38	
Total fat mass (g)			
Baseline	19308.1 (6098.9)	18483 (6564.7)	
7 days post treatment	19222.1 (6012.2)	18344.1 (6565.8)	
Change over 7 days	-86.1 (462.6)	-138.9 (710.4)	0.78
Difference within group (p value)	0.48	0.46	
Android lean tissue (g)			
Baseline	4094.9 (521.8)	3814.5 (514.3)	
7 days post treatment	4121.7 (495.3)	3817.3 (493.8)	
Change over 7 days	26.7 (174.2)	2.9 (131.8)	0.72
Difference within group (p value)	0.56	0.93	
Gynoid lean tissue (g)			
Baseline	9330.9 (1001)	9030.4 (1181)	
7 days post treatment	9407.4 (1196.4)	9010.3 (1131.3)	

Change over 7 days	76.5 (283.2)	-20.1 (307.8)	0.4
Difference within group (p value)	0.31	0.8	
Total lean mass (g)			
Baseline	60181.7 (7231.1)	56422.3 (5958.4)	
7 days post treatment	60803.5 (7384.2)	56610.5 (5766.5)	
Change over 7 days	621.8 (989.5)	188.2 (1178.3)	0.26
Difference within group (p value)	0.029	0.55	

Table 4-4 *The effect of AZD4017 + prednisolone and placebo + prednisolone on other secondary outcomes during a two-step hyperinsulinaemic euglycaemic clamp. Data are mean (SD) or median (IQR).*

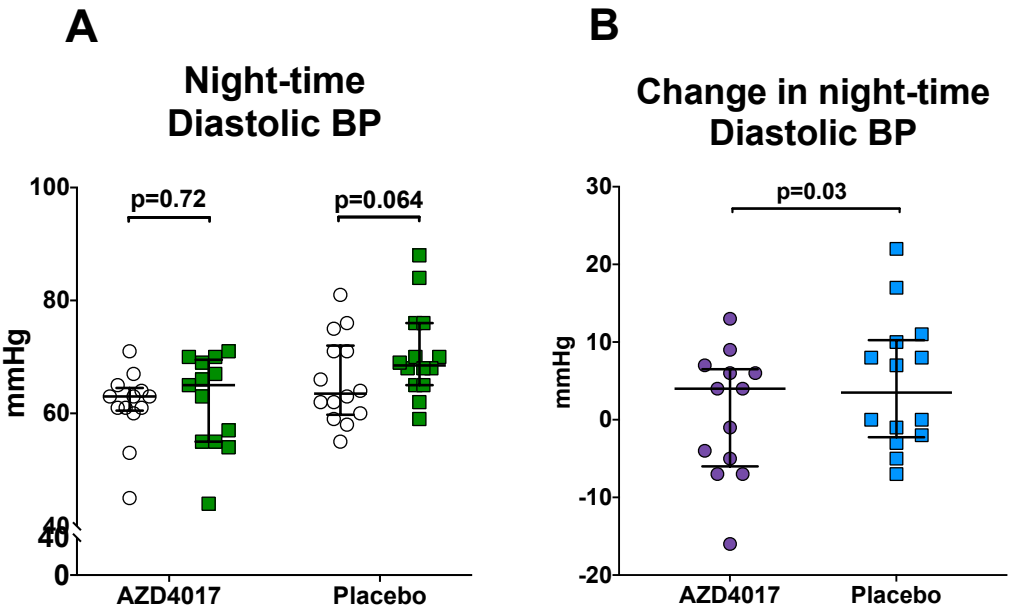

Figure 4.3-6 *The effect of prednisolone + AZD4017 and prednisolone + placebo on night-time diastolic blood pressure (BP) (A). Change refers to the difference between pre- and post-treatment values (B). Data are medians and error bars are IQR. Datapoints represent individual patients. White circles represent pre-treatment levels and green squares post-treatment levels (7 days), purple circles are AZD4017 and blue squares, placebo.*

4.3.7 DEXA scan

DEXA scans performed showed an increase in total lean tissue following prednisolone and AZD4017 but no other significant differences post treatment in either group (**Table 4-4**). In particular the parameters that remained the same in both

groups included % android fat mass, % gynoid fat mass, % fat mass, android tissue mass, gynoid tissue mass, total tissue mass, android fat tissue, gynoid fat tissue, total fat mass, android lean tissue and gynoid lean tissue.

4.3.8 Serum Osteocalcin

Serum osteocalcin levels are a GC-sensitive marker of bone turnover (252, 253). Osteocalcin levels decreased following administration of prednisolone + placebo (9.12 (7.44 to 9.76) vs. 4.16 (3.46 to 5.04) ng/ml, p<0.0001, pre- vs. post-treatment) and this was entirely prevented with co-administration of AZD4017 (7.79 (6.18 to 11.69) vs. 8.13 (6.80 to 10.31) ng/ml, p=0.64, pre- vs. post-treatment) (**Table 4-4**, **Figure 4.3-7** A). The absolute changes in osteocalcin levels were significantly different between the 2 groups (0.00 (-3.46 to 2.18) vs. -3.86 (-5.78 to -2.7), p<0.0001, AZD4017 vs. placebo) (**Table 4-2**, **Figure 4.3-7** B).

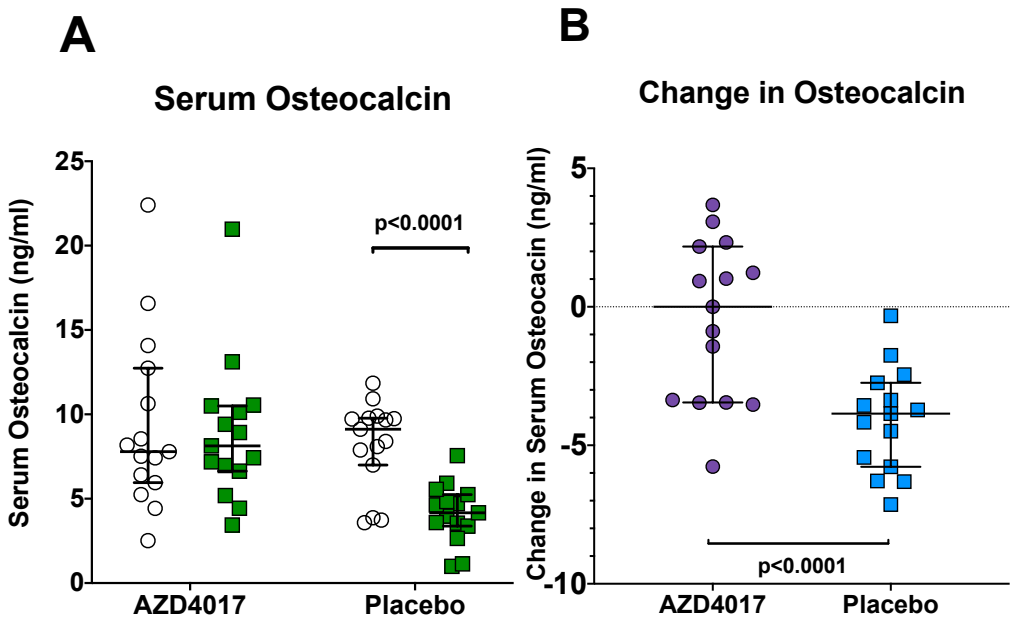

Figure 4.3-7 *The effect of prednisolone + AZD4017 and prednisolone + placebo on serum osteocalcin levels (A). Change refers to the difference between pre- and post-treatment values (B). Data are medians and error bars are IQR. Datapoints represent individual patients. White circles represent pre-treatment levels and green squares post-treatment levels (7 days), purple circles are AZD4017 and blue squares, placebo.*

4.3.9 Immune inflammatory response

The immune-suppressive action of prednisolone was measured using the OX40 assay. Treatment with both prednisolone + placebo and prednisolone + AZD4017 decreased the percentage of CD25+CD134+ cells following exposal to both VZV and PHA in the OX40 assay. Whilst there was no significant difference in the response to VZV exposure when comparing the two arms of the study 0.40 (-0.55 to -0.10) vs. -0.30 (-1.85 to 0.00), p=0.81, AZD4017 vs. placebo), the response to PHA was more marked in the prednisolone + placebo group (-10.2 (14.4) vs. -21.7 (14.0), p=0.046, AZD4017 vs. placebo) (**Table 4-2**, **Figure 4.3-8** A-D).

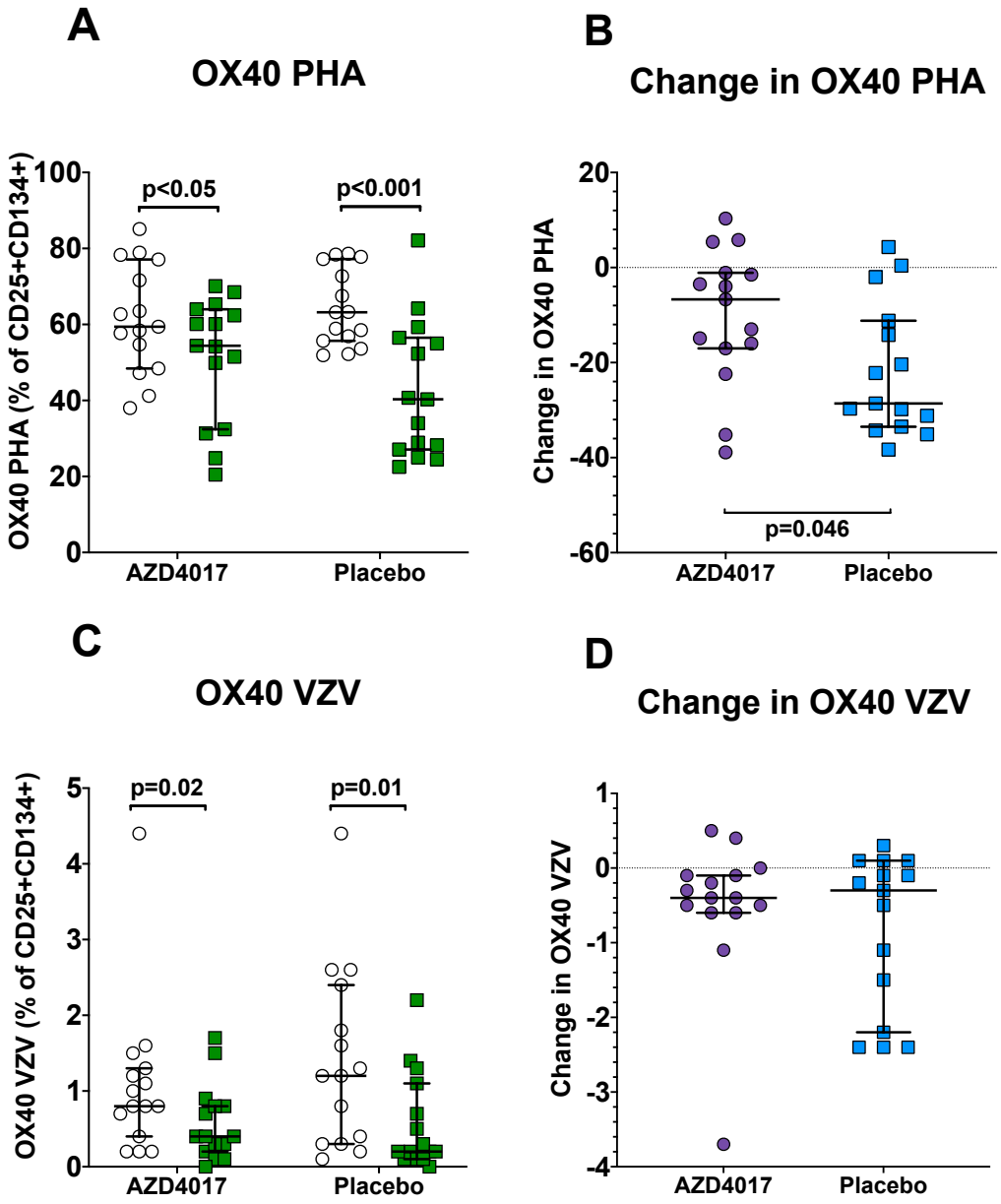

Figure 4.3-8 *The effect of prednisolone + AZD4017 and prednisolone + placebo on serum osteocalcin levels (A). Change refers to the difference between pre- and post-treatment values (B). Data are medians and error bars are IQR. Datapoints represent individual patients. White circles represent pre-treatment levels and green squares post-treatment levels (7 days), purple circles are AZD4017 and blue squares, placebo.*

4.3.10 Skeletal muscle gene expression

RNA sequencing analysis identifed 19 genes whose expression was significantly changed following treatment with placebo + prednisolone (DHCR24, APOD, HBA2, HBB, HBA1, TSPYL2, HMOX1, ALAS2, RASD1, S100A8, SNCA, S100A9,

FABP7, MMP3, PADI4, TRIM58, AKR1B10, HBD and CA1). In the AZD4017 + prednisolone group, there were only two genes that were identified as significantly different in expression (RASD1 and AKR1B10).

The most relevant genes (as evident by their expression magnitude and function) are DHCR24, which is involved in cholesterol biosynthesis and APOD, which is involed in lipoprotein metabolism. This indicates that treatment with prednisolone + placebo is involved in upregulating these two genes and thus suggesting that prednisolone induces its metabolic effects in the skeletal muscle through these pathways. The fact that these genes's expression is not altered following AZD4017 + placebo, signifies that, as expected, AZD4017 inhibits the action of prednisolone at the pre-receptor level.

4.3.11 Subcutaneous adipose tissue gene expression

Subcutaneous adipose tissue RNA sequencing analysis identified only 7 genes (FAM13A, PLA2G2A, ARHGAP20, KLHL25, SPINK2, DACT2 and KCNQ3) that were regulated by placebo + prednisolone treatment. There no changes in expression in any gene in the AZD4017 + prednisolone group. Of the 7 identified genes, the most relevant gene (as evident by its expression magnitude and function), was PLA2G2A. This gene is known to be involved in several lipid metabolism pathways such as glycerophospholipid metabolism, ether lipid metabolism, arachidonic acid metabolism, linoleic acid metabolism and alpha-linolenic acid metabolism. It is also known to be involved in the ras signalling pathway. This gene was also upregulated in the subcutaneous adipose tissue following treatment with prednisolone in the FindIt2 study (**Chapter 3**).

4.3.12 Adverse events and tolerability

There were four adverse events reported in the AZD4017 group, comprising transient headache (three participants) and an elevated TSH (one participant) which normalised by day 14. There was one reported adverse event in the placebo group (irritability). No other adverse events were reported throughout the duration of the study, or in the 30 days after the final administration of AZD4017 or placebo.

4.4 Discussion

The results of the first randomised, double blind, placebo-controlled study, show that inhibition of 11β-HSD1 using AZD4017 can limit the adverse metabolic and bone effects, of oral prednisolone treatment. This proof-of-concept study represents the first endorsement of a developing body of preclinical data demonstrating the potent ability of 11β-HSD1 to regulate the action of exogenous GCs. In addition, it challenges currently held views with regards to GC action, suggesting that tissue-specific GC metabolism (inactivation and regeneration), rather circulating levels in the blood, is critical in controlling the biological impact of GCs.

The metabolic effects of 11β-HSD1 deficiency or inhibition have been extensively investigated in animal models. 11β-HSD1 KO mice have reduced visceral adipose tissue accumulation on a HFD and resist the development of insulin resistance and T2DM (123, 134). Selective 11β-HSD1 inhibitors have also been trialled in animal models where they reduce fasting blood glucose, insulin and cholesterol levels (169-171), as well as decreasing mesenteric fat mass and hepatic steatosis (172, 173). In addition, they improve insulin sensitivity and reduce hepatic glucose production (182). However, in humans, selective 11β-HSD1 inhibitors have only demonstrated

relatively modest improvements in glycaemic control and hyperlipidaemia and blood pressure in patients with T2DM (107, 183-185).

Cushing's syndrome as a result of excess prescribed GC therapy is a significant clinical and economic burden. The use of prescribed glucocorticoids is widespread, particularly amongst the elderly who may be more susceptible to their adverse effects, and is associated with increased cardiovascular and cerebrovascular morbidity and mortality (254).

To date, the potential to modulate the adverse effects of prescribed GCs through manipulation of 11β-HSD1 activity and expression has only been examined in rodent models. 11β-HSD1 KO mice fail to develop a classical Cushing's phenotype following corticosterone (the predominant circulating GC in rodents); this was critically dependent upon adipose tissue (but not liver) 11β-HSD1 expression (135). More recently, Fenton et al. (2019) reported protection from trabecular bone loss, following GC administration, in 11β-HSD1 KO mice (245). The phenotype observed in these rodent models mirrors the observations for our clinical study in terms of the beneficial impact of 11β-HSD1 inhibition to limit the impact of prednisolone on glucose disposal, insulin sensitivity, blood pressure and osteocalcin.

Our data represent the first interventional study in humans, however, Cooper et al. (2003) examined the effect on bone formation and turnover markers following administration of prednisolone (5mg twice daily). Bone formation markers decreased in all subjects, however, the magnitude of the reduction was greatest in those individuals with the highest 11β-HSD1 activity at baseline (156). The data from our

study would appear to endorse these observations and therefore 11β-HSD1 inhibition may have the potential as a therapy not only to limit the adverse metabolic effects associated with GC use, but also to limit GC-induced bone loss. As anticipated, we did not observe many significant changes in tissues types after 7 days of treatment in either group. This is likely due to the relatively short duration of treatment course as we would not expect to see large changes in weight or fat distribution.

GCs are most commonly prescribed for their immune-suppressive and anti-inflammatory actions. 11β-HSD1 is highly expressed in the liver and adipose tissue, but is only expressed at very low levels in T-cells and other immune-inflammatory response cells. It has been suggested that 11β-HSD1 may have a role in controlling the endogenous anti-inflammatory response; 11β-HSD1 KO mice develop a greater inflammatory reaction in response to joint inflammation, peritonitis and lung inflammation and have a slower recovery (153). However, the response to exogenous GC therapy in these models in 11β-HSD1 KO mice has not been examined. In clinical studies, global 11β-HSD1 activity is increased in patients with rheumatoid arthritis (154) as well as in those with inflammatory bowel disease (155). As in the mouse models, the response to GCs in the presence of 11β-HSD1 deficiency or inhibition has not been studied. Our data demonstrate that the impact of prednisolone on the OX40 response is preserved following co-administration of AZD4017. We would speculate that the differential impact of AZD4017 metabolic and immune inflammatory cells is a reflection of levels of expression. In tissue where 11β-HSD1 is highly expressed, circulating levels are amplified through the conversion of prednisone to prednisolone, whereas in tissues and cells where there is little 11β-HSD1, the impact of GCs reflect circulating levels (and hence no difference between

placebo-treated and AZD4017-treated groups in our study). It is important to note that the participants in this study were healthy volunteers without any underlying immune or inflammatory conditions.

A small number of clinical studies have tried to address the issue of protection form the adverse metabolic effects of prescribed GCs, most commonly using established anti-diabetic agents. Glucagon-like peptide 1 (GLP-1) analogues appear to limit dysglycaemia associated with prednisolone use as well as improving pancreatic islet cell function (255). In case series and retrospective analyses, dipeptidyl peptidase-4 (DPP-4) inhibitors improved glycated haemoglobin and post-prandial glucose levels in patients with chronic medical conditions treated with GC therapy (256, 257). However, in a randomised, double-blind placebo-controlled study, there was no improvement in GC-induced glucose intolerance in non-diabetic individuals (258).

More recently, Pernicova et al. (2020) examined the impact of metformin in patients already prescribed glucocorticoid therapy (259). As well as reporting improvement in carbohydrate and lipid metabolism, they demonstrated improvements in the incidence of pneumonia and all-cause hospital admissions. Metformin administration improved some of the metabolic profiles of GC-treated patients. However, the participants in this study were all already taking GC therapy (and there was little deterioration in metabolic phenotype in the placebo group over time) and therefore it is not possible to say if the observed benefits of metformin were independent of the effects of GC therapy.

There are no published data on the effect of GCs in gene expressions in skeletal muscle tissue. Almon et al. (2008) published their finding on the genomic response

of rats' skeletal muscle to methylprednisolone (260). They also reported upregulation of HMOX1, S100A8 and S100A9 but did not report any changes to the expression of DHCR24 or APOD. DHCR24 catalyzes the conversion of desmosterol to cholesterol and is known to be involved in glucose metabolism as its expression decreased in obese patients with T2DM following bariatric surgery (261). Sex steroids can upregulate the expression of this gene but it is not currently known how GCs influence its expression (262).

11β-HSD1 inhibition appears to convey multiple metabolic benefits (not simply glycaemic control); we propose that this results from the specific targeting of a critical component of the tissue-specific action of GCs, whereby their impact in metabolic tissues is amplified (as a result of high 11β-HSD1 expression and active GC regeneration) leading to unwanted adverse side effects.

The strengths of this study are it is randomized, double-blinded with balanced groups. This is the first time the effect of a selective 11β-HSD1 inhibitor on the metabolic and bone effects of GC has been reported. There are some limitations to the current study; the sample size is modest, although the trial was designed as an early phase II, proof-of-concept study, it was only conducted in healthy male volunteers and over a relatively short duration. Therefore no conclusions can be drawn with regards to the potential benefits in women (although the drug has been administered to women for up to 12 weeks, and was well tolerated (248). Importantly, the participants in this study did not have underlying immune or inflammatory conditions and therefore, the next step would be to conduct a larger, more prolonged trial in patients with an inflammatory condition who are initiated on glucocorticoid therapy.

In conclusion, this is the first time that 11β-HSD1 inhibition, using AZD4017, has been demonstrated to limit the adverse metabolic and bone side-effects of prednisolone in healthy male participants. In the future, it remains plausible, that 11β-HSD1 inhibitors may prove to be an important protective adjunctive therapy alongside prescribed GCs.

5 Discussion

5.1 Pre-receptor metabolism regulates the action of exogenous GCs

Pre-receptor GC metabolism is an important element to the regulation of endogenous and exogenous GC actions. In this thesis, I have presented the effects of prednisolone action when two keys enzymes involved in GC metabolism are inhibited. This is the first time that the combination of either of these inhibitors was investigated in conjunction with prednisolone. Even though the studies were of relatively short duration (7 days), the metabolic effects of prednisolone at 10mg daily and at 20mg daily on insulin action in the muscle, liver and adipose tissue was evident. These effects however, were augmented when given alongside with a 5αRI and limited following co-administration with an 11β-HSD1 inhibitor, demonstrating their significance on exogenous GC action.

I have also demonstrated that the metabolic effects of exogenous GCs, which occur at the metabolic tissues such as liver, skeletal muscle and adipose tissue, do not correlate with the circulating levels of GCs. In fact, the pre-receptor metabolism plays a key role in the development of adverse effects. This raises an interesting point about how we could predict response as well as risk of side-effects in patients requiring treatment with GCs, by assessing the pre-receptor enzyme activity. This can be done by analysing the urine steroid profile. This way we could begin personalized treatment, guided by pre-receptor pattern activity.

11β-HSD1 inhibition, as mentioned in **Chapter 1**, has been investigated as a possible therapeutic target in treating conditions such as metabolic syndrome. However, the biggest caveat in 11β-HSD1 inhibition is the subsequent HPA axis activation. This results in ACTH elevation and thus increase of DHEA and other androgens which

could potentially cause hirsutism in women. Additionally, adrenal hypertrophy/hyperplasia is also a plausible consequence which could eventually lead to tumour development. Another concern is that HPA axis activation could predispose individuals to depression. In the TICSI study, there was no change in the ACTH levels following treatment with both prednisolone and AZD4017, but a decrease was noted after treatment with prednisolone and placebo. 11β-HSD1 is expressed in the brain which can explain this result. This finding suggests that 11β-HSD1 inhibition could protect against HPA axis suppression and thus eliminating the need for tapering the GCs dose following prolonged treatments. In **Chapter 4**, I have shown that 11β-HSD1 inhibition can ameliorate metabolic and bone side-effects of GCs as evident by blocking the GC-induced effects on glucose disposal, hepatic and peripheral insulin sensitivity and osteocalcin levels. This postulates an exciting new therapeutic approach which could be used in conjunction with GCs to reduce the risk of developing metabolic side-effects particularly in patients that are on prolonged GC therapy.

Conversely, inhibition of 5αR can trigger the opposite effects to 11β-HSD1 inhibition, as discussed in **Chapter 3**. As mentioned previously, 5αR metabolise active GC into its inactive metabolites in key metabolic tissues where 5αR enzymes are expressed, such as the liver, adipose tissue and skeletal muscle. Subsequently, co-administration of 5αRI and GC exacerbate the metabolic side-effects of GCs. This raises an important clinical question regarding surveillance into the development of side-effects, such as hyperglycaemia and hypertension. This would be of particular importance in patients with pre-disposition to these conditions, such as patients who are overweight or have a family history.

More recently, another class of medications, selective glucocorticoid receptor modulators (SEGRMs), have been investigated for their potential use as anti-inflammatory agents. SEGRMs enter the cell, bind to GR and trigger transrepression. Unlike GCs they do not also initiate transactivation. Thus, they are able to act as anti-inflammatory agents, in a similar way to GCs but do not induce side-effects that are predominantly mediated by transactivation such as hyperglycaemia and muscle wasting. There is emerging evidence of the efficacy and safety of some of these compounds (such as PF-04171327), however, many SEGRMs are halted at the pre-clinical phase (263).

5.2 Future plans

The clinical studies that were presented here were performed on healthy male volunteers and whilst the results have provided an indication of the change in metabolic profile following prednisolone administration and a 5αRI or an 11β-HSD1 inhibitor, it cannot be verified that these parameters will alter in a similar way in an inflammatory cohort. The results of the TICSI clinical study, which were described in **Chapter 4**, alluded that co-administration with an 11β-HSD1 inhibitor could be used to limit GC-induced metabolic and bone side-effects. Therefore, the next step, would be to trial this medication to patients requiring long-term GC treatment and to investigate its effects on immune response, in addition to assessing any metabolic changes. A possible cohort would be patients with polymyalgia rheumatica who often require long-term courses of exogenous GCs at moderate to high doses. The aim of such trial would be to confirm the effects of AZD4017 on limiting GC-induced metabolic changes as well as confirm that the anti-inflammatory actions of GCs are unchanged in the presence of this medication. AZD4017 could then be trialled in

combination with GCs in other inflammatory conditions such as arthritis and asthma. There is also potential of its use in endogenous GC excess conditions such as Cushing's syndrome. The gold standard treatment for this condition is to remove the mischievous growth in either the pituitary or adrenal gland or from an ectopic source. However, there are some patients that are not able to undergo surgery, in whom an 11β-HSD1 inhibitor could potentially be used to control the deleterious metabolic side-effects of excess cortisol, as current medical treatment is often not well tolerated. Additionally, there is emerging evidence that mild autonomous Cushing's syndrome or subclinical Cushing's, caused by adrenal adenomas, also increase the risk of cardiovascular events and mortality (264). Surgical treatment is not always performed in these cases and thus treatment with an 11β-HSD1 inhibitor could be a suitable medical therapy.

6 References

1. Mason HL, Myers, C.S., Kendall, E.C. The chemistry of crystalline substances isolated from the suprarenal gland. J Biol Chem. 1936;114(613-631).

2. Mason HL, Hoehn, W.M., McKenzie, B.F., Kendall, E.C. Chemical studies of the suprarenal cortex III. The structures of compounds A, B, H. J Biol Chem. 1937;120:719-41.

3. Reichstein T. The properties of adrenal cortex. VI. Segregative methods, plus isolation of the substances F a H and J. Helv Chim Acta. 1936;19(1107-1126).

4. Reichstein T. On components of kindey lobes. X. On knowledge of cortico-sterones. Helv Chim Acta. 1937;20(953-969).

5. Hench PS, Kendall EC, Slocumb CH, Polley HF. Effects of cortisone acetate and pituitary ACTH on rheumatoid arthritis, rheumatic fever and certain other conditions. Arch Intern Med (Chic). 1950;85(4):545-666.

6. Hollander JL, Brown EM, Jr., Jessar RA, Brown CY. Hydrocortisone and cortisone injected into arthritic joints; comparative effects of and use of hydrocortisone as a local antiarthritic agent. J Am Med Assoc. 1951;147(17):1629-35.

7. Amelung D, Hubener HJ, Roka L, Meyerheim G. Conversion of cortisone to compound F. J Clin Endocrinol Metab. 1953;13(9):1125-6.

8. Burton AF. Inhibition of 11-beta-hydroxysteroid dhydrogenase activity in rat and mouse tissues in vitro and in vivo. Endocrinology. 1965;77(2):325-31.

9. Koerner DR. 11 beta-hydroxysteroid dehydrogenase of lung and testis. Endocrinology. 1966;79(5):935-8.

10. Lakshmi V, Monder C. Purification and characterization of the corticosteroid 11 beta-dehydrogenase component of the rat liver 11 beta-hydroxysteroid dehydrogenase complex. Endocrinology. 1988;123(5):2390-8.

11. Maser E, Volker B, Friebertshauser J. 11 Beta-hydroxysteroid dehydrogenase type 1 from human liver: dimerization and enzyme cooperativity support its postulated role as glucocorticoid reductase. Biochemistry. 2002;41(7):2459-65.

12. Clore JN, Thurby-Hay L. Glucocorticoid-induced hyperglycemia. Endocr Pract. 2009;15(5):469-74.

13. Jeong IK, Oh SH, Kim BJ, Chung JH, Min YK, Lee MS, et al. The effects of dexamethasone on insulin release and biosynthesis are dependent on the dose and duration of treatment. Diabetes Res Clin Pract. 2001;51(3):163-71.

14. Raul Ariza-Andraca C, Barile-Fabris LA, Frati-Munari AC, Baltazar-Montufar P. Risk factors for steroid diabetes in rheumatic patients. Arch Med Res. 1998;29(3):259-62.

15. Hjelmesaeth J, Hartmann A, Kofstad J, Stenstrom J, Leivestad T, Egeland T, et al. Glucose intolerance after renal transplantation depends upon prednisolone dose and recipient age. Transplantation. 1997;64(7):979-83.

16. Uzu T, Harada T, Sakaguchi M, Kanasaki M, Isshiki K, Araki S, et al. Glucocorticoid-induced diabetes mellitus: prevalence and risk factors in primary renal diseases. Nephron Clin Pract. 2007;105(2):c54-7.

17. Besse C, Nicod N, Tappy L. Changes in insulin secretion and glucose metabolism induced by dexamethasone in lean and obese females. Obes Res. 2005;13(2):306-11.

18. Frazier B, Hsiao CW, Deuster P, Poth M. African Americans and Caucasian Americans: differences in glucocorticoid-induced insulin resistance. Horm Metab Res. 2010;42(12):887-91.

19. Davidson J, Wilkinson A, Dantal J, Dotta F, Haller H, Hernandez D, et al. New-onset diabetes after transplantation: 2003 International consensus guidelines. Proceedings of an international expert panel meeting. Barcelona, Spain, 19 February 2003. Transplantation. 2003;75(10 Suppl):SS3-24.

20. Henriksen JE, Alford F, Ward GM, Beck-Nielsen H. Risk and mechanism of dexamethasone-induced deterioration of glucose tolerance in non-diabetic first-degree relatives of NIDDM patients. Diabetologia. 1997;40(12):1439-48.

21. Depczynski B, Daly B, Campbell LV, Chisholm DJ, Keogh A. Predicting the occurrence of diabetes mellitus in recipients of heart transplants. Diabet Med. 2000;17(1):15-9.

22. McMahon M, Gerich J, Rizza R. Effects of glucocorticoids on carbohydrate metabolism. Diabetes Metab Rev. 1988;4(1):17-30.

23. Vegiopoulos A, Herzig S. Glucocorticoids, metabolism and metabolic diseases. Mol Cell Endocrinol. 2007;275(1-2):43-61.

24. van Raalte DH, Ouwens DM, Diamant M. Novel insights into glucocorticoid-mediated diabetogenic effects: towards expansion of therapeutic options? Eur J Clin Invest. 2009;39(2):81-93.

25. Dirlewanger M, Schneiter PH, Paquot N, Jequier E, Rey V, Tappy L. Effects of glucocorticoids on hepatic sensitivity to insulin and glucagon in man. Clin Nutr. 2000;19(1):29-34.

26. Kraus-Friedmann N. Hormonal regulation of hepatic gluconeogenesis. Physiol Rev. 1984;64(1):170-259.

27. Andrews RC, Walker BR. Glucocorticoids and insulin resistance: old hormones, new targets. Clin Sci (Lond). 1999;96(5):513-23.

28. Bernal-Mizrachi C, Weng S, Feng C, Finck BN, Knutsen RH, Leone TC, et al. Dexamethasone induction of hypertension and diabetes is PPAR-alpha dependent in LDL receptor-null mice. Nat Med. 2003;9(8):1069-75.

29. Bernal-Mizrachi C, Xiaozhong L, Yin L, Knutsen RH, Howard MJ, Arends JJ, et al. An afferent vagal nerve pathway links hepatic PPARalpha activation to glucocorticoid-induced insulin resistance and hypertension. Cell Metab. 2007;5(2):91-102.

30. Weinstein SP, Wilson CM, Pritsker A, Cushman SW. Dexamethasone inhibits insulin-stimulated recruitment of GLUT4 to the cell surface in rat skeletal muscle. Metabolism. 1998;47(1):3-6.

31. Oda N, Nakai A, Mokuno T, Sawai Y, Nishida Y, Mano T, et al. Dexamethasone-induced changes in glucose transporter 4 in rat heart muscle, skeletal muscle and adipocytes. Eur J Endocrinol. 1995;133(1):121-6.

32. Coderre L, Vallega GA, Pilch PF, Chipkin SR. In vivo effects of dexamethasone and sucrose on glucose transport (GLUT-4) protein tissue distribution. Am J Physiol. 1996;271(4 Pt 1):E643-8.

33. Weinstein SP, Paquin T, Pritsker A, Haber RS. Glucocorticoid-induced insulin resistance: dexamethasone inhibits the activation of glucose transport in rat skeletal muscle by both insulin- and non-insulin-related stimuli. Diabetes. 1995;44(4):441-5.

34. Dimitriadis G, Leighton B, Parry-Billings M, Sasson S, Young M, Krause U, et al. Effects of glucocorticoid excess on the sensitivity of glucose transport and metabolism to insulin in rat skeletal muscle. Biochem J. 1997;321 (Pt 3):707-12.

35. Ruzzin J, Wagman AS, Jensen J. Glucocorticoid-induced insulin resistance in skeletal muscles: defects in insulin signalling and the effects of a selective glycogen synthase kinase-3 inhibitor. Diabetologia. 2005;48(10):2119-30.

36. Henriksen JE, Alford F, Vaag A, Handberg A, Beck-Nielsen H. Intracellular skeletal muscle glucose metabolism is differentially altered by dexamethasone treatment of normoglycemic relatives of type 2 diabetic patients. Metabolism. 1999;48(9):1128-35.

37. Ekstrand A, Schalin-Jantti C, Lofman M, Parkkonen M, Widen E, Franssila-Kallunki A, et al. The effect of (steroid) immunosuppression on skeletal muscle glycogen metabolism in patients after kidney transplantation. Transplantation. 1996;61(6):889-93.

38. Krebs M, Krssak M, Bernroider E, Anderwald C, Brehm A, Meyerspeer M, et al. Mechanism of amino acid-induced skeletal muscle insulin resistance in humans. Diabetes. 2002;51(3):599-605.

39. Rizza RA, Mandarino LJ, Gerich JE. Cortisol-induced insulin resistance in man: impaired suppression of glucose production and stimulation of glucose utilization due to a postreceptor detect of insulin action. J Clin Endocrinol Metab. 1982;54(1):131-8.

40. Elks ML. Fat oxidation and diabetes of obesity: the Randle hypothesis revisited. Med Hypotheses. 1990;33(4):257-60.

41. Perseghin G, Petersen K, Shulman GI. Cellular mechanism of insulin resistance: potential links with inflammation. Int J Obes Relat Metab Disord. 2003;27 Suppl 3:S6-11.

42. Boden G, Shulman GI. Free fatty acids in obesity and type 2 diabetes: defining their role in the development of insulin resistance and beta-cell dysfunction. Eur J Clin Invest. 2002;32 Suppl 3:14-23.

43. Delaunay F, Khan A, Cintra A, Davani B, Ling ZC, Andersson A, et al. Pancreatic beta cells are important targets for the diabetogenic effects of glucocorticoids. J Clin Invest. 1997;100(8):2094-8.

44. van Raalte DH, Nofrate V, Bunck MC, van Iersel T, Elassaiss Schaap J, Nassander UK, et al. Acute and 2-week exposure to prednisolone impair different aspects of beta-cell function in healthy men. Eur J Endocrinol. 2010;162(4):729-35.

45. Wajngot A, Giacca A, Grill V, Vranic M, Efendic S. The diabetogenic effects of glucocorticoids are more pronounced in low- than in high-insulin responders. Proc Natl Acad Sci U S A. 1992;89(13):6035-9.

46. Shamoon H, Soman V, Sherwin RS. The influence of acute physiological increments of cortisol on fuel metabolism and insulin binding to monocytes in normal humans. J Clin Endocrinol Metab. 1980;50(3):495-501.

47. Kalhan SC, Adam PA. Inhibitory effect of prednisone on insulin secretion in man: model for duplication of blood glucose concentration. J Clin Endocrinol Metab. 1975;41(3):600-10.

48. Grill V, Pigon J, Hartling SG, Binder C, Efendic S. Effects of dexamethasone on glucose-induced insulin and proinsulin release in low and high insulin responders. Metabolism. 1990;39(3):251-8.

49. Larsson H, Ahren B. Insulin resistant subjects lack islet adaptation to short-term dexamethasone-induced reduction in insulin sensitivity. Diabetologia. 1999;42(8):936-43.

50. Beard JC, Halter JB, Best JD, Pfeifer MA, Porte D, Jr. Dexamethasone-induced insulin resistance enhances B cell responsiveness to glucose level in normal men. Am J Physiol. 1984;247(5 Pt 1):E592-6.

51. Matsumoto K, Yamasaki H, Akazawa S, Sakamaki H, Ishibashi M, Abiru N, et al. High-dose but not low-dose dexamethasone impairs glucose tolerance by inducing compensatory failure of pancreatic beta-cells in normal men. J Clin Endocrinol Metab. 1996;81(7):2621-6.

52. Dessein PH, Joffe BI. Insulin resistance and impaired beta cell function in rheumatoid arthritis. Arthritis Rheum. 2006;54(9):2765-75.

53. Stumvoll M, Goldstein BJ, van Haeften TW. Type 2 diabetes: principles of pathogenesis and therapy. Lancet. 2005;365(9467):1333-46.

54. Hamamdzic D, Duzic E, Sherlock JD, Lanier SM. Regulation of alpha 2-adrenergic receptor expression and signaling in pancreatic beta-cells. Am J Physiol. 1995;269(1 Pt 1):E162-71.

55. Ullrich S, Berchtold S, Ranta F, Seebohm G, Henke G, Lupescu A, et al. Serum- and glucocorticoid-inducible kinase 1 (SGK1) mediates glucocorticoid-induced inhibition of insulin secretion. Diabetes. 2005;54(4):1090-9.

56. Kanis JA, Johansson H, Oden A, Johnell O, de Laet C, Melton IL, et al. A meta-analysis of prior corticosteroid use and fracture risk. J Bone Miner Res. 2004;19(6):893-9.

57. Weinstein RS. Clinical practice. Glucocorticoid-induced bone disease. N Engl J Med. 2011;365(1):62-70.

58. Van Staa TP, Leufkens HG, Abenhaim L, Zhang B, Cooper C. Use of oral corticosteroids and risk of fractures. J Bone Miner Res. 2000;15(6):993-1000.

59. De Vries F, Bracke M, Leufkens HG, Lammers JW, Cooper C, Van Staa TP. Fracture risk with intermittent high-dose oral glucocorticoid therapy. Arthritis Rheum. 2007;56(1):208-14.

60. van Staa TP, Leufkens HG, Abenhaim L, Zhang B, Cooper C. Oral corticosteroids and fracture risk: relationship to daily and cumulative doses. Rheumatology (Oxford). 2000;39(12):1383-9.

61. van Staa TP, Leufkens HG, Cooper C. The epidemiology of corticosteroid-induced osteoporosis: a meta-analysis. Osteoporos Int. 2002;13(10):777-87.

62. Amiche MA, Albaum JM, Tadrous M, Pechlivanoglou P, Levesque LE, Adachi JD, et al. Fracture risk in oral glucocorticoid users: a Bayesian meta-regression leveraging control arms of osteoporosis clinical trials. Osteoporos Int. 2016;27(5):1709-18.

63. Balasubramanian A, Wade SW, Adler RA, Lin CJF, Maricic M, O'Malley CD, et al. Glucocorticoid exposure and fracture risk in patients with new-onset rheumatoid arthritis. Osteoporos Int. 2016;27(11):3239-49.

64. Lems WF, Van Veen GJ, Gerrits MI, Jacobs JW, Houben HH, Van Rijn HJ, et al. Effect of low-dose prednisone (with calcium and calcitriol supplementation) on calcium and bone metabolism in healthy volunteers. Br J Rheumatol. 1998;37(1):27-33.

65. Kauh E, Mixson L, Malice MP, Mesens S, Ramael S, Burke J, et al. Prednisone affects inflammation, glucose tolerance, and bone turnover within hours of treatment in healthy individuals. Eur J Endocrinol. 2012;166(3):459-67.

66. Kuroki Y, Kaji H, Kawano S, Kanda F, Takai Y, Kajikawa M, et al. Short-term effects of glucocorticoid therapy on biochemical markers of bone metabolism in Japanese patients: a prospective study. J Bone Miner Metab. 2008;26(3):271-8.

67. Kaji H, Kuroki Y, Murakawa Y, Funakawa I, Funasaka Y, Kanda F, et al. Effect of alendronate on bone metabolic indices and bone mineral density in patients

treated with high-dose glucocorticoid: a prospective study. Osteoporos Int. 2010;21(9):1565-71.

68. Perez P, Page A, Bravo A, Del Rio M, Gimenez-Conti I, Budunova I, et al. Altered skin development and impaired proliferative and inflammatory responses in transgenic mice overexpressing the glucocorticoid receptor. FASEB J. 2001;15(11):2030-2.

69. Schacke H, Docke WD, Asadullah K. Mechanisms involved in the side effects of glucocorticoids. Pharmacol Ther. 2002;96(1):23-43.

70. Kojima M, Shui YB, Sasaki K. Topographic distribution of prednisolone in the lens after organ culture. Ophthalmic Res. 1995;27 Suppl 1:25-33.

71. Tripathi RC, Parapuram SK, Tripathi BJ, Zhong Y, Chalam KV. Corticosteroids and glaucoma risk. Drugs Aging. 1999;15(6):439-50.

72. Zhou L, Li Y, Yue BY. Glucocorticoid effects on extracellular matrix proteins and integrins in bovine trabecular meshwork cells in relation to glaucoma. Int J Mol Med. 1998;1(2):339-46.

73. Hall RC, Popkin MK, Stickney SK, Gardner ER. Presentation of the steroid psychoses. J Nerv Ment Dis. 1979;167(4):229-36.

74. Carpenter WT, Jr., Gruen PH. Cortisol's effects on human mental functioning. J Clin Psychopharmacol. 1982;2(2):91-101.

75. Sapolsky RM, Uno H, Rebert CS, Finch CE. Hippocampal damage associated with prolonged glucocorticoid exposure in primates. J Neurosci. 1990;10(9):2897-902.

76. Watanabe Y, Gould E, Daniels DC, Cameron H, McEwen BS. Tianeptine attenuates stress-induced morphological changes in the hippocampus. Eur J Pharmacol. 1992;222(1):157-62.

77. Magarinos AM, Verdugo JM, McEwen BS. Chronic stress alters synaptic terminal structure in hippocampus. Proc Natl Acad Sci U S A. 1997;94(25):14002-8.

78. Uno H, Lohmiller L, Thieme C, Kemnitz JW, Engle MJ, Roecker EB, et al. Brain damage induced by prenatal exposure to dexamethasone in fetal rhesus macaques. I. Hippocampus. Brain Res Dev Brain Res. 1990;53(2):157-67.

79. Gould E, Tanapat P, McEwen BS, Flugge G, Fuchs E. Proliferation of granule cell precursors in the dentate gyrus of adult monkeys is diminished by stress. Proc Natl Acad Sci U S A. 1998;95(6):3168-71.

80. Lawrence MS, Sapolsky RM. Glucocorticoids accelerate ATP loss following metabolic insults in cultured hippocampal neurons. Brain Res. 1994;646(2):303-6.

81. Virgin CE, Jr., Ha TP, Packan DR, Tombaugh GC, Yang SH, Horner HC, et al. Glucocorticoids inhibit glucose transport and glutamate uptake in hippocampal astrocytes: implications for glucocorticoid neurotoxicity. J Neurochem. 1991;57(4):1422-8.

82. Stein-Behrens BA, Lin WJ, Sapolsky RM. Physiological elevations of glucocorticoids potentiate glutamate accumulation in the hippocampus. J Neurochem. 1994;63(2):596-602.

83. Julius D. Molecular biology of serotonin receptors. Annu Rev Neurosci. 1991;14:335-60.

84. Wissink S, Meijer O, Pearce D, van Der Burg B, van Der Saag PT. Regulation of the rat serotonin-1A receptor gene by corticosteroids. J Biol Chem. 2000;275(2):1321-6.

85. Funder JW, Pearce PT, Smith R, Smith AI. Mineralocorticoid action: target tissue specificity is enzyme, not receptor, mediated. Science. 1988;242(4878):583-5.

86. Sholter DE, Armstrong PW. Adverse effects of corticosteroids on the cardiovascular system. Can J Cardiol. 2000;16(4):505-11.

87. Sato A, Funder JW, Okubo M, Kubota E, Saruta T. Glucocorticoid-induced hypertension in the elderly. Relation to serum calcium and family history of essential hypertension. Am J Hypertens. 1995;8(8):823-8.

88. Di Fazano CS, Messica O, Quennesson S, Quennesson ER, Inaoui R, Vergne P, et al. Two new cases of glucocorticoid-induced pancreatitis. Rev Rhum Engl Ed. 1999;66(4):235.

89. Kennedy WA, Laurier C, Gautrin D, Ghezzo H, Pare M, Malo JL, et al. Occurrence and risk factors of oral candidiasis treated with oral antifungals in seniors using inhaled steroids. J Clin Epidemiol. 2000;53(7):696-701.

90. Richardson CT. Pathogenetic factors in peptic ulcer disease. Am J Med. 1985;79(2C):1-7.

91. Pivonello R, Isidori AM, De Martino MC, Newell-Price J, Biller BM, Colao A. Complications of Cushing's syndrome: state of the art. Lancet Diabetes Endocrinol. 2016;4(7):611-29.

92. Overman RA, Yeh JY, Deal CL. Prevalence of oral glucocorticoid usage in the United States: a general population perspective. Arthritis Care Res (Hoboken). 2013;65(2):294-8.

93. van Staa TP, Leufkens HG, Abenhaim L, Begaud B, Zhang B, Cooper C. Use of oral corticosteroids in the United Kingdom. QJM. 2000;93(2):105-11.

94. Fardet L, Petersen I, Nazareth I. [Description of oral glucocorticoid prescriptions in general population]. Rev Med Interne. 2011;32(10):594-9.

95. Benard-Laribiere A, Pariente A, Pambrun E, Begaud B, Fardet L, Noize P. Prevalence and prescription patterns of oral glucocorticoids in adults: a retrospective cross-sectional and cohort analysis in France. BMJ Open. 2017;7(7):e015905.

96. Tomlinson JW, Draper N, Mackie J, Johnson AP, Holder G, Wood P, et al. Absence of Cushingoid phenotype in a patient with Cushing's disease due to defective cortisone to cortisol conversion. J Clin Endocrinol Metab. 2002;87(1):57-62.

97. Arai H, Kobayashi N, Nakatsuru Y, Masuzaki H, Nambu T, Takaya K, et al. A case of cortisol producing adrenal adenoma without phenotype of Cushing's syndrome due to impaired 11beta-hydroxysteroid dehydrogenase 1 activity. Endocr J. 2008;55(4):709-15.

98. Fenton C, Martin C, Jones R, Croft A, Campos J, Naylor AJ, et al. Local steroid activation is a critical mediator of the anti-inflammatory actions of therapeutic glucocorticoids. Ann Rheum Dis. 2020.

99. Tomlinson JW, Walker EA, Bujalska IJ, Draper N, Lavery GG, Cooper MS, et al. 11beta-hydroxysteroid dehydrogenase type 1: a tissue-specific regulator of glucocorticoid response. Endocr Rev. 2004;25(5):831-66.

100. Odermatt A, Arnold P, Stauffer A, Frey BM, Frey FJ. The N-terminal anchor sequences of 11beta-hydroxysteroid dehydrogenases determine their orientation in the endoplasmic reticulum membrane. J Biol Chem. 1999;274(40):28762-70.

101. Draper N, Walker EA, Bujalska IJ, Tomlinson JW, Chalder SM, Arlt W, et al. Mutations in the genes encoding 11beta-hydroxysteroid dehydrogenase type 1 and hexose-6-phosphate dehydrogenase interact to cause cortisone reductase deficiency. Nat Genet. 2003;34(4):434-9.

102. Tannin GM, Agarwal AK, Monder C, New MI, White PC. The human gene for 11 beta-hydroxysteroid dehydrogenase. Structure, tissue distribution, and chromosomal localization. J Biol Chem. 1991;266(25):16653-8.

103. Gomez-Sanchez EP, Ganjam V, Chen YJ, Liu Y, Zhou MY, Toroslu C, et al. Regulation of 11 beta-hydroxysteroid dehydrogenase enzymes in the rat kidney by estradiol. Am J Physiol Endocrinol Metab. 2003;285(2):E272-9.

104. Lavery GG, Walker EA, Tiganescu A, Ride JP, Shackleton CH, Tomlinson JW, et al. Steroid biomarkers and genetic studies reveal inactivating mutations in hexose-6-phosphate dehydrogenase in patients with cortisone reductase deficiency. J Clin Endocrinol Metab. 2008;93(10):3827-32.

105. Lawson AJ, Walker EA, Lavery GG, Bujalska IJ, Hughes B, Arlt W, et al. Cortisone-reductase deficiency associated with heterozygous mutations in 11beta-hydroxysteroid dehydrogenase type 1. Proc Natl Acad Sci U S A. 2011;108(10):4111-6.

106. Lavery GG, Idkowiak J, Sherlock M, Bujalska I, Ride JP, Saqib K, et al. Novel H6PDH mutations in two girls with premature adrenarche: 'apparent' and 'true' CRD can be differentiated by urinary steroid profiling. Eur J Endocrinol. 2013;168(2):K19-26.

107. Gathercole LL, Lavery GG, Morgan SA, Cooper MS, Sinclair AJ, Tomlinson JW, et al. 11beta-Hydroxysteroid dehydrogenase 1: translational and therapeutic aspects. Endocr Rev. 2013;34(4):525-55.

108. Rahman TJ, Walker EA, Mayosi BM, Hall DH, Avery PJ, Connell JM, et al. Genotype at the P554L variant of the hexose-6 phosphate dehydrogenase gene is associated with carotid intima-medial thickness. PLoS One. 2011;6(8):e23248.

109. Wellcome Trust Case Control C, Australo-Anglo-American Spondylitis C, Burton PR, Clayton DG, Cardon LR, Craddock N, et al. Association scan of 14,500 nonsynonymous SNPs in four diseases identifies autoimmunity variants. Nat Genet. 2007;39(11):1329-37.

110. Alcina A, Fernandez O, Gonzalez JR, Catala-Rabasa A, Fedetz M, Ndagire D, et al. Tag-SNP analysis of the GFI1-EVI5-RPL5-FAM69 risk locus for multiple sclerosis. Eur J Hum Genet. 2010;18(7):827-31.

111. San Millan JL, Botella-Carretero JI, Alvarez-Blasco F, Luque-Ramirez M, Sancho J, Moghetti P, et al. A study of the hexose-6-phosphate dehydrogenase gene R453Q and 11beta-hydroxysteroid dehydrogenase type 1 gene 83557insA polymorphisms in the polycystic ovary syndrome. J Clin Endocrinol Metab. 2005;90(7):4157-62.

112. Martinez-Garcia MA, San-Millan JL, Escobar-Morreale HF. The R453Q and D151A polymorphisms of hexose-6-phosphate dehydrogenase gene (H6PD) influence the polycystic ovary syndrome (PCOS) and obesity. Gene. 2012;497(1):38-44.

113. Veilleux A, Rheaume C, Daris M, Luu-The V, Tchernof A. Omental adipose tissue type 1 11 beta-hydroxysteroid dehydrogenase oxoreductase activity, body fat distribution, and metabolic alterations in women. J Clin Endocrinol Metab. 2009;94(9):3550-7.

114. Morton NM, Ramage L, Seckl JR. Down-regulation of adipose 11beta-hydroxysteroid dehydrogenase type 1 by high-fat feeding in mice: a potential adaptive mechanism counteracting metabolic disease. Endocrinology. 2004;145(6):2707-12.

115. Bujalska IJ, Gathercole LL, Tomlinson JW, Darimont C, Ermolieff J, Fanjul AN, et al. A novel selective 11beta-hydroxysteroid dehydrogenase type 1 inhibitor prevents human adipogenesis. J Endocrinol. 2008;197(2):297-307.

116. Chapman K, Holmes M, Seckl J. 11beta-hydroxysteroid dehydrogenases: intracellular gate-keepers of tissue glucocorticoid action. Physiol Rev. 2013;93(3):1139-206.

117. Travison TG, O'Donnell AB, Araujo AB, Matsumoto AM, McKinlay JB. Cortisol levels and measures of body composition in middle-aged and older men. Clin Endocrinol (Oxf). 2007;67(1):71-7.

118. Woods CP, Corrigan M, Gathercole L, Taylor A, Hughes B, Gaoatswe G, et al. Tissue specific regulation of glucocorticoids in severe obesity and the response to significant weight loss following bariatric surgery (BARICORT). J Clin Endocrinol Metab. 2015;100(4):1434-44.

119. Mlinar B, Marc J, Jensterle M, Bokal EV, Jerin A, Pfeifer M. Expression of 11beta-hydroxysteroid dehydrogenase type 1 in visceral and subcutaneous adipose tissues of patients with polycystic ovary syndrome is associated with adiposity. J Steroid Biochem Mol Biol. 2011;123(3-5):127-32.

120. Michailidou Z, Jensen MD, Dumesic DA, Chapman KE, Seckl JR, Walker BR, et al. Omental 11beta-hydroxysteroid dehydrogenase 1 correlates with fat cell size independently of obesity. Obesity (Silver Spring). 2007;15(5):1155-63.

121. Goedecke JH, Wake DJ, Levitt NS, Lambert EV, Collins MR, Morton NM, et al. Glucocorticoid metabolism within superficial subcutaneous rather than visceral

adipose tissue is associated with features of the metabolic syndrome in South African women. Clin Endocrinol (Oxf). 2006;65(1):81-7.

122. Masuzaki H, Paterson J, Shinyama H, Morton NM, Mullins JJ, Seckl JR, et al. A transgenic model of visceral obesity and the metabolic syndrome. Science. 2001;294(5549):2166-70.

123. Morton NM, Paterson JM, Masuzaki H, Holmes MC, Staels B, Fievet C, et al. Novel adipose tissue-mediated resistance to diet-induced visceral obesity in 11 beta-hydroxysteroid dehydrogenase type 1-deficient mice. Diabetes. 2004;53(4):931-8.

124. Ricketts ML, Verhaeg JM, Bujalska I, Howie AJ, Rainey WE, Stewart PM. Immunohistochemical localization of type 1 11beta-hydroxysteroid dehydrogenase in human tissues. J Clin Endocrinol Metab. 1998;83(4):1325-35.

125. Jamieson PM, Chapman KE, Edwards CR, Seckl JR. 11 beta-hydroxysteroid dehydrogenase is an exclusive 11 beta- reductase in primary cultures of rat hepatocytes: effect of physicochemical and hormonal manipulations. Endocrinology. 1995;136(11):4754-61.

126. Ricketts ML, Shoesmith KJ, Hewison M, Strain A, Eggo MC, Stewart PM. Regulation of 11 beta-hydroxysteroid dehydrogenase type 1 in primary cultures of rat and human hepatocytes. J Endocrinol. 1998;156(1):159-68.

127. Stimson RH, Andrew R, McAvoy NC, Tripathi D, Hayes PC, Walker BR. Increased whole-body and sustained liver cortisol regeneration by 11beta-hydroxysteroid dehydrogenase type 1 in obese men with type 2 diabetes provides a target for enzyme inhibition. Diabetes. 2011;60(3):720-5.

128. Torrecilla E, Fernandez-Vazquez G, Vicent D, Sanchez-Franco F, Barabash A, Cabrerizo L, et al. Liver upregulation of genes involved in cortisol production and action is associated with metabolic syndrome in morbidly obese patients. Obes Surg. 2012;22(3):478-86.

129. Shukla R, Basu AK, Mandal B, Mukhopadhyay P, Maity A, Chakraborty S, et al. 11beta Hydroxysteroid dehydrogenase - 1 activity in type 2 diabetes mellitus: a comparative study. BMC Endocr Disord. 2019;19(1):15.

130. Deary IJ, Hayward C, Permana PA, Nair S, Whalley LJ, Starr JM, et al. Polymorphisms in the gene encoding 11B-hydroxysteroid dehydrogenase type 1 (HSD11B1) and lifetime cognitive change. Neurosci Lett. 2006;393(1):74-7.

131. Dube S, Slama MQ, Basu A, Rizza RA, Basu R. Glucocorticoid Excess Increases Hepatic 11beta-HSD-1 Activity in Humans: Implications in Steroid-Induced Diabetes. J Clin Endocrinol Metab. 2015;100(11):4155-62.

132. Paterson JM, Morton NM, Fievet C, Kenyon CJ, Holmes MC, Staels B, et al. Metabolic syndrome without obesity: Hepatic overexpression of 11beta-hydroxysteroid dehydrogenase type 1 in transgenic mice. Proc Natl Acad Sci U S A. 2004;101(18):7088-93.

133. Lavery GG, Zielinska AE, Gathercole LL, Hughes B, Semjonous N, Guest P, et al. Lack of significant metabolic abnormalities in mice with liver-specific disruption of 11beta-hydroxysteroid dehydrogenase type 1. Endocrinology. 2012;153(7):3236-48.

134. Morton NM, Holmes MC, Fievet C, Staels B, Tailleux A, Mullins JJ, et al. Improved lipid and lipoprotein profile, hepatic insulin sensitivity, and glucose tolerance in 11beta-hydroxysteroid dehydrogenase type 1 null mice. J Biol Chem. 2001;276(44):41293-300.

135. Morgan SA, McCabe EL, Gathercole LL, Hassan-Smith ZK, Larner DP, Bujalska IJ, et al. 11beta-HSD1 is the major regulator of the tissue-specific effects of circulating glucocorticoid excess. Proc Natl Acad Sci U S A. 2014;111(24):E2482-91.

136. Whorwood CB, Donovan SJ, Wood PJ, Phillips DI. Regulation of glucocorticoid receptor alpha and beta isoforms and type I 11beta-hydroxysteroid dehydrogenase expression in human skeletal muscle cells: a key role in the pathogenesis of insulin resistance? J Clin Endocrinol Metab. 2001;86(5):2296-308.

137. Abdallah BM, Beck-Nielsen H, Gaster M. Increased expression of 11beta-hydroxysteroid dehydrogenase type 1 in type 2 diabetic myotubes. Eur J Clin Invest. 2005;35(10):627-34.

138. Zhang M, Lv XY, Li J, Xu ZG, Chen L. Alteration of 11beta-hydroxysteroid dehydrogenase type 1 in skeletal muscle in a rat model of type 2 diabetes. Mol Cell Biochem. 2009;324(1-2):147-55.

139. Hassan-Smith ZK, Morgan SA, Sherlock M, Hughes B, Taylor AE, Lavery GG, et al. Gender-Specific Differences in Skeletal Muscle 11beta-HSD1 Expression Across Healthy Aging. J Clin Endocrinol Metab. 2015;100(7):2673-81.

140. Swali A, Walker EA, Lavery GG, Tomlinson JW, Stewart PM. 11beta-Hydroxysteroid dehydrogenase type 1 regulates insulin and glucagon secretion in pancreatic islets. Diabetologia. 2008;51(11):2003-11.

141. Davani B, Khan A, Hult M, Martensson E, Okret S, Efendic S, et al. Type 1 11beta -hydroxysteroid dehydrogenase mediates glucocorticoid activation and insulin release in pancreatic islets. J Biol Chem. 2000;275(45):34841-4.

142. Turban S, Liu X, Ramage L, Webster SP, Walker BR, Dunbar DR, et al. Optimal elevation of beta-cell 11beta-hydroxysteroid dehydrogenase type 1 is a compensatory mechanism that prevents high-fat diet-induced beta-cell failure. Diabetes. 2012;61(3):642-52.

143. Ortsater H, Alberts P, Warpman U, Engblom LO, Abrahmsen L, Bergsten P. Regulation of 11beta-hydroxysteroid dehydrogenase type 1 and glucose-stimulated insulin secretion in pancreatic islets of Langerhans. Diabetes Metab Res Rev. 2005;21(4):359-66.

144. Duplomb L, Lee Y, Wang MY, Park BH, Takaishi K, Agarwal AK, et al. Increased expression and activity of 11beta-HSD-1 in diabetic islets and prevention with troglitazone. Biochem Biophys Res Commun. 2004;313(3):594-9.

145. Walker BR, Yau JL, Brett LP, Seckl JR, Monder C, Williams BC, et al. 11 beta-hydroxysteroid dehydrogenase in vascular smooth muscle and heart: implications for cardiovascular responses to glucocorticoids. Endocrinology. 1991;129(6):3305-12.

146. Small GR, Hadoke PW, Sharif I, Dover AR, Armour D, Kenyon CJ, et al. Preventing local regeneration of glucocorticoids by 11beta-hydroxysteroid dehydrogenase type 1 enhances angiogenesis. Proc Natl Acad Sci U S A. 2005;102(34):12165-70.

147. Gomez-Sanchez EP, Romero DG, de Rodriguez AF, Warden MP, Krozowski Z, Gomez-Sanchez CE. Hexose-6-phosphate dehydrogenase and 11beta-hydroxysteroid dehydrogenase-1 tissue distribution in the rat. Endocrinology. 2008;149(2):525-33.

148. Sooy K, Webster SP, Noble J, Binnie M, Walker BR, Seckl JR, et al. Partial deficiency or short-term inhibition of 11beta-hydroxysteroid dehydrogenase type 1 improves cognitive function in aging mice. J Neurosci. 2010;30(41):13867-72.

149. Sandeep TC, Yau JL, MacLullich AM, Noble J, Deary IJ, Walker BR, et al. 11Beta-hydroxysteroid dehydrogenase inhibition improves cognitive function in

healthy elderly men and type 2 diabetics. Proc Natl Acad Sci U S A. 2004;101(17):6734-9.

150. Rauz S, Walker EA, Shackleton CH, Hewison M, Murray PI, Stewart PM. Expression and putative role of 11 beta-hydroxysteroid dehydrogenase isozymes within the human eye. Invest Ophthalmol Vis Sci. 2001;42(9):2037-42.

151. Coutinho AE KT, Zhang Z, Esteves C, Gilmour JS, Cailhier JF, Hughes J, Seckl JR,, Savill JS CK. Dynamic regulation of 11-hydroxysteroid dehydrogenase type 1 in neutrophils during an inflammatory response. Endocr Rev. 2011;32:2-575.

152. Freeman L, Hewison M, Hughes SV, Evans KN, Hardie D, Means TK, et al. Expression of 11beta-hydroxysteroid dehydrogenase type 1 permits regulation of glucocorticoid bioavailability by human dendritic cells. Blood. 2005;106(6):2042-9.

153. Coutinho AE, Gray M, Brownstein DG, Salter DM, Sawatzky DA, Clay S, et al. 11beta-Hydroxysteroid dehydrogenase type 1, but not type 2, deficiency worsens acute inflammation and experimental arthritis in mice. Endocrinology. 2012;153(1):234-40.

154. Hardy R, Rabbitt EH, Filer A, Emery P, Hewison M, Stewart PM, et al. Local and systemic glucocorticoid metabolism in inflammatory arthritis. Ann Rheum Dis. 2008;67(9):1204-10.

155. Cooper MS, Kriel H, Sayers A, Fraser WD, Williams AM, Stewart PM, et al. Can 11beta-hydroxysteroid dehydrogenase activity predict the sensitivity of bone to therapeutic glucocorticoids in inflammatory bowel disease? Calcif Tissue Int. 2011;89(3):246-51.

156. Cooper MS, Blumsohn A, Goddard PE, Bartlett WA, Shackleton CH, Eastell R, et al. 11beta-hydroxysteroid dehydrogenase type 1 activity predicts the effects of glucocorticoids on bone. J Clin Endocrinol Metab. 2003;88(8):3874-7.

157. Tiganescu A, Walker EA, Hardy RS, Mayes AE, Stewart PM. Localization, age- and site-dependent expression, and regulation of 11beta-hydroxysteroid dehydrogenase type 1 in skin. J Invest Dermatol. 2011;131(1):30-6.

158. Vukelic S, Stojadinovic O, Pastar I, Rabach M, Krzyzanowska A, Lebrun E, et al. Cortisol synthesis in epidermis is induced by IL-1 and tissue injury. J Biol Chem. 2011;286(12):10265-75.

159. Terao M, Murota H, Kimura A, Kato A, Ishikawa A, Igawa K, et al. 11beta-Hydroxysteroid dehydrogenase-1 is a novel regulator of skin homeostasis and a candidate target for promoting tissue repair. PLoS One. 2011;6(9):e25039.

160. Hennebert O, Chalbot S, Alran S, Morfin R. Dehydroepiandrosterone 7alpha-hydroxylation in human tissues: possible interference with type 1 11beta-hydroxysteroid dehydrogenase-mediated processes. J Steroid Biochem Mol Biol. 2007;104(3-5):326-33.

161. Classen-Houben D, Schuster D, Da Cunha T, Odermatt A, Wolber G, Jordis U, et al. Selective inhibition of 11beta-hydroxysteroid dehydrogenase 1 by 18alpha-glycyrrhetinic acid but not 18beta-glycyrrhetinic acid. J Steroid Biochem Mol Biol. 2009;113(3-5):248-52.

162. Diederich S, Grossmann C, Hanke B, Quinkler M, Herrmann M, Bahr V, et al. In the search for specific inhibitors of human 11beta-hydroxysteroid-dehydrogenases (11beta-HSDs): chenodeoxycholic acid selectively inhibits 11beta-HSD-I. Eur J Endocrinol. 2000;142(2):200-7.

163. Livingstone DE, Walker BR. Is 11beta-hydroxysteroid dehydrogenase type 1 a therapeutic target? Effects of carbenoxolone in lean and obese Zucker rats. J Pharmacol Exp Ther. 2003;305(1):167-72.

164. Sharma RA, McLelland HR, Hill KA, Ireson CR, Euden SA, Manson MM, et al. Pharmacodynamic and pharmacokinetic study of oral Curcuma extract in patients with colorectal cancer. Clin Cancer Res. 2001;7(7):1894-900.

165. Zhao L, Pan Y, Peng K, Wang Z, Li J, Li D, et al. Inhibition of 11beta-HSD1 by LG13 improves glucose metabolism in type 2 diabetic mice. J Mol Endocrinol. 2015;55(2):119-31.

166. Hintzpeter J, Stapelfeld C, Loerz C, Martin HJ, Maser E. Green tea and one of its constituents, Epigallocatechine-3-gallate, are potent inhibitors of human 11beta-hydroxysteroid dehydrogenase type 1. PLoS One. 2014;9(1):e84468.

167. Tagawa N, Yuda R, Kubota S, Wakabayashi M, Yamaguchi Y, Kiyonaga D, et al. 17Beta-estradiol inhibits 11beta-hydroxysteroid dehydrogenase type 1 activity in rodent adipocytes. J Endocrinol. 2009;202(1):131-9.

168. Cao J, Gao L, Chen Y, Sun W, Wang F, Li H, et al. Citrinal B, natural 11 beta-hydroxysteroid dehydrogennase type 1 inhibitor identified from structure-based virtual screening. Fitoterapia. 2017;123:29-34.

169. Barf T, Vallgarda J, Emond R, Haggstrom C, Kurz G, Nygren A, et al. Arylsulfonamidothiazoles as a new class of potential antidiabetic drugs. Discovery of potent and selective inhibitors of the 11beta-hydroxysteroid dehydrogenase type 1. J Med Chem. 2002;45(18):3813-5.

170. Alberts P, Engblom L, Edling N, Forsgren M, Klingstrom G, Larsson C, et al. Selective inhibition of 11beta-hydroxysteroid dehydrogenase type 1 decreases blood glucose concentrations in hyperglycaemic mice. Diabetologia. 2002;45(11):1528-32.

171. Alberts P, Nilsson C, Selen G, Engblom LO, Edling NH, Norling S, et al. Selective inhibition of 11 beta-hydroxysteroid dehydrogenase type 1 improves hepatic insulin sensitivity in hyperglycemic mice strains. Endocrinology. 2003;144(11):4755-62.

172. Berthiaume M, Laplante M, Festuccia WT, Cianflone K, Turcotte LP, Joanisse DR, et al. 11beta-HSD1 inhibition improves triglyceridemia through reduced liver VLDL secretion and partitions lipids toward oxidative tissues. Am J Physiol Endocrinol Metab. 2007;293(4):E1045-52.

173. Berthiaume M, Laplante M, Festuccia W, Gelinas Y, Poulin S, Lalonde J, et al. Depot-specific modulation of rat intraabdominal adipose tissue lipid metabolism by pharmacological inhibition of 11beta-hydroxysteroid dehydrogenase type 1. Endocrinology. 2007;148(5):2391-7.

174. Park SB, Park JS, Jung WH, Kim HY, Kwak HJ, Ahn JH, et al. Anti-inflammatory effect of a selective 11beta-hydroxysteroid dehydrogenase type 1 inhibitor via the stimulation of heme oxygenase-1 in LPS-activated mice and J774.1 murine macrophages. J Pharmacol Sci. 2016;131(4):241-50.

175. Park SB, Jung WH, Kang NS, Park JS, Bae GH, Kim HY, et al. Anti-diabetic and anti-inflammatory effect of a novel selective 11beta-HSD1 inhibitor in the diet-induced obese mice. Eur J Pharmacol. 2013;721(1-3):70-9.

176. Ryu JH, Lee JA, Kim S, Shin YA, Yang J, Han HY, et al. Discovery of 2-((R)-4-(2-Fluoro-4-(methylsulfonyl)phenyl)-2-methylpiperazin-1-yl)-N-((1R,2s,3S ,5S,7S)-5-hydroxyadamantan-2-yl)pyrimidine-4-carboxamide (SKI2852): A Highly Potent, Selective, and Orally Bioavailable Inhibitor of 11beta-Hydroxysteroid Dehydrogenase Type 1 (11beta-HSD1). J Med Chem. 2016;59(22):10176-89.

177. Oh H, Jeong KH, Han HY, Son HJ, Kim SS, Lee HJ, et al. A potent and selective 11beta-hydroxysteroid dehydrogenase type 1 inhibitor, SKI2852, ameliorates metabolic syndrome in diabetic mice models. Eur J Pharmacol. 2015;768:139-48.

178. Byun SY, Shin YJ, Nam KY, Hong SP, Ahn SK. A novel highly potent and selective 11beta-hydroxysteroid dehydrogenase type 1 inhibitor, UI-1499. Life Sci. 2015;120:1-7.

179. Freude S, Heise T, Woerle HJ, Jungnik A, Rauch T, Hamilton B, et al. Safety, pharmacokinetics and pharmacodynamics of BI 135585, a selective 11beta-hydroxysteroid dehydrogenase-1 (HSD1) inhibitor in humans: liver and adipose tissue 11beta-HSD1 inhibition after acute and multiple administrations over 2 weeks. Diabetes Obes Metab. 2016;18(5):483-90.

180. Hamilton BS, Himmelsbach F, Nar H, Schuler-Metz A, Krosky P, Guo J, et al. Pharmacological characterization of the selective 11beta-hydroxysteroid dehydrogenase 1 inhibitor, BI 135585, a clinical candidate for the treatment of type 2 diabetes. Eur J Pharmacol. 2015;746:50-5.

181. Wan ZK, Chenail E, Li HQ, Ipek M, Xiang J, Suri V, et al. Discovery of HSD-621 as a Potential Agent for the Treatment of Type 2 Diabetes. ACS Med Chem Lett. 2013;4(1):118-23.

182. Edgerton DS, Basu R, Ramnanan CJ, Farmer TD, Neal D, Scott M, et al. Effect of 11 beta-hydroxysteroid dehydrogenase-1 inhibition on hepatic glucose metabolism in the conscious dog. Am J Physiol Endocrinol Metab. 2010;298(5):E1019-26.

183. A study of the effect of INCB013739 on cortisone reducing enzyme activity in obese people predisposed to diabetes. National Institutes of Health 2012.

184. Rosenstock J, Banarer S, Fonseca VA, Inzucchi SE, Sun W, Yao W, et al. The 11-beta-hydroxysteroid dehydrogenase type 1 inhibitor INCB13739 improves hyperglycemia in patients with type 2 diabetes inadequately controlled by metformin monotherapy. Diabetes Care. 2010;33(7):1516-22.

185. Feig PU, Shah S, Hermanowski-Vosatka A, Plotkin D, Springer MS, Donahue S, et al. Effects of an 11beta-hydroxysteroid dehydrogenase type 1 inhibitor, MK-0916, in patients with type 2 diabetes mellitus and metabolic syndrome. Diabetes Obes Metab. 2011;13(6):498-504.

186. AstraZeneca Mechanism of action: 11beta-hydroxysteroid dehydrogenase type 1 (11beta-HSD1) inhibitor. 2017 [Available from: https://openinnovation.astrazeneca.com/azd4017.html.

187. Russell DW, Wilson JD. Steroid 5 alpha-reductase: two genes/two enzymes. Annu Rev Biochem. 1994;63:25-61.

188. Uemura M, Tamura K, Chung S, Honma S, Okuyama A, Nakamura Y, et al. Novel 5 alpha-steroid reductase (SRD5A3, type-3) is overexpressed in hormone-refractory prostate cancer. Cancer Sci. 2008;99(1):81-6.

189. Tamura K, Furihata M, Tsunoda T, Ashida S, Takata R, Obara W, et al. Molecular features of hormone-refractory prostate cancer cells by genome-wide gene expression profiles. Cancer Res. 2007;67(11):5117-25.

190. Tomkins GM, Yielding KL, Curran JF. The influence of diethylstilbestrol and adenosine diphosphate on pyridine nucleotide coenzyme binding by glutamic dehydrogenase. J Biol Chem. 1962;237:1704-8.

191. Poletti A, Coscarella A, Negri-Cesi P, Colciago A, Celotti F, Martini L. 5 alpha-reductase isozymes in the central nervous system. Steroids. 1998;63(5-6):246-51.

192. Gisleskog PO, Hermann D, Hammarlund-Udenaes M, Karlsson MO. A model for the turnover of dihydrotestosterone in the presence of the irreversible 5 alpha-reductase inhibitors GI198745 and finasteride. Clin Pharmacol Ther. 1998;64(6):636-47.

193. Andersson S, Russell DW. Structural and biochemical properties of cloned and expressed human and rat steroid 5 alpha-reductases. Proc Natl Acad Sci U S A. 1990;87(10):3640-4.

194. Normington K, Russell DW. Tissue distribution and kinetic characteristics of rat steroid 5 alpha-reductase isozymes. Evidence for distinct physiological functions. J Biol Chem. 1992;267(27):19548-54.

195. Samtani R, Bajpai M, Ghosh PK, Saraswathy KN. SRD5A2 gene mutations--a population-based review. Pediatr Endocrinol Rev. 2010;8(1):34-40.

196. Jakimiuk AJ, Weitsman SR, Magoffin DA. 5alpha-reductase activity in women with polycystic ovary syndrome. J Clin Endocrinol Metab. 1999;84(7):2414-8.

197. Labrie F, Dupont A, Simard J, Luu-The V, Belanger A. Intracrinology: the basis for the rational design of endocrine therapy at all stages of prostate cancer. Eur Urol. 1993;24 Suppl 2:94-105.

198. Dowman JK, Hopkins LJ, Reynolds GM, Armstrong MJ, Nasiri M, Nikolaou N, et al. Loss of 5alpha-reductase type 1 accelerates the development of hepatic steatosis but protects against hepatocellular carcinoma in male mice. Endocrinology. 2013;154(12):4536-47.

199. Livingstone DE, Barat P, Di Rollo EM, Rees GA, Weldin BA, Rog-Zielinska EA, et al. 5alpha-Reductase type 1 deficiency or inhibition predisposes to insulin

resistance, hepatic steatosis, and liver fibrosis in rodents. Diabetes. 2015;64(2):447-58.

200. Blumenfeld Z, Kaidar G, Zuckerman-Levin N, Dumin E, Knopf C, Hochberg Z. Cortisol-Metabolizing Enzymes in Polycystic Ovary Syndrome. Clin Med Insights Reprod Health. 2016;10:9-13.

201. Crowley RK, Hughes B, Gray J, McCarthy T, Hughes S, Shackleton CH, et al. Longitudinal changes in glucocorticoid metabolism are associated with later development of adverse metabolic phenotype. Eur J Endocrinol. 2014;171(4):433-42.

202. Tomlinson JW, Finney J, Gay C, Hughes BA, Hughes SV, Stewart PM. Impaired glucose tolerance and insulin resistance are associated with increased adipose 11beta-hydroxysteroid dehydrogenase type 1 expression and elevated hepatic 5alpha-reductase activity. Diabetes. 2008;57(10):2652-60.

203. Tomlinson JW, Finney J, Hughes BA, Hughes SV, Stewart PM. Reduced glucocorticoid production rate, decreased 5alpha-reductase activity, and adipose tissue insulin sensitization after weight loss. Diabetes. 2008;57(6):1536-43.

204. Tsilchorozidou T, Honour JW, Conway GS. Altered cortisol metabolism in polycystic ovary syndrome: insulin enhances 5alpha-reduction but not the elevated adrenal steroid production rates. J Clin Endocrinol Metab. 2003;88(12):5907-13.

205. Vassiliadi DA, Barber TM, Hughes BA, McCarthy MI, Wass JA, Franks S, et al. Increased 5 alpha-reductase activity and adrenocortical drive in women with polycystic ovary syndrome. J Clin Endocrinol Metab. 2009;94(9):3558-66.

206. Zyirek M, Flood C, Longcope C. 5 alpha-reductase activity in rat adipose tissue. Proc Soc Exp Biol Med. 1987;186(2):134-8.

207. Perel E, Daniilescu D, Kindler S, Kharlip L, Killinger DW. The formation of 5 alpha-reduced androgens in stromal cells from human breast adipose tissue. J Clin Endocrinol Metab. 1986;62(2):314-8.

208. Upreti R, Hughes KA, Livingstone DE, Gray CD, Minns FC, Macfarlane DP, et al. 5alpha-reductase type 1 modulates insulin sensitivity in men. J Clin Endocrinol Metab. 2014;99(8):E1397-406.

209. Campelo AE, Cutini PH, Massheimer VL. Cellular actions of testosterone in vascular cells: mechanism independent of aromatization to estradiol. Steroids. 2012;77(11):1033-40.

210. Quinkler M, Bumke-Vogt C, Meyer B, Bahr V, Oelkers W, Diederich S. The human kidney is a progesterone-metabolizing and androgen-producing organ. J Clin Endocrinol Metab. 2003;88(6):2803-9.

211. Mak TCS, Livingstone DEW, Nixon M, Walker BR, Andrew R. Role of Hepatic Glucocorticoid Receptor in Metabolism in Models of 5alphaR1 Deficiency in Male Mice. Endocrinology. 2019;160(9):2061-73.

212. Nasiri M, Nikolaou N, Parajes S, Krone NP, Valsamakis G, Mastorakos G, et al. 5alpha-Reductase Type 2 Regulates Glucocorticoid Action and Metabolic Phenotype in Human Hepatocytes. Endocrinology. 2015;156(8):2863-71.

213. Hazlehurst JM, Oprescu AI, Nikolaou N, Di Guida R, Grinbergs AE, Davies NP, et al. Dual-5alpha-Reductase Inhibition Promotes Hepatic Lipid Accumulation in Man. J Clin Endocrinol Metab. 2016;101(1):103-13.

214. Wei L, Lai EC, Kao-Yang YH, Walker BR, MacDonald TM, Andrew R. Incidence of type 2 diabetes mellitus in men receiving steroid 5alpha-reductase inhibitors: population based cohort study. BMJ. 2019;365:l1204.

215. Steele R. Influences of glucose loading and of injected insulin on hepatic glucose output. Ann N Y Acad Sci. 1959;82:420-30.

216. Folch J, Lees M, Sloane Stanley GH. A simple method for the isolation and purification of total lipides from animal tissues. J Biol Chem. 1957;226(1):497-509.

217. Burdge GC, Wright P, Jones AE, Wootton SA. A method for separation of phosphatidylcholine, triacylglycerol, non-esterified fatty acids and cholesterol esters from plasma by solid-phase extraction. Br J Nutr. 2000;84(5):781-7.

218. Vella A, Rizza RA. Application of isotopic techniques using constant specific activity or enrichment to the study of carbohydrate metabolism. Diabetes. 2009;58(10):2168-74.

219. Chong MF, Fielding BA, Frayn KN. Mechanisms for the acute effect of fructose on postprandial lipemia. Am J Clin Nutr. 2007;85(6):1511-20.

220. Elia M, Livesey G. Energy expenditure and fuel selection in biological systems: the theory and practice of calculations based on indirect calorimetry and tracer methods. World Rev Nutr Diet. 1992;70:68-131.

221. Liapi C CG. Glucocorticoids. In: Jaffe SJ AJe, editor. Pediatric Pharmacology. 2nd ed. Philadelphia: WB Saunders Co; 1992. p. 466-75.

222. Foisy MM, Yakiwchuk EM, Chiu I, Singh AE. Adrenal suppression and Cushing's syndrome secondary to an interaction between ritonavir and fluticasone: a review of the literature. HIV Med. 2008;9(6):389-96.

223. Kozower M, Veatch L, Kaplan MM. Decreased clearance of prednisolone, a factor in the development of corticosteroid side effects. J Clin Endocrinol Metab. 1974;38(3):407-12.

224. Ahi S, Beotra A, Dubey S, Upadhyay A, Jain S. Simultaneous identification of prednisolone and its ten metabolites in human urine by high performance liquid chromatography-tandem mass spectrometry. Drug Test Anal. 2012;4(6):460-7.

225. Lamble S, Batty E, Attar M, Buck D, Bowden R, Lunter G, et al. Improved workflows for high throughput library preparation using the transposome-based Nextera system. BMC Biotechnol. 2013;13:104.

226. Dobin A, Davis CA, Schlesinger F, Drenkow J, Zaleski C, Jha S, et al. STAR: ultrafast universal RNA-seq aligner. Bioinformatics. 2013;29(1):15-21.

227. Harrow J, Frankish A, Gonzalez JM, Tapanari E, Diekhans M, Kokocinski F, et al. GENCODE: the reference human genome annotation for The ENCODE Project. Genome Res. 2012;22(9):1760-74.

228. Liao Y, Smyth GK, Shi W. featureCounts: an efficient general purpose program for assigning sequence reads to genomic features. Bioinformatics. 2014;30(7):923-30.

229. Robinson MD, McCarthy DJ, Smyth GK. edgeR: a Bioconductor package for differential expression analysis of digital gene expression data. Bioinformatics. 2010;26(1):139-40.

230. Venneri MA, Hasenmajer V, Fiore D, Sbardella E, Pofi R, Graziadio C, et al. Circadian Rhythm of Glucocorticoid Administration Entrains Clock Genes in Immune Cells: A DREAM Trial Ancillary Study. J Clin Endocrinol Metab. 2018;103(8):2998-3009.

231. Lee H, Kim M, Park YH, Park JB. Dexamethasone downregulates SIRT1 and IL6 and upregulates EDN1 genes in stem cells derived from gingivae via the AGE/RAGE pathway. Biotechnol Lett. 2018;40(3):509-19.

232. Sasse SK, Altonsy MO, Kadiyala V, Cao G, Panettieri RA, Jr., Gerber AN. Glucocorticoid and TNF signaling converge at A20 (TNFAIP3) to repress airway smooth muscle cytokine expression. Am J Physiol Lung Cell Mol Physiol. 2016;311(2):L421-32.

233. Mostafa MM, Rider CF, Shah S, Traves SL, Gordon PMK, Miller-Larsson A, et al. Glucocorticoid-driven transcriptomes in human airway epithelial cells: commonalities, differences and functional insight from cell lines and primary cells. BMC Med Genomics. 2019;12(1):29.

234. den Uyl D, van Raalte DH, Nurmohamed MT, Lems WF, Bijlsma JW, Hoes JN, et al. Metabolic effects of high-dose prednisolone treatment in early rheumatoid arthritis: balance between diabetogenic effects and inflammation reduction. Arthritis Rheum. 2012;64(3):639-46.

235. van Raalte DH, Brands M, van der Zijl NJ, Muskiet MH, Pouwels PJ, Ackermans MT, et al. Low-dose glucocorticoid treatment affects multiple aspects of intermediary metabolism in healthy humans: a randomised controlled trial. Diabetologia. 2011;54(8):2103-12.

236. van Raalte DH, Diamant M, Ouwens DM, Ijzerman RG, Linssen MM, Guigas B, et al. Glucocorticoid treatment impairs microvascular function in healthy men in association with its adverse effects on glucose metabolism and blood pressure: a randomised controlled trial. Diabetologia. 2013;56(11):2383-91.

237. Petersons CJ, Mangelsdorf BL, Jenkins AB, Poljak A, Smith MD, Greenfield JR, et al. Effects of low-dose prednisolone on hepatic and peripheral insulin sensitivity, insulin secretion, and abdominal adiposity in patients with inflammatory rheumatologic disease. Diabetes Care. 2013;36(9):2822-9.

238. Petersons CJ, Mangelsdorf BL, Poljak A, Smith MD, Greenfield JR, Thompson CH, et al. Low dose prednisolone and insulin sensitivity differentially affect arterial stiffness and endothelial function: An open interventional and cross-sectional study. Atherosclerosis. 2017;258:34-9.

239. Hazlehurst JM, Gathercole LL, Nasiri M, Armstrong MJ, Borrows S, Yu J, et al. Glucocorticoids fail to cause insulin resistance in human subcutaneous adipose tissue in vivo. J Clin Endocrinol Metab. 2013;98(4):1631-40.

240. Traish A, Haider KS, Doros G, Haider A. Long-term dutasteride therapy in men with benign prostatic hyperplasia alters glucose and lipid profiles and increases severity of erectile dysfunction. Horm Mol Biol Clin Investig. 2017;30(3).

241. Nixon M, Upreti R, Andrew R. 5alpha-Reduced glucocorticoids: a story of natural selection. J Endocrinol. 2012;212(2):111-27.

242. Saberi P, Phengrasamy T, Nguyen DP. Inhaled corticosteroid use in HIV-positive individuals taking protease inhibitors: a review of pharmacokinetics, case reports and clinical management. HIV Med. 2013;14(9):519-29.

243. Renner E, Horber FF, Jost G, Frey BM, Frey FJ. Effect of liver function on the metabolism of prednisone and prednisolone in humans. Gastroenterology. 1986;90(4):819-28.

244. Cooper MS, Rabbitt EH, Goddard PE, Bartlett WA, Hewison M, Stewart PM. Osteoblastic 11beta-hydroxysteroid dehydrogenase type 1 activity increases with age and glucocorticoid exposure. J Bone Miner Res. 2002;17(6):979-86.

245. Fenton CG, Doig CL, Fareed S, Naylor A, Morrell AP, Addison O, et al. 11beta-HSD1 plays a critical role in trabecular bone loss associated with systemic glucocorticoid therapy. Arthritis Res Ther. 2019;21(1):188.

246. Stefan N, Ramsauer M, Jordan P, Nowotny B, Kantartzis K, Machann J, et al. Inhibition of 11beta-HSD1 with RO5093151 for non-alcoholic fatty liver disease: a multicentre, randomised, double-blind, placebo-controlled trial. Lancet Diabetes Endocrinol. 2014;2(5):406-16.

247. Scott JS, Bowker SS, Deschoolmeester J, Gerhardt S, Hargreaves D, Kilgour E, et al. Discovery of a potent, selective, and orally bioavailable acidic 11beta-hydroxysteroid dehydrogenase type 1 (11beta-HSD1) inhibitor: discovery of 2-[(3S)-1-[5-(cyclohexylcarbamoyl)-6-propylsulfanylpyridin-2-yl]-3-piperidyl]acet ic acid (AZD4017). J Med Chem. 2012;55(12):5951-64.

248. Markey K, Mitchell, J., Botfield, H. et al. 11b-Hydroxysteroid dehydrogenase type 1 inhibition in idiopathic intracranial hypertension: a double-blind randomized controlled trial2020; 2.

249. Sadler R, Bateman EA, Heath V, Patel SY, Schwingshackl PP, Cullinane AC, et al. Establishment of a healthy human range for the whole blood "OX40" assay for the detection of antigen-specific CD4+ T cells by flow cytometry. Cytometry B Clin Cytom. 2014;86(5):350-61.

250. Vulto A, Minovic I, de Vries LV, Timmermans AC, van Faassen M, Gomes Neto AW, et al. Endogenous urinary glucocorticoid metabolites and mortality in prednisolone-treated renal transplant recipients. Clin Transplant. 2020;34(4):e13824.

251. de Jong WHA, Buitenwerf E, Pranger AT, Riphagen IJ, Wolffenbuttel BHR, Kerstens MN, et al. Determination of reference intervals for urinary steroid profiling

using a newly validated GC-MS/MS method. Clin Chem Lab Med. 2017;56(1):103-12.

252. Nielsen HK, Charles P, Mosekilde L. The effect of single oral doses of prednisone on the circadian rhythm of serum osteocalcin in normal subjects. J Clin Endocrinol Metab. 1988;67(5):1025-30.

253. Meeran K, Hattersley A, Burrin J, Shiner R, Ibbertson K. Oral and inhaled corticosteroids reduce bone formation as shown by plasma osteocalcin levels. Am J Respir Crit Care Med. 1995;151(2 Pt 1):333-6.

254. Souverein PC, Berard A, Van Staa TP, Cooper C, Egberts AC, Leufkens HG, et al. Use of oral glucocorticoids and risk of cardiovascular and cerebrovascular disease in a population based case-control study. Heart. 2004;90(8):859-65.

255. van Raalte DH, van Genugten RE, Linssen MM, Ouwens DM, Diamant M. Glucagon-like peptide-1 receptor agonist treatment prevents glucocorticoid-induced glucose intolerance and islet-cell dysfunction in humans. Diabetes Care. 2011;34(2):412-7.

256. Ohashi N, Tsuji N, Naito Y, Iwakura T, Isobe S, Ono M, et al. Alogliptin improves steroid-induced hyperglycemia in treatment-naive Japanese patients with chronic kidney disease by decrease of plasma glucagon levels. Med Sci Monit. 2014;20:587-93.

257. Katsuyama H, Sako A, Adachi H, Hamasaki H, Yanai H. Effects of 6-month sitagliptin treatment on metabolic parameters in diabetic patients taking oral glucocorticoids: a retrospective cohort study. J Clin Med Res. 2015;7(6):479-84.

258. van Genugten RE, van Raalte DH, Muskiet MH, Heymans MW, Pouwels PJ, Ouwens DM, et al. Does dipeptidyl peptidase-4 inhibition prevent the diabetogenic effects of glucocorticoids in men with the metabolic syndrome? A randomized controlled trial. Eur J Endocrinol. 2014;170(3):429-39.

259. Pernicova I, Kelly S, Ajodha S, Sahdev A, Bestwick JP, Gabrovska P, et al. Metformin to reduce metabolic complications and inflammation in patients on systemic glucocorticoid therapy: a randomised, double-blind, placebo-controlled, proof-of-concept, phase 2 trial. Lancet Diabetes Endocrinol. 2020;8(4):278-91.

260. Almon RR, Yang E, Lai W, Androulakis IP, Ghimbovschi S, Hoffman EP, et al. Relationships between circadian rhythms and modulation of gene expression by glucocorticoids in skeletal muscle. Am J Physiol Regul Integr Comp Physiol. 2008;295(4):R1031-47.

261. Berisha SZ, Serre D, Schauer P, Kashyap SR, Smith JD. Changes in whole blood gene expression in obese subjects with type 2 diabetes following bariatric surgery: a pilot study. PLoS One. 2011;6(3):e16729.

262. Bonaccorsi L, Luciani P, Nesi G, Mannucci E, Deledda C, Dichiara F, et al. Androgen receptor regulation of the seladin-1/DHCR24 gene: altered expression in prostate cancer. Lab Invest. 2008;88(10):1049-56.

263. Safy M, de Hair MJH, Jacobs JWG, Buttgereit F, Kraan MC, van Laar JM. Efficacy and safety of selective glucocorticoid receptor modulators in comparison to glucocorticoids in arthritis, a systematic review. PLoS One. 2017;12(12):e0188810.

264. Di Dalmazi G, Berr CM, Fassnacht M, Beuschlein F, Reincke M. Adrenal function after adrenalectomy for subclinical hypercortisolism and Cushing's syndrome: a systematic review of the literature. J Clin Endocrinol Metab. 2014;99(8):2637-45.